Full-field x-ray imaging

Goal: Basic understanding of key imaging concepts and guide as a potential user

Outline

Part 1: Key concepts for imaging
Part 2: Practical issues and instruments
Part 3: Imaging techniques and examples
Part 4: Current frontiers

Outline

Part 1: Key concepts for imaging
Part 2: Practical issues and instruments
Part 3: Imaging techniques and examples
Part 4: Current frontiers

Key concept: the sample transmission function

Away from Bragg conditions, x-ray interaction with materials can be characterized by the material index of refraction: $n = 1 - \delta + i\beta$

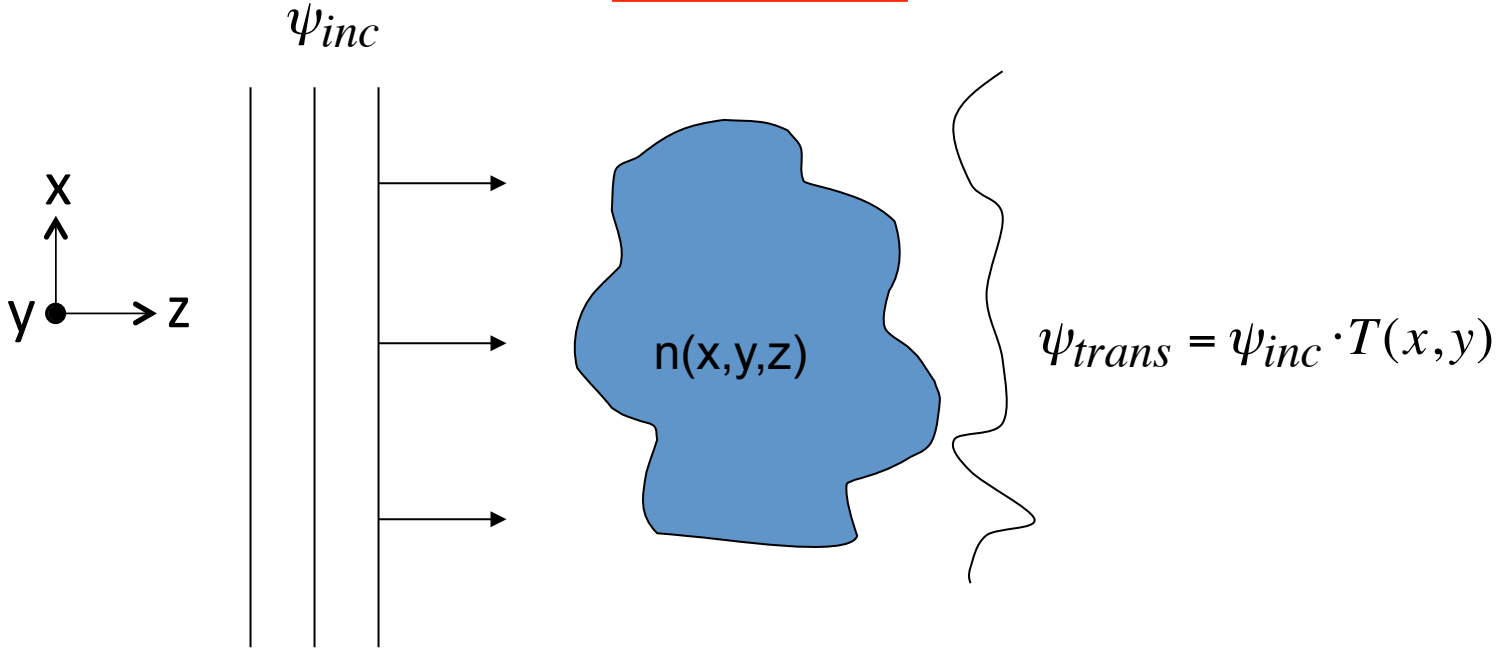

$$T(x,y) = e^{ik\int n(x,y,z)dz} = e^{ik\int [1-\delta(x,y,z)+i\beta(x,y,z)]dz} = e^{-k\int \beta(x,y,z)dz} e^{ik\int dz} e^{-ik\int \delta(x,y,z)dz}$$

Drop constant phase term $e^{ik\int dz}$

$$T(x,y) = e^{-k\int \beta(x,y,z)dz} e^{-ik\int \delta(x,y,z)dz} = A(x,y)e^{i\phi(x,y)}$$

$A(x,y)$ *is the wave amplitude*

$\phi(x,y)$ *is the accumulated phase difference*

Visual guide

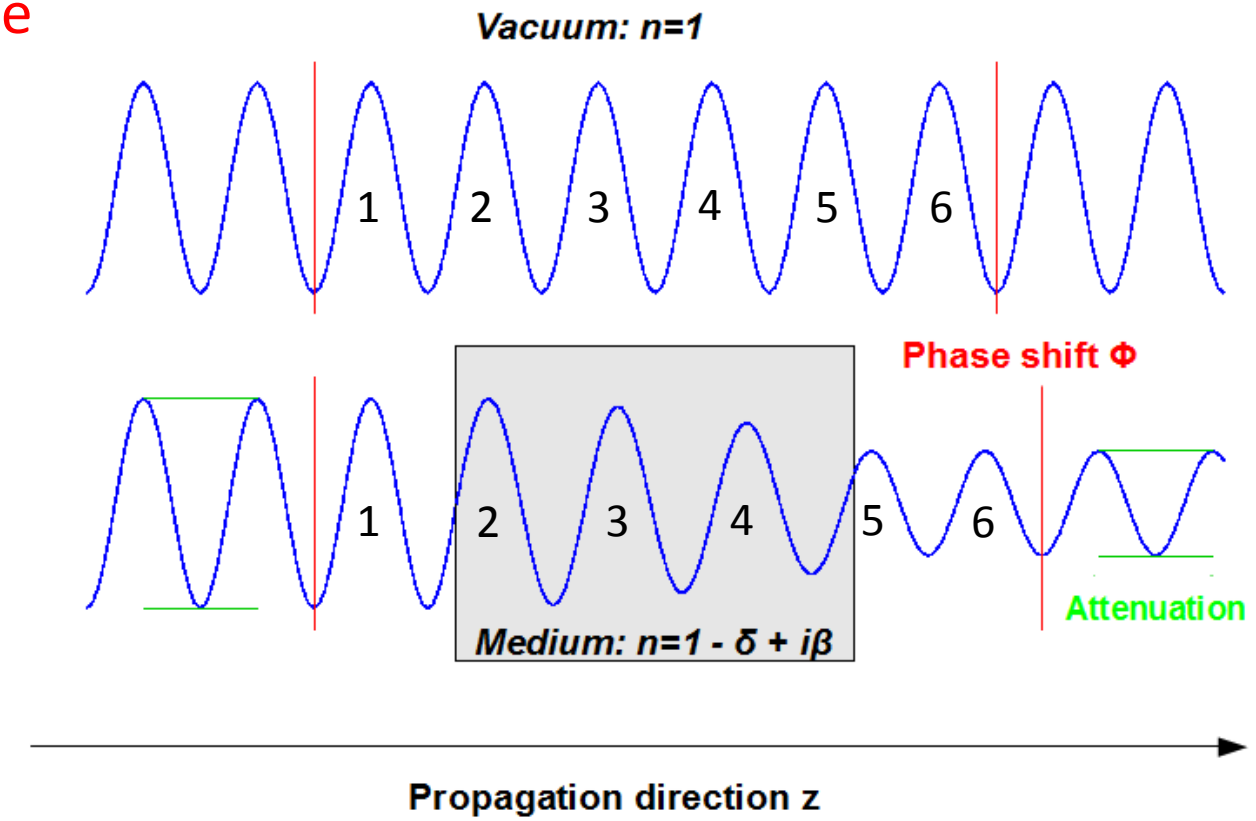

Samples does two things to the incident wave:

1. Attenuates the wave amplitude via absorption (β term)
2. Affects the phase of the wave (δ term).

For x-rays, the wave accumulates less phase when going through material. The phase term (ϕ) is the integral of δ and it reflects how fewer cycles the wave has gone through to get to some particular point in space (from some other point in space) relative to vacuum.

$$\beta \propto \lambda^4$$

$$\mu = \frac{4\pi\beta}{\lambda} \quad \propto \quad \lambda^3$$

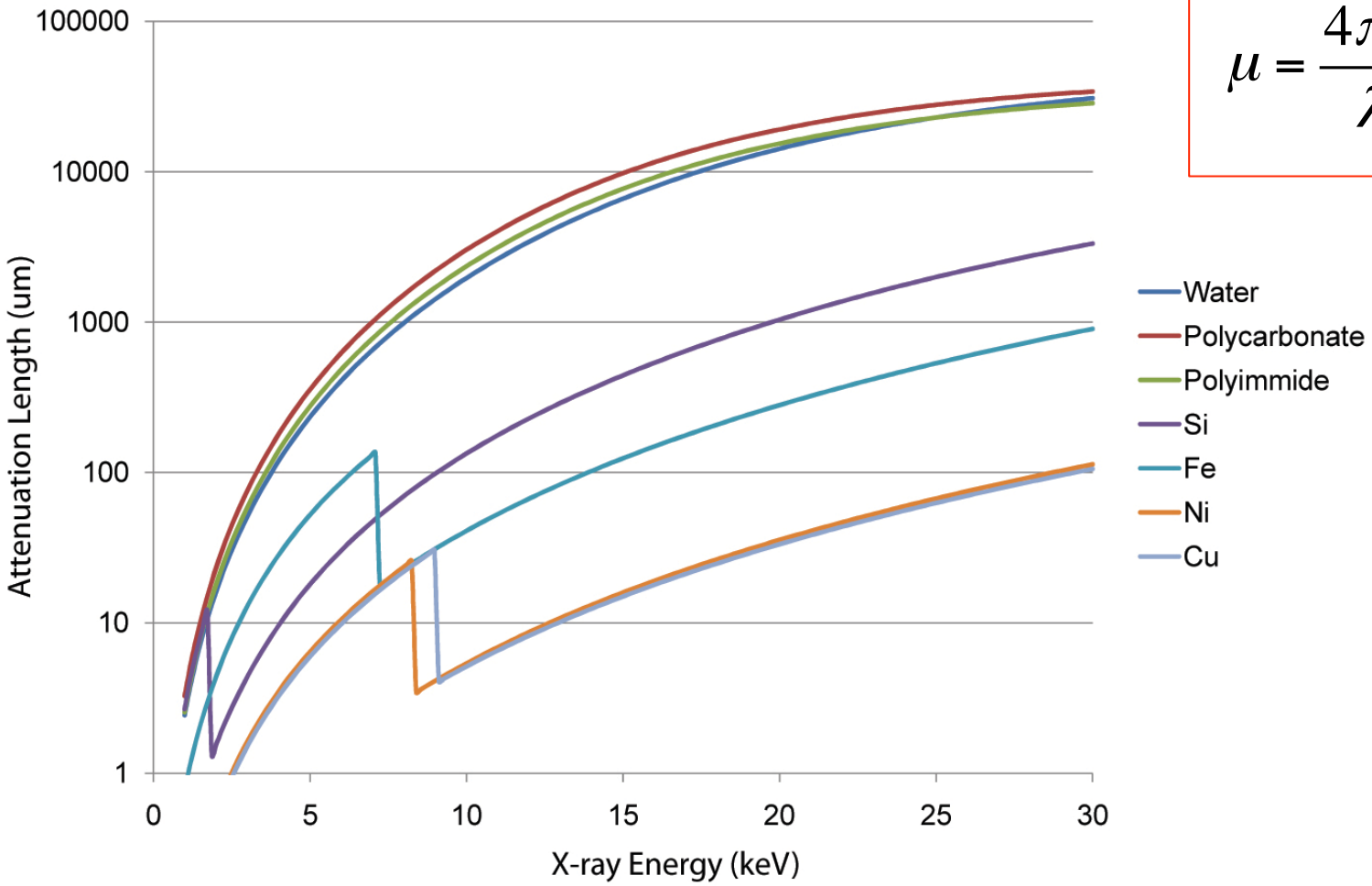

For ‘soft’ materials, 10 keV is good for few mm thickness

For ‘hard’ materials, 10 keV is only good for 0.01 – 0.1 mm thick

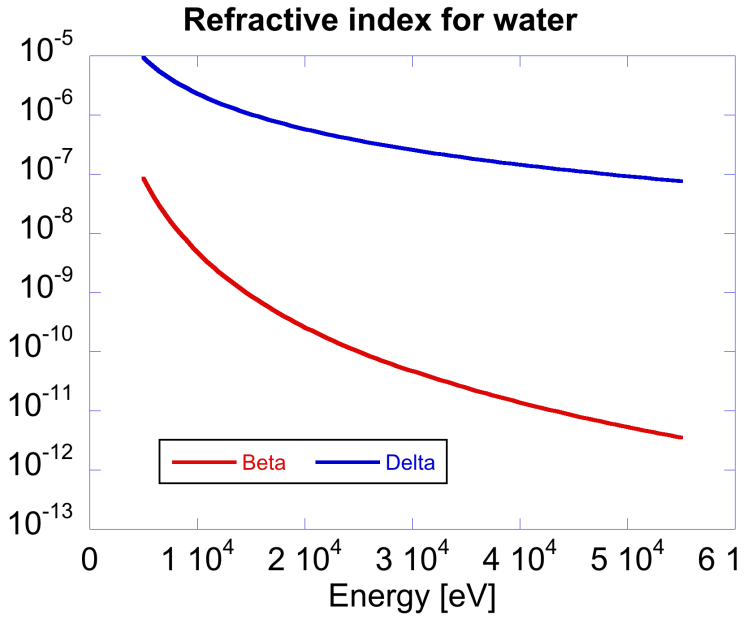

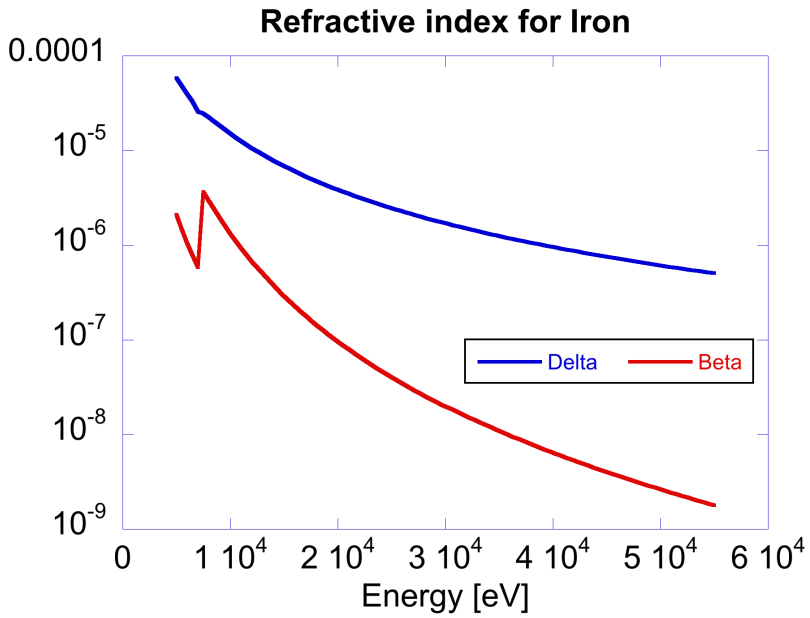

1/e attenuation length: $\Delta t = \dfrac{\lambda}{4\pi\beta}$

Pi phase shift length: $\Delta t = \dfrac{\lambda}{2\delta}$

Eg. 20 keV, λ = 12.4/20 = 0.62 Å

For Al at 20 keV, β = 4e-9 and δ = 1.4e-6

1/e length = 0.62e-10/(4x3.14x4e-9) = 1.2 mm

Pi phase shift length = 0.62e-10/(2x1.4xe-6) = 0.02 mm

Phase and wavefront

For x-rays, real part of refractive index is < 1

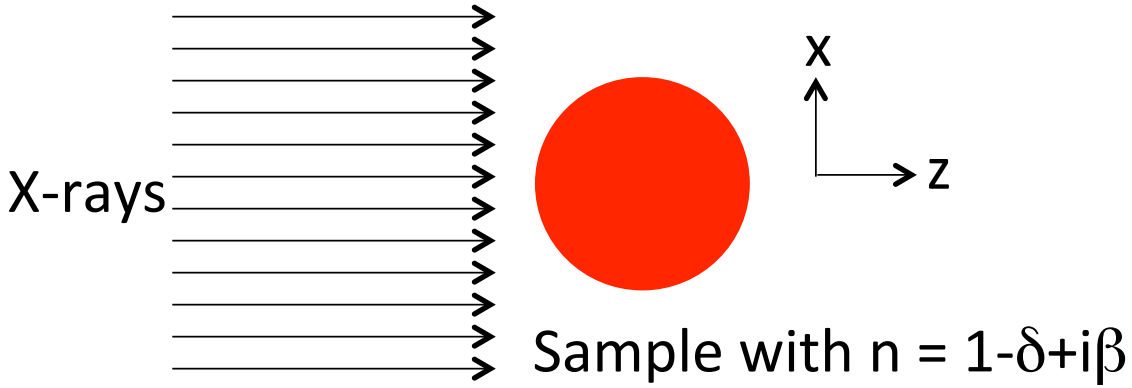

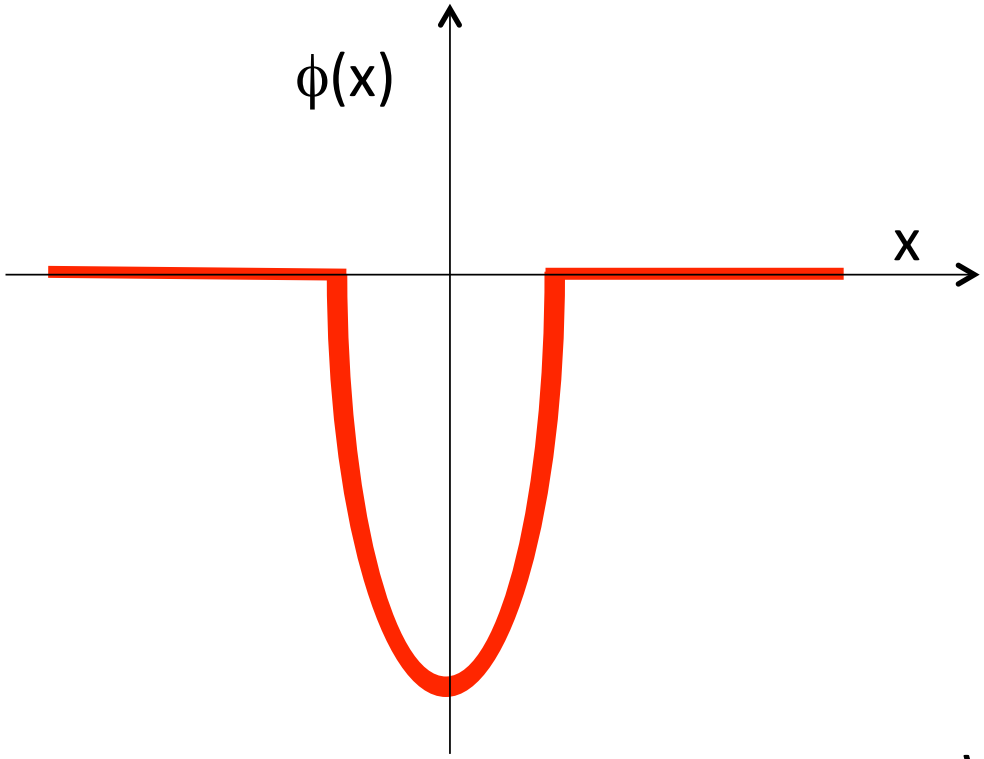

Phase immediately after sample
Wave through sample has accumulated less phase

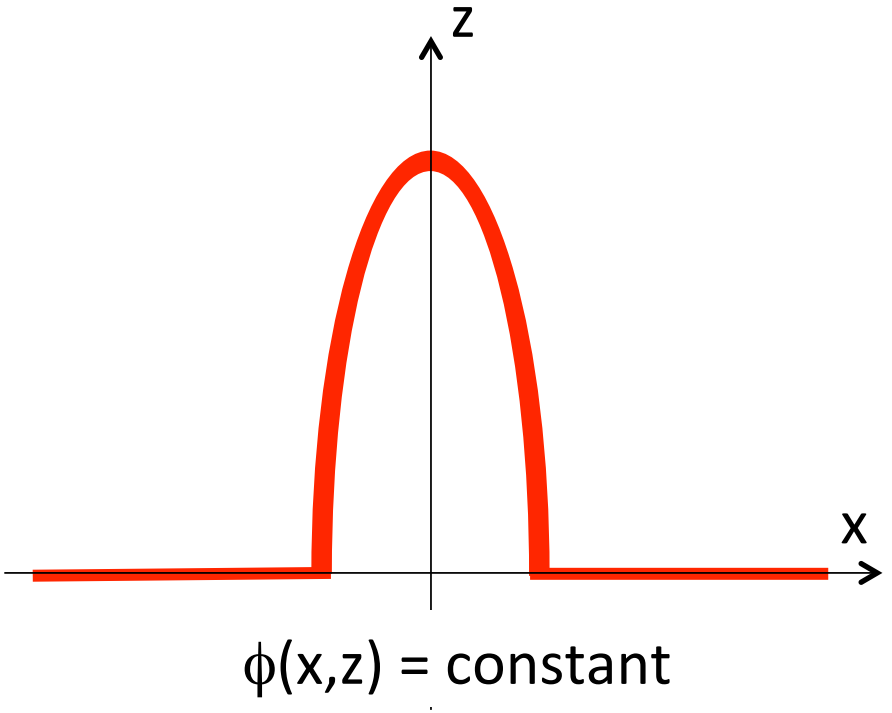

Wavefront immediately after sample
Phase velocity through sample is higher than through vacuum

Key concept: Huygens, Fresnel & Kirchoff diffraction

Huygens: Every point on a wavefront is a secondary source of spherical waves. The wavefront at a later time is due to interference and sum of all these secondary waves.

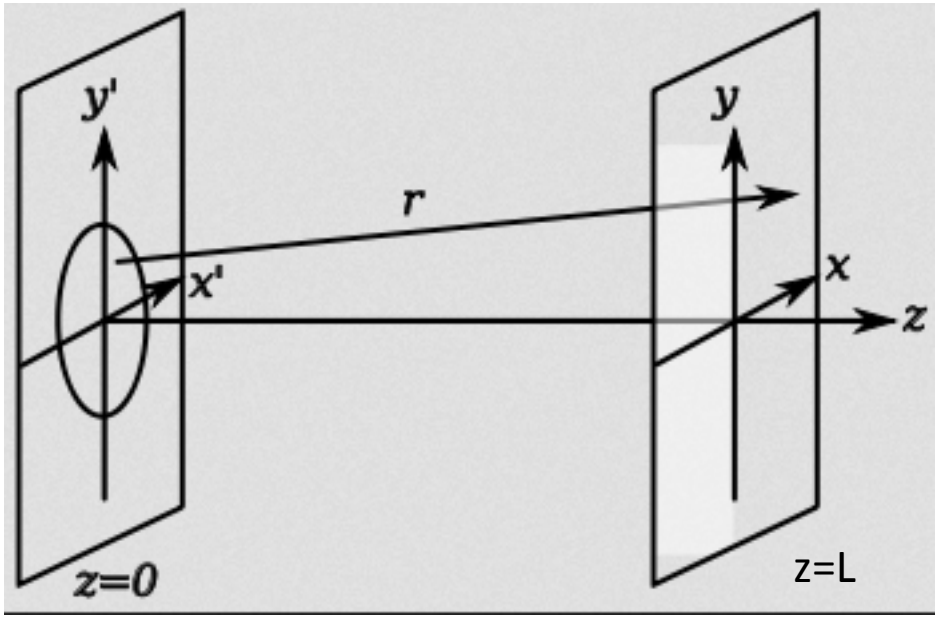

$$\psi_0(x',y') \equiv \psi(x',y',z=0) \qquad \psi_L(x,y) \equiv \psi(x,y,z=L)$$

$$\psi_L(x,y) = \frac{1}{i\lambda}\iint \psi_0(x',y')\frac{e^{ikr}}{r}\,dx'\,dy'$$

For synchrotrons, we have ignored an 'obliquity factor' in the integral

Approximate r with Taylor series
Fraunhofer diffraction: Only keep linear terms
Fresnel diffraction: Keep quadratic terms

$$\psi_L(x,y) = \frac{e^{ikL}}{i\lambda L}\iint \psi_0(x',y')\exp\left[\frac{i\pi}{\lambda L}\left[(x-x')^2+(y-y')^2\right]\right]dx'\,dy'$$

Define a Fresnel propagator:

$$P_L(x,y) = \frac{e^{ikL}}{i\lambda L}\exp\left[\frac{i\pi}{\lambda L}(x^2+y^2)\right]$$

Free space propagation of a wave is thus a convolution of the initial wave with the propagator

$$\psi_L(x,y) = \psi_0(x,y) \otimes P_L(x,y)$$

If you know the wavefunction at z, you can calculate the wavefunction at z+L

Key concept: 'Local' direction of the wave is normal to the wave front

For a wave written as: $\psi(x,y) = A(x,y)e^{ik\phi(x,y)}$

'Local' direction of the wave is normal to the wave front

$$\vec{k}_{out} \approx \frac{\partial\phi(x,y)}{\partial x}\hat{x} + \frac{\partial\phi(x,y)}{\partial y}\hat{y} + k\hat{z}$$

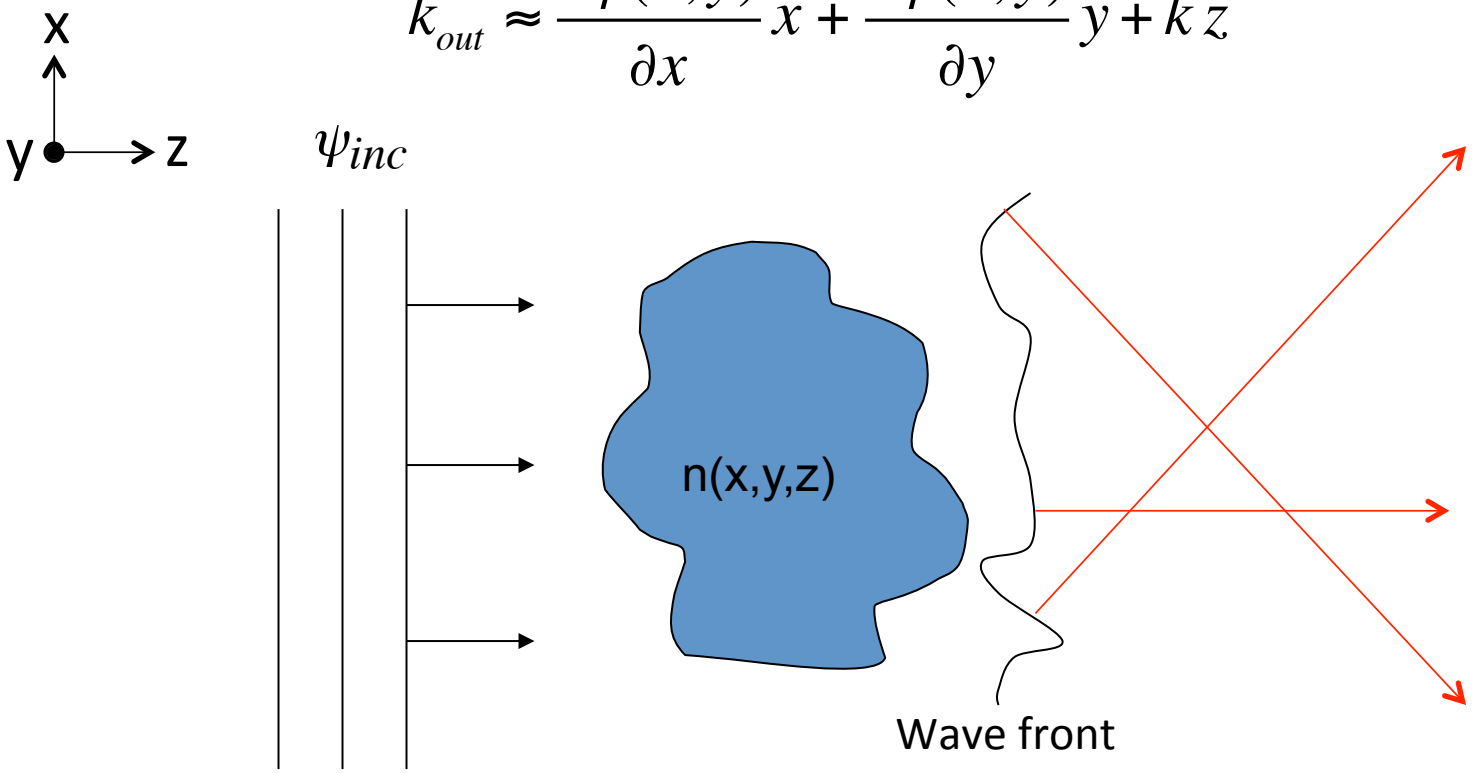

Phase gradients result in angular changes of the rays.
Large phase gradients (rapid phase change) leads to large angular deviations.
Small phase gradients (gradual phase change) leads to small angular deviations.

Visual guide

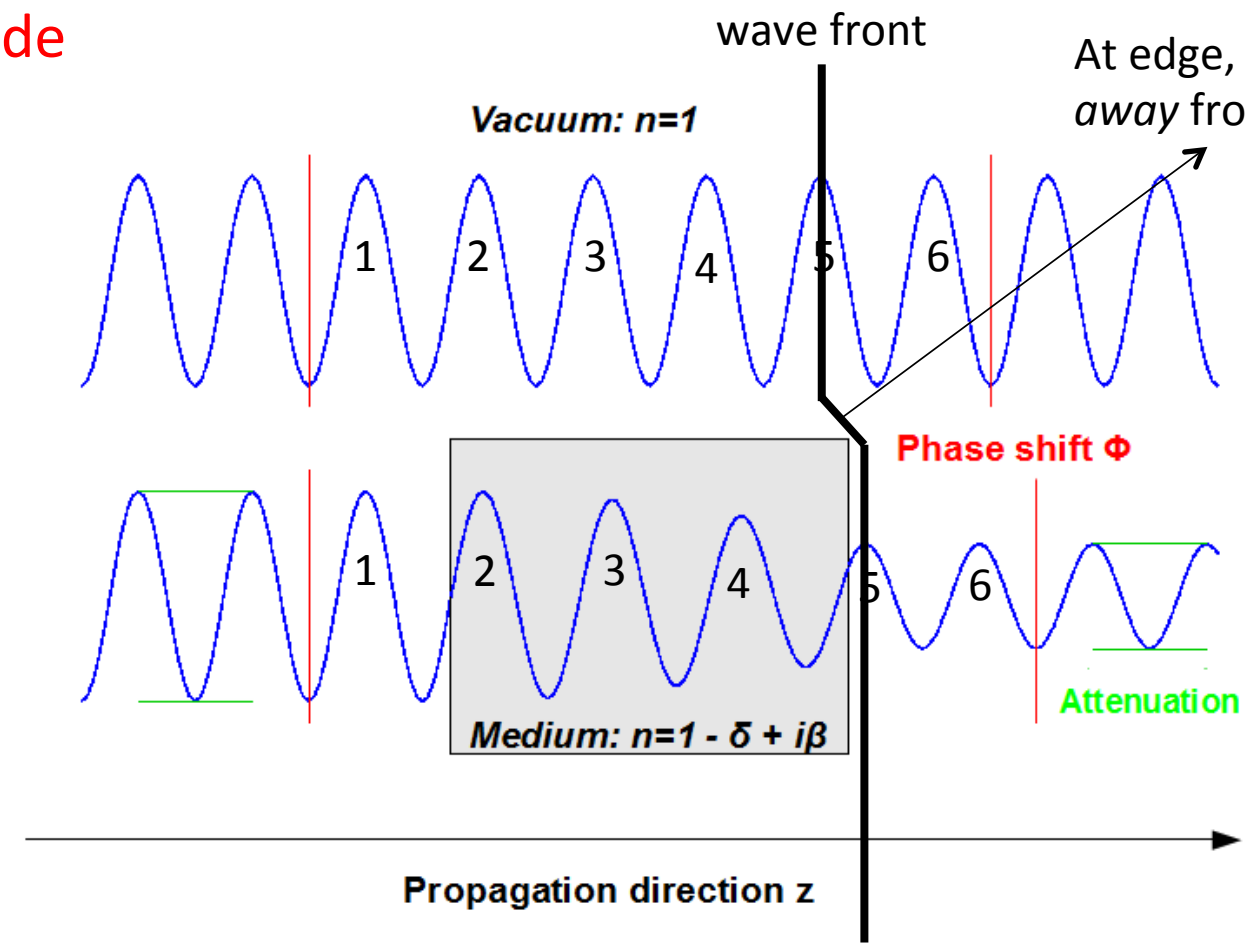

For visible light, δ is large and negative.
For x-rays, δ is very small and positive.

Key Concept: Crystals

Hyperphysics.phy-astr.gsu.edu

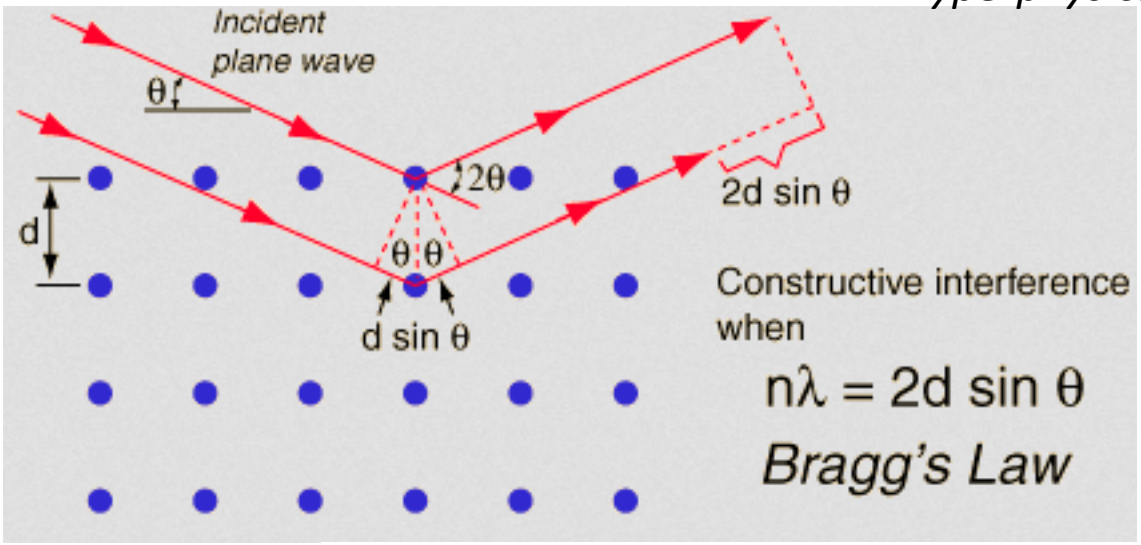

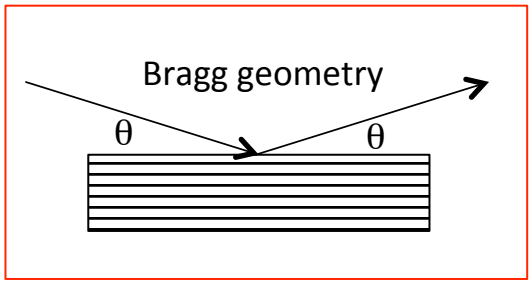

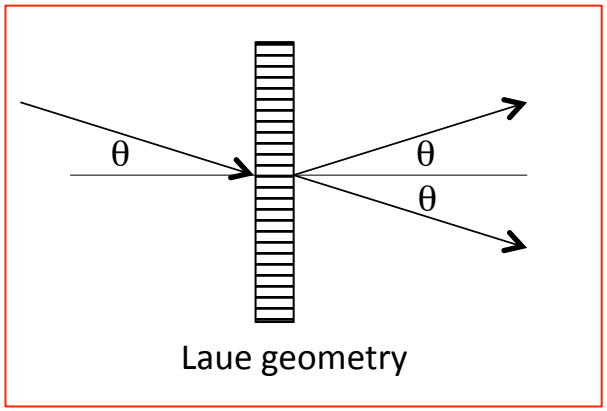

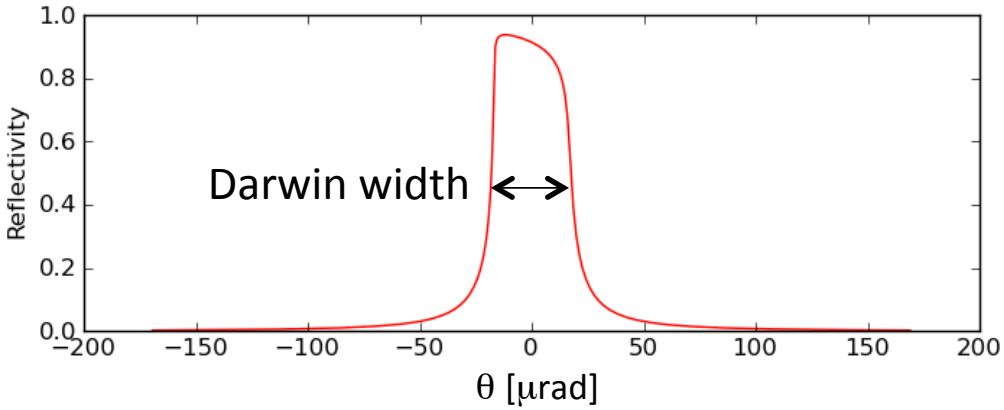

- For a monochromatic incident beam, crystal reflects over a very small angular range (Darwin width).
- Sides of the reflectivity curve are very steep – very sensitive to angular changes

Key concept: Small structures scatter to large angles

Consider scattering from grating

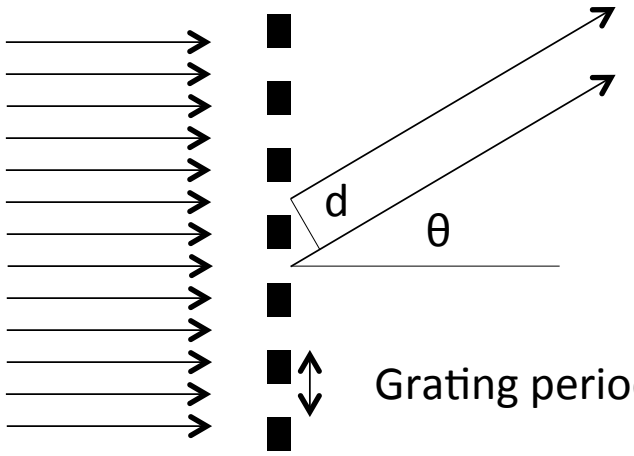

Path difference d = a sin θ

Constructive interference when: a sin θ = nλ
For n=1 (first order) , θ = λ/a
That is, small a -> large θ

Recall Qun Shen presentation
Scattering theory: Scattered wave amplitude is the Fourier transform of the electron density.
Small features scatter to high 'q'.

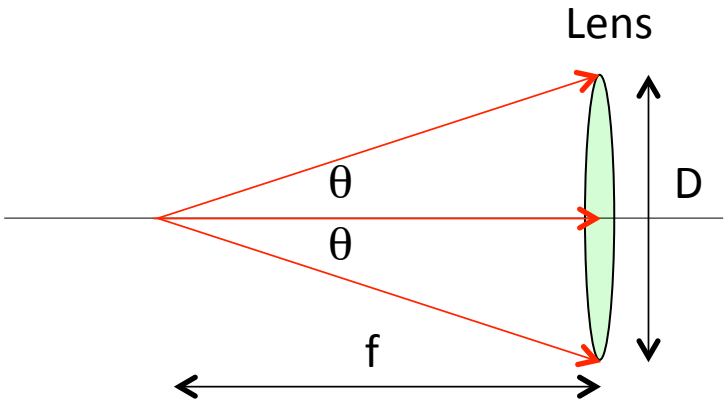

Lens terminology: numerical aperture (NA)
NA = sin(θ) = lens radius/focal distance =D/2f

Key concept: Abbe theory

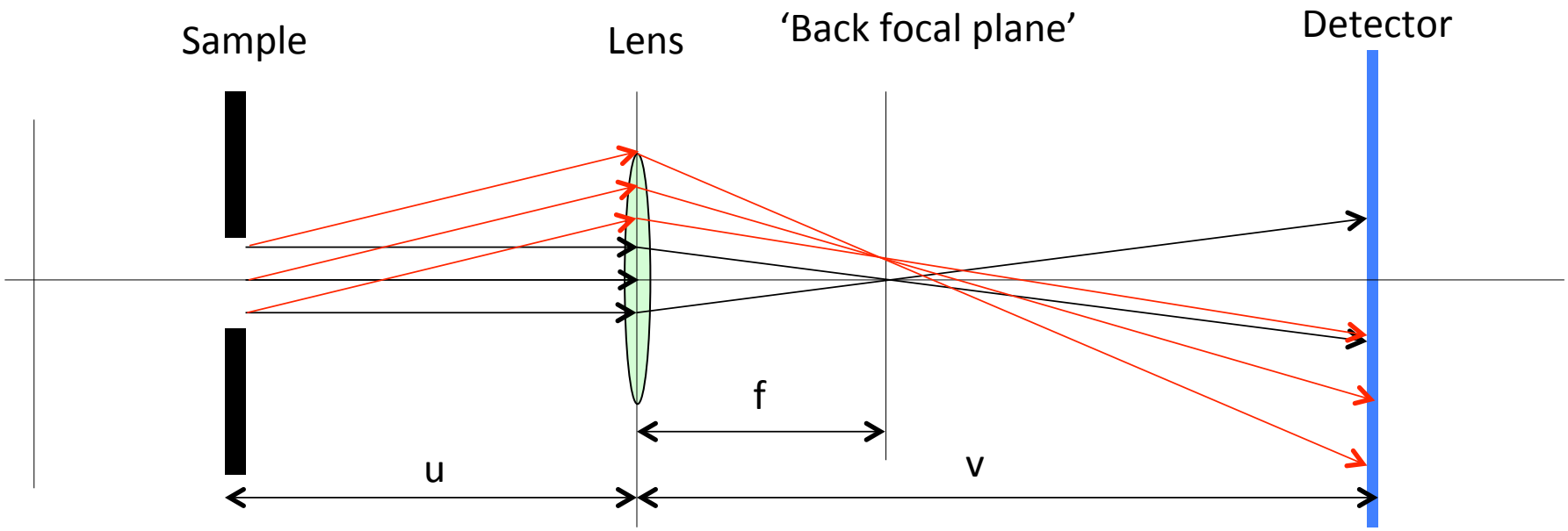

Assume thin lens: $1/u + 1/v = 1/f$

Lens imaging is a two step Fourier transform:

At back focal plane = Fourier transform of sample plane wavefunction

At detector plane = Inverse Fourier transform of back focal plane wavefunction

Key concept: The resolution of the lens-based imaging system depends on how high in angle of the scattered beam from the sample is collected by the lens. Higher lens numerical aperture leads to better spatial resolution.

Lens imaging resolution

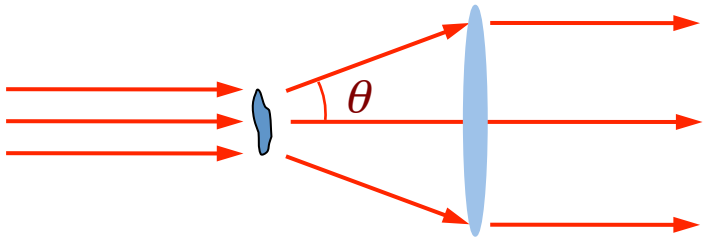

On-axis illumination.
Highest scattered angle captured by lens = θ
Expect highest 'resolution' ~ $\lambda/\theta = \lambda/NA$

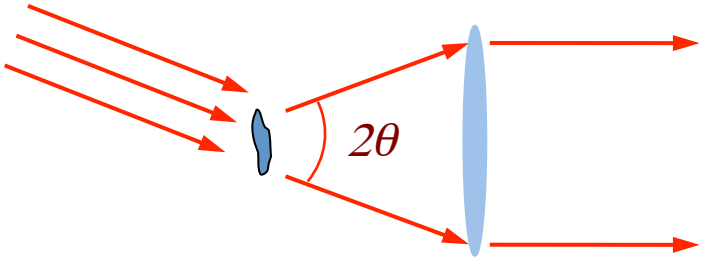

Oblique illumination.
Highest scattered angle captured by lens = 2θ
Expect highest 'resolution' ~ $\lambda/2\theta = \lambda/2NA$

Note: These are 'rules of thumb'. Actual definition of 'resolution' is more nuanced.

Key concept: Talbot effect

$$\psi_L(x) = \psi_0(x) \otimes P_L(x) \quad \rightarrow \quad \tilde{\psi}_L(f) = \tilde{\psi}_0(f).\tilde{P}_L(f)$$

$$P_L(x) = \frac{e^{ikL}}{i\lambda L}\exp\left[\frac{i\pi x^2}{\lambda L}\right] \quad \rightarrow \quad \tilde{P}(f) = \exp[-i\pi\lambda L f^2]$$

$$If\ \psi_0(x)\ is\ periodic\ with\ period\ a, then\ \tilde{\psi}_0(f) = A_n\,\delta(\frac{n}{a})\ where\ n \in integer$$

$$\tilde{\psi}_L(f) = \sum_n A_n \delta\left(\frac{n}{a}\right).\tilde{P}_L(f) = \sum_n A_n \exp\left[-i\pi\lambda L\left(\frac{n}{a}\right)^2\right]$$

$$\text{At multiples of the Talbot distance } L_T = \frac{2a^2}{\lambda},\ \tilde{P}(f)=1$$

Talbot effect: An image of a periodic sample is formed at multiples of Talbot distance downstream of the sample.

Fractional Talbot effect: Images *related* to periodic sample are formed at fractional Talbot distances.

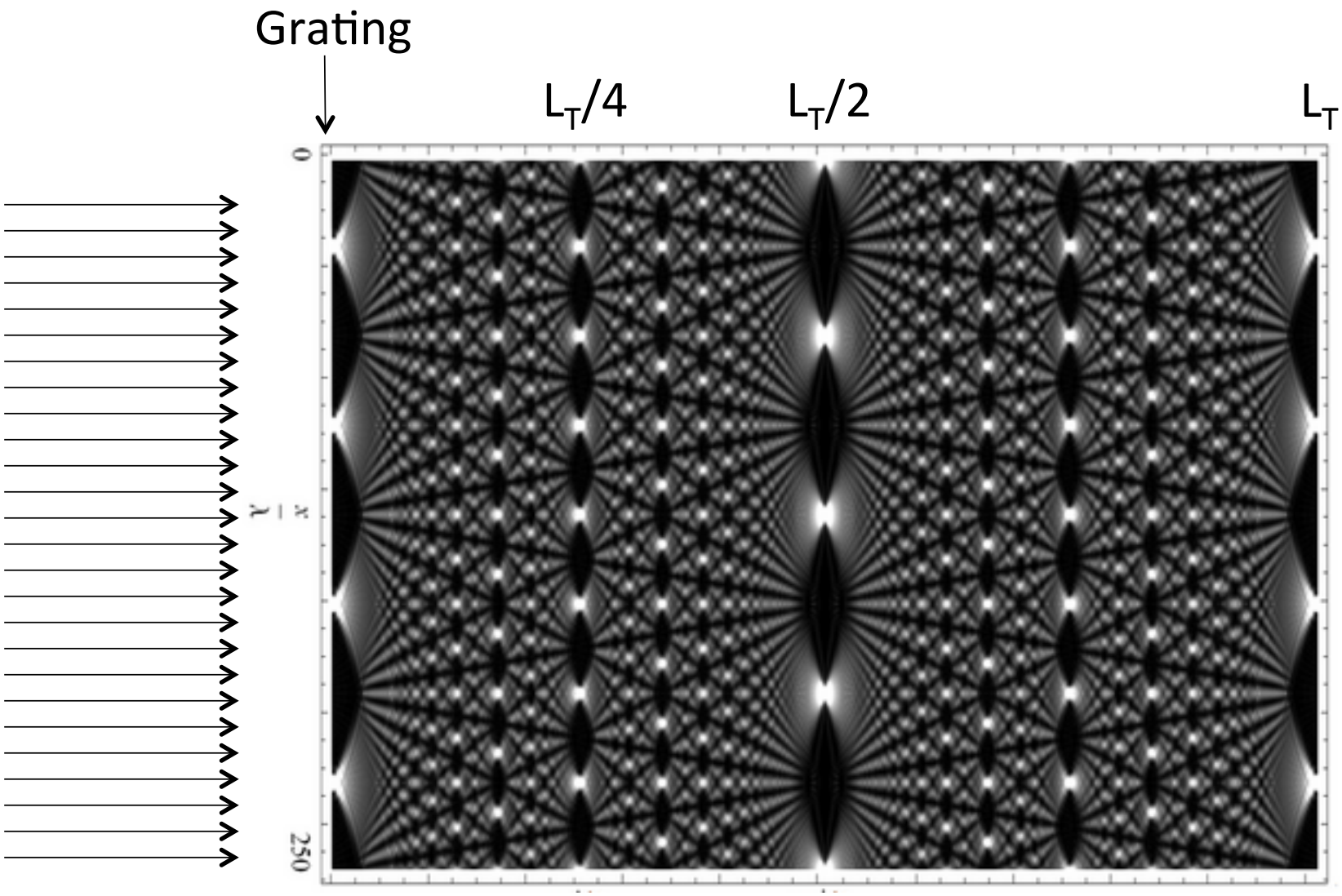

At certain fractional Talbot distances, shifts and/or frequency multiples

wikipedia

Key concept: Tomography – Fourier slice theorem

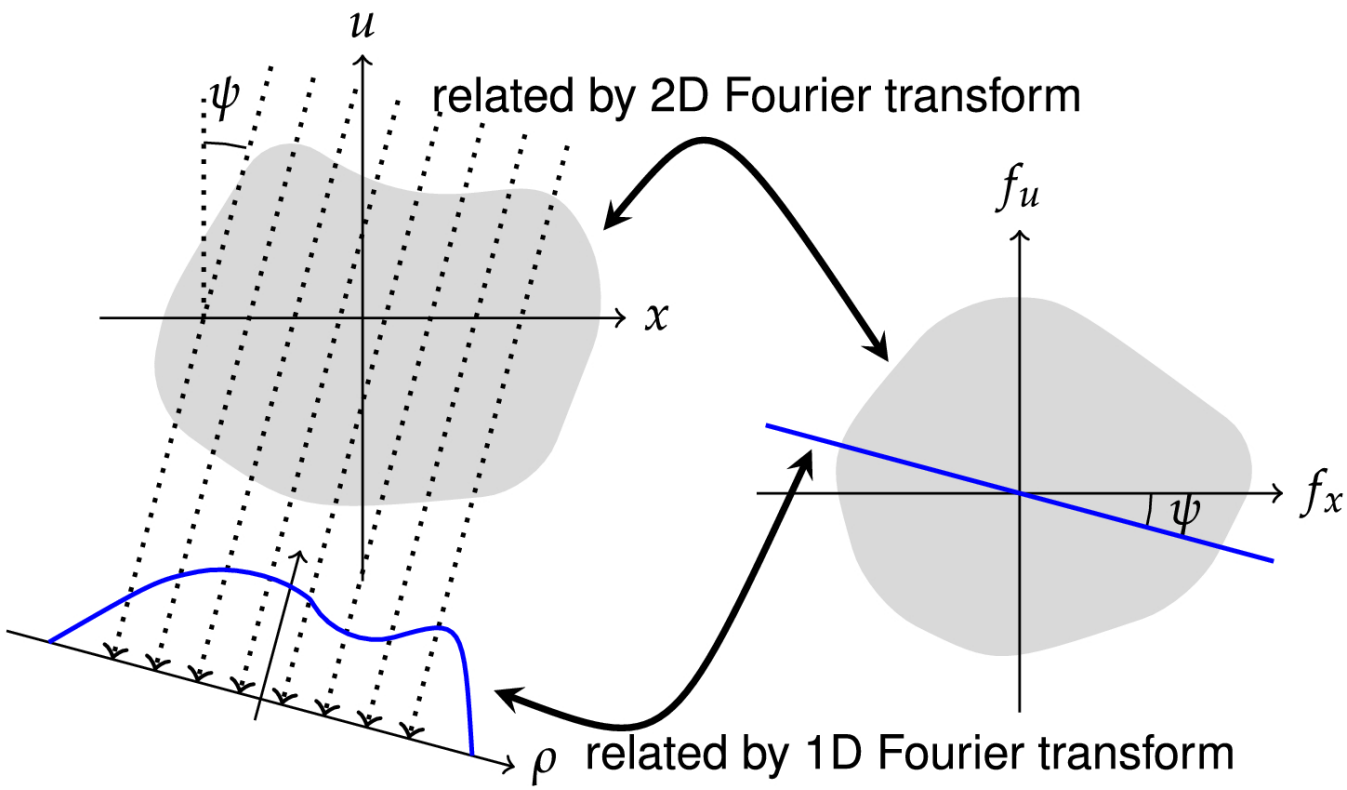

Fourier transform of projection image <-> A slice in the Fourier transform of the object

So, taking many projections at different angles, you can fully fill out the 3D Fourier transform of the object. A inverse Fourier transform gives you the 3D object in real space.

Citation
Edmund Y. Lam, "Computational photography with plenoptic camera and light field capture: tutorial," J. Opt. Soc. Am. A **32,** 2021-2032 (2015);
https://www.osapublishing.org/josaa/abstract.cfm?uri=josaa-32-11-2021

OSA
The Optical Society

Sketch from www.esrf.eu

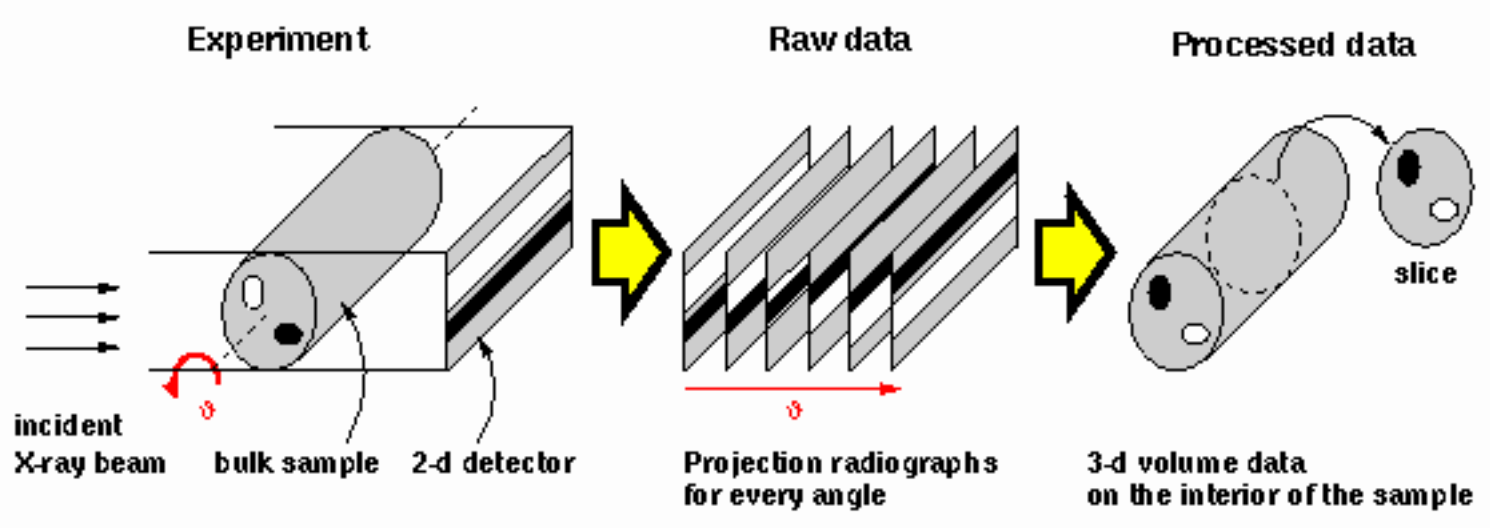

Requirements:

- Projection must reflect the line integral of some local function. Eg $\int \mu(x,y,z)\,dz$

- Sample projection must be smaller than detector field of view in direction perpendicular to rotation axis.
- Sufficient sample transmission at the 'most absorbed' regions.
- Best samples are rods; worst samples are plates.
- Very good rotation stage with minimal run-out.
- Number of projections ~ number of pixels in direction perpendicular to rotation axis.

Because of FOV requirement, FOV/resolution < #pixels in direction perpendicular to rotation axis
With typical 2K x 2K sensors, FOV/resolution ~ 2K.

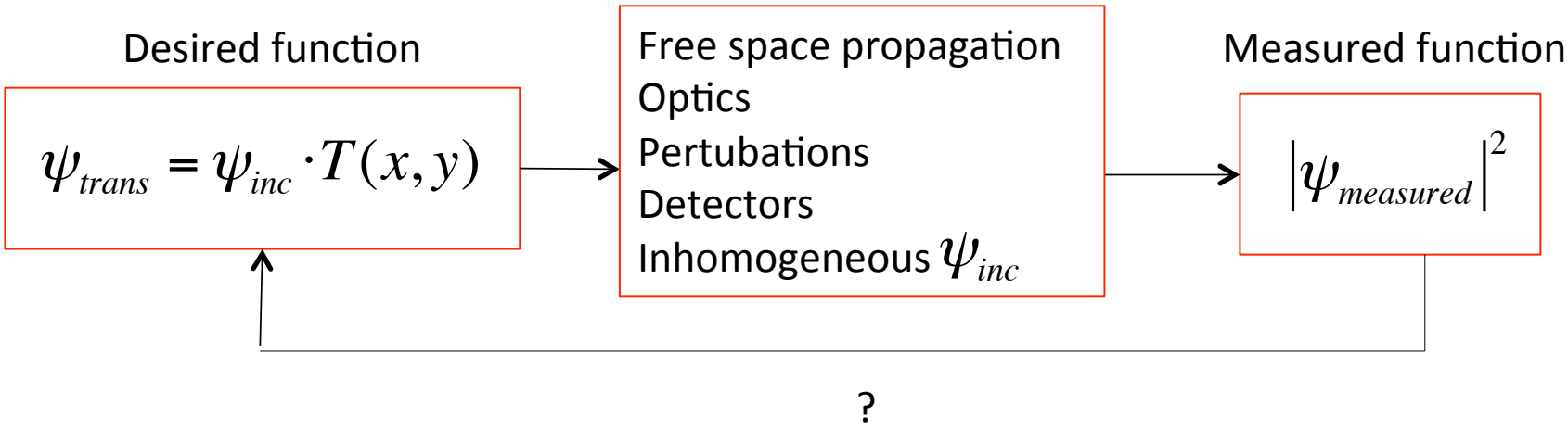

In Quantitative Imaging, want to obtain $\beta(x,y,z)$ or $\delta(x,y,z)$

Majority of x-ray imaging is not quantitative – but for visualization

Outline

Part 1: Key concepts for imaging
Part 2: Practical issues and instruments
Part 3: Imaging techniques and examples
Part 4: Current frontiers

Detection setups

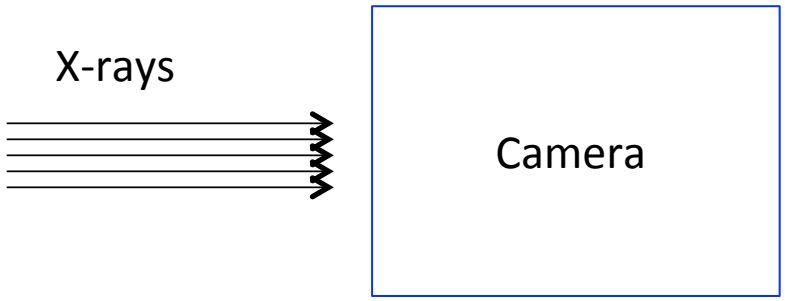

Direct detection: x-rays hit sensor chip
Chip pixel size determines resolution
Mostly for low x-ray energy < 10 keV

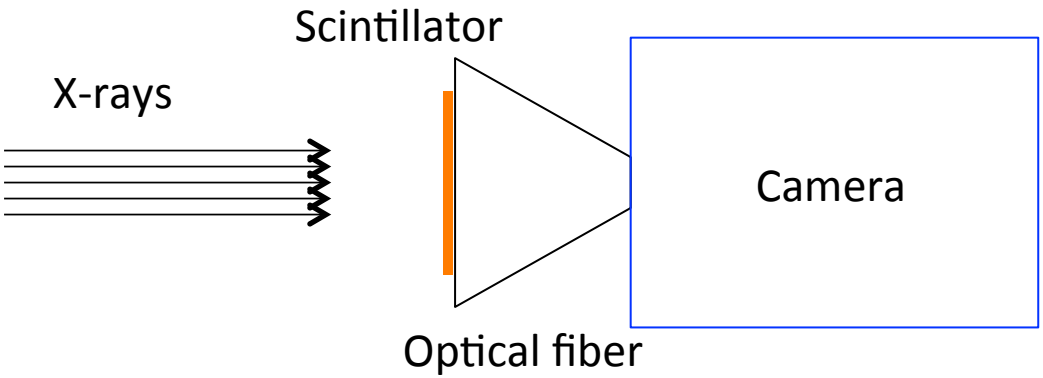

Scintillator converts x-ray to visible light
Optical fiber demagnifies image to fit sensor chip
For imaging large samples
Spatial resolution poor.

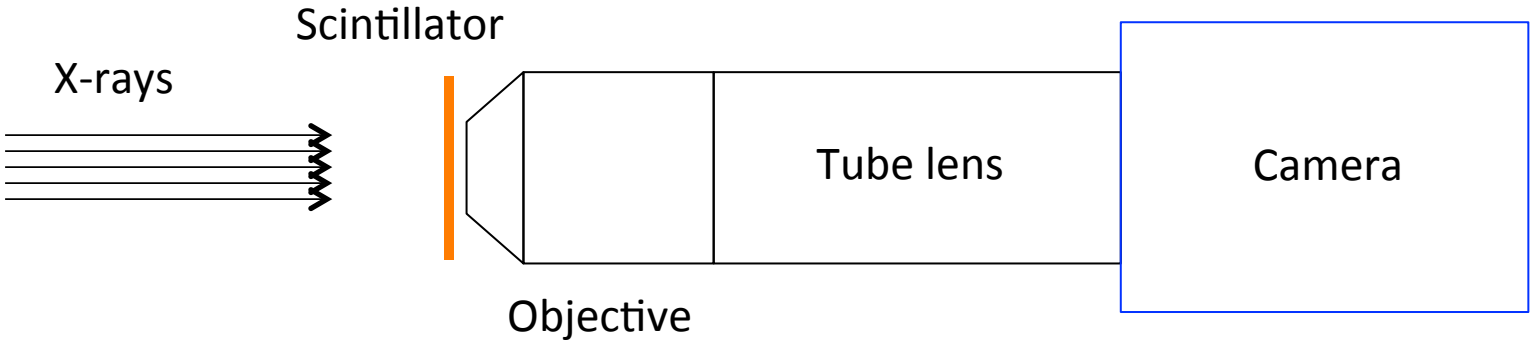

Scintillator screen converts x-rays to visible light
Visible light optics magnifies image onto sensor chip
~ 1 um overall resolution

Detection setups

Most common:

Add a mirror to move camera and optics away from X-ray incident direction.

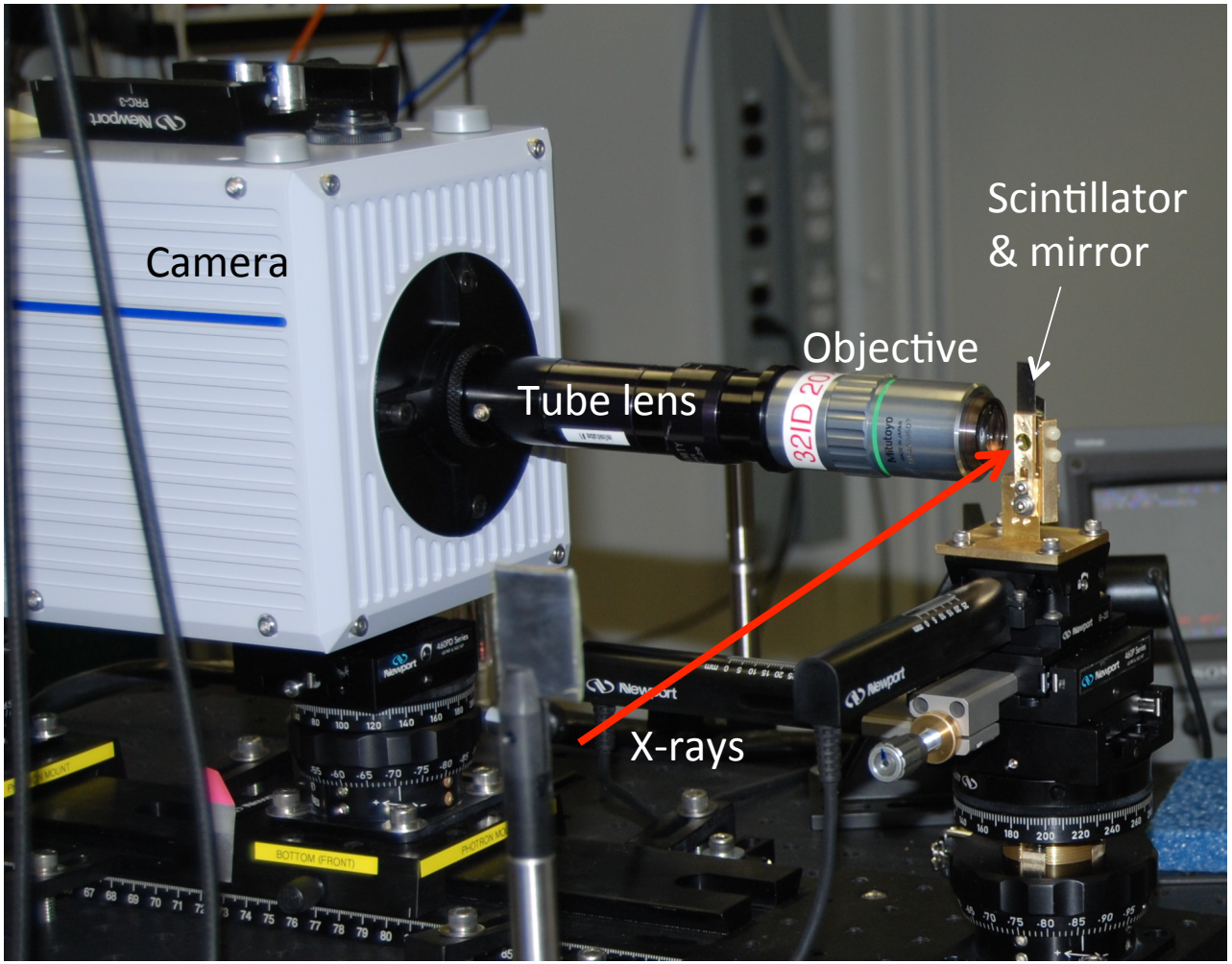

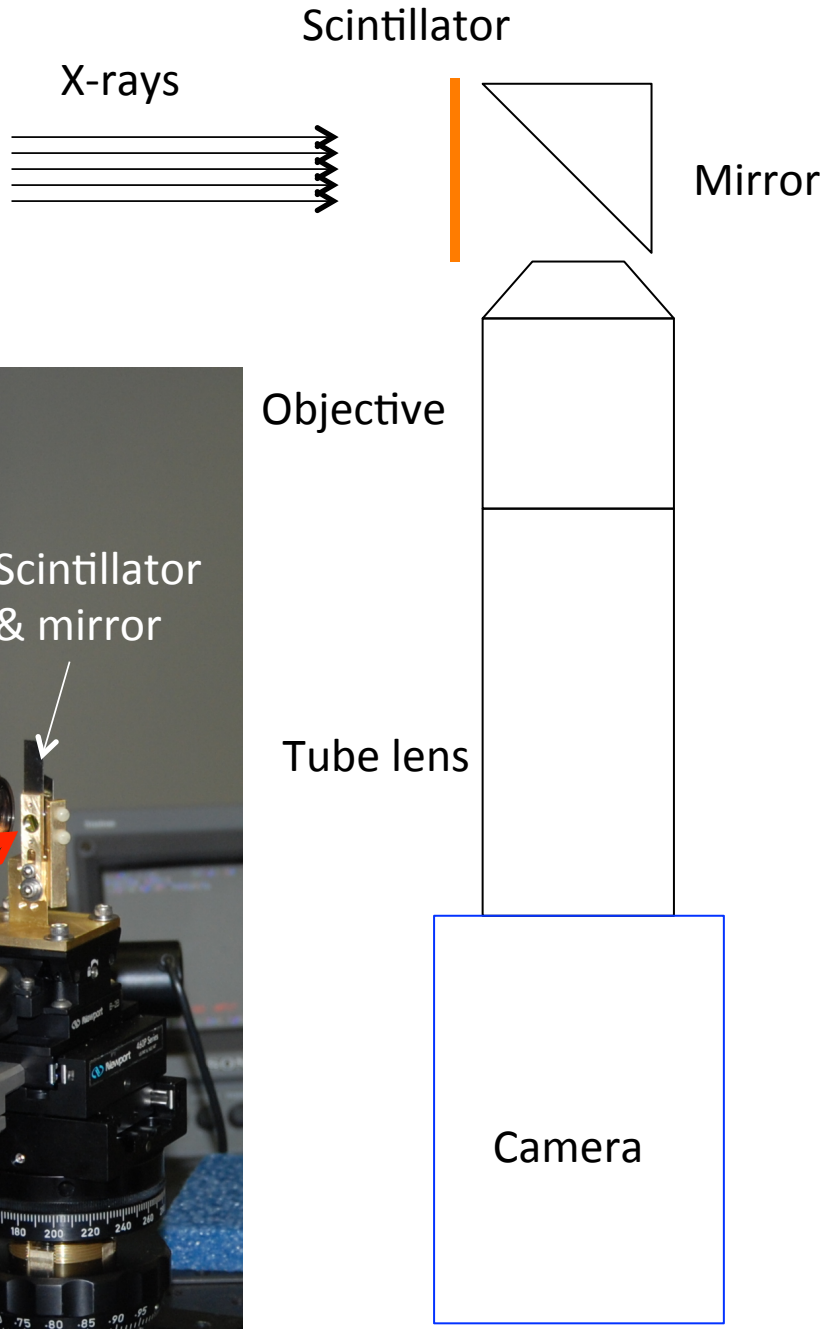

Spatial resolution

Source size – penumbral broadening
Camera pixel size
Detection
- scintillator thickness
- analyzer crystal – extinction length, Borrman fan etc
- numerical aperture of optics

Simplest and most common approach is to add all the contributions in quadruture

$$\text{Resulting resolution} = \sqrt{\sigma_{so}^2 + \sigma_p^2 + \sigma_{sc}^2 + \sigma_c^2 + \sigma_o^2}$$

Spatial resolution: Source penumbral blurring

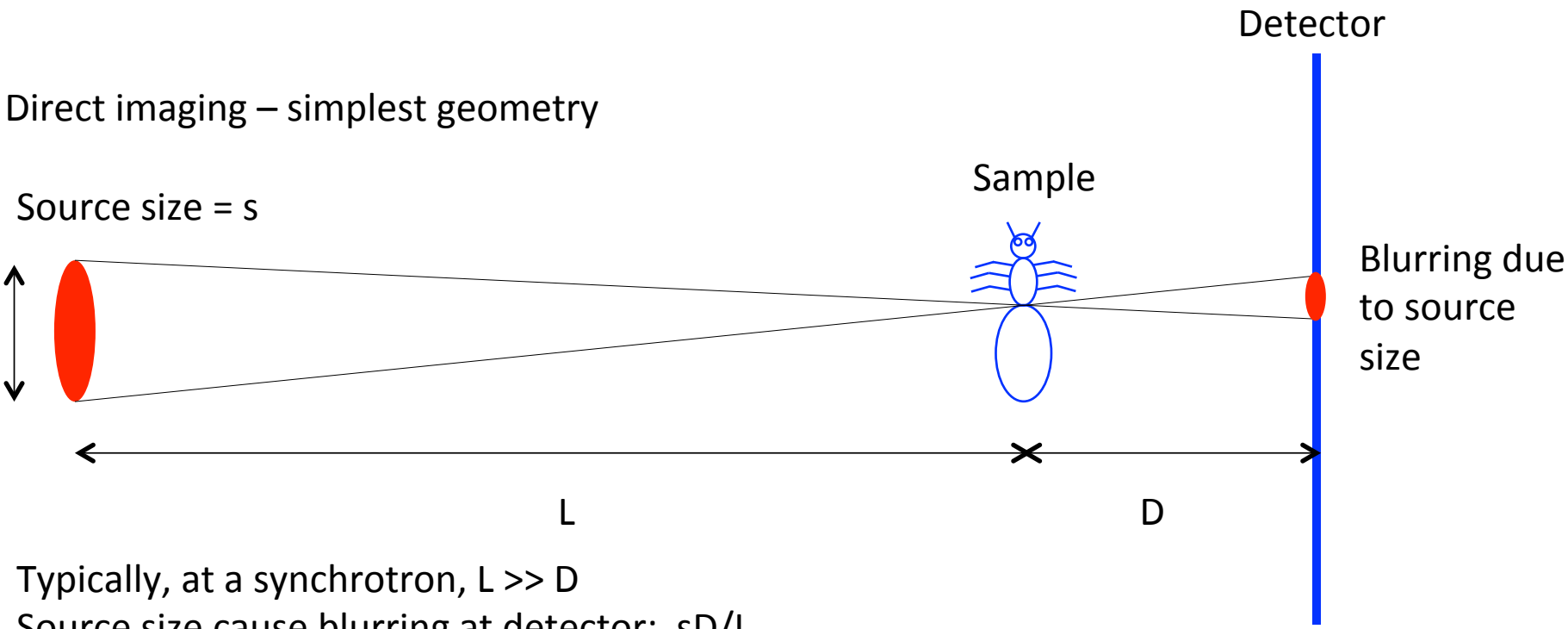

Typically, at a synchrotron, L >> D
Source size cause blurring at detector: sD/L

Example: APS 32ID L = 60 m. D is about 2 cm. Horizontal s = 275 um (rms)
So, blur = 275 um x 2 cm/6000 cm = 0.1 um (rms)
But if D = 1 m, blur = 275 um x 1/60 = 4.6 um (rms)
NSLSII, low/hi beta beta section, horizontal s = 28 or 99 um (rms)
At D = 1 m, blur Is much smaller!

Magnification = (D+L)/L – usually negligible at synchrotron
Imperfections in beamline optics can effectively make L appear smaller

Spatial resolution: Scintillators

X-ray imaging with scintillators and lens coupling. Identical visible-light images are created by the X-ray beam in different planes of the scintillator. An image in plane z0 is focused onto the CCD. An image in plane z0 + δz is out of focus at the CCD.

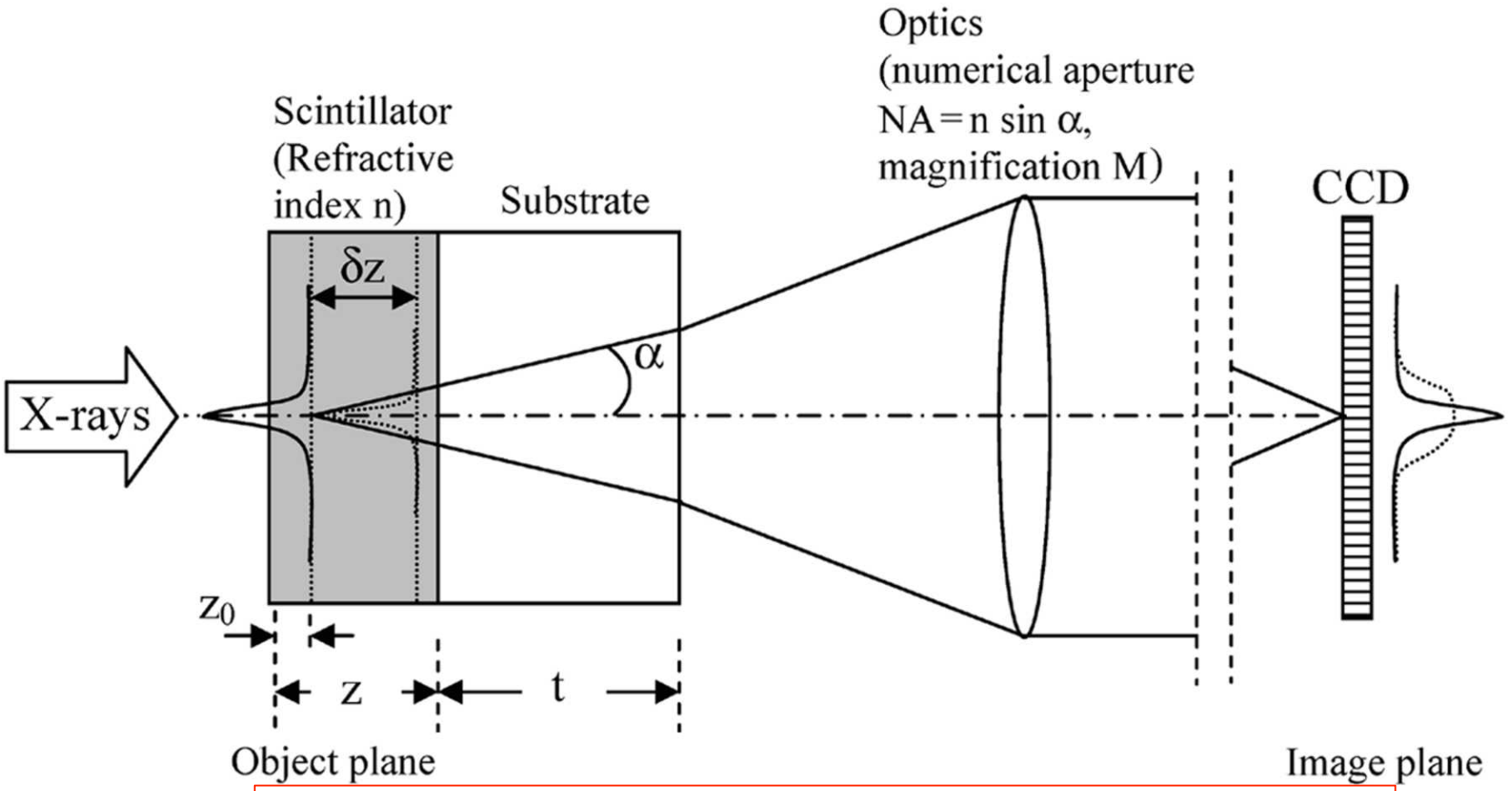

Challenge: Thin scintillator for good focus; but thick scintillator for better x-ray stopping power (efficiency)

JOURNAL OF SYNCHROTRON RADIATION

Martin & Koch

Volume 13 | **Part 2** | March 2006 | Pages 180–194 | 10.1107/S0909049506000550

Spatial resolution: Cameras

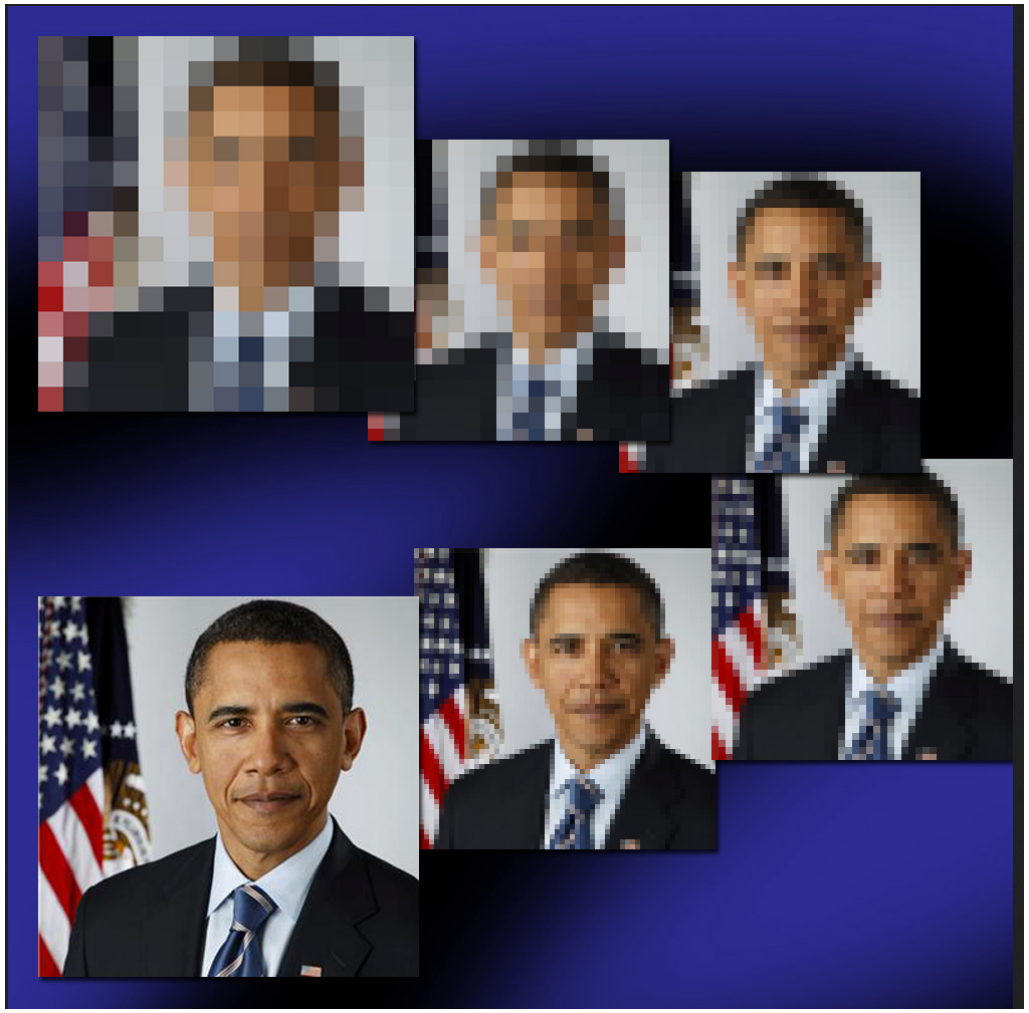

Detector pixel sizes usually 6-100 um

For um or below resolution, magnification upstream of camera is needed.

solarweek.org

Spatial resolution: Crystal effects

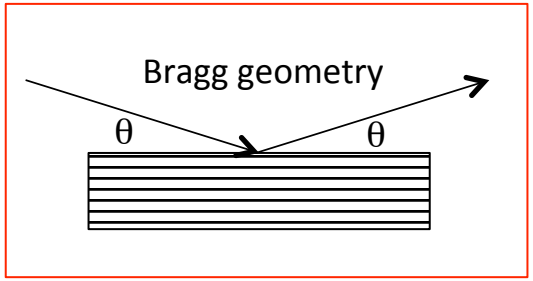

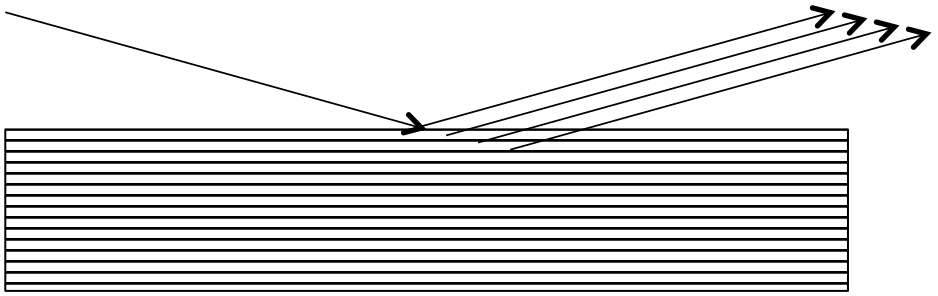

X-rays penetrate crystal (extinction length). Reflected beam is blurred.

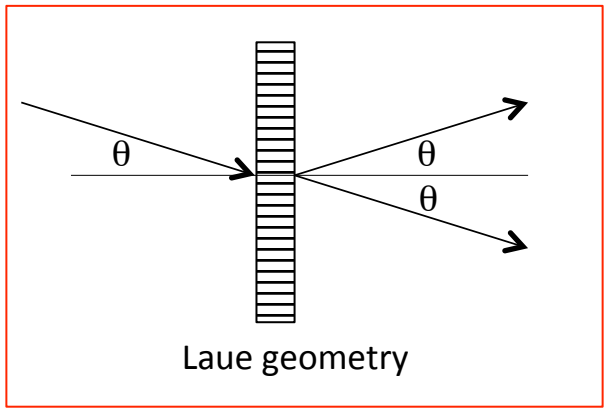

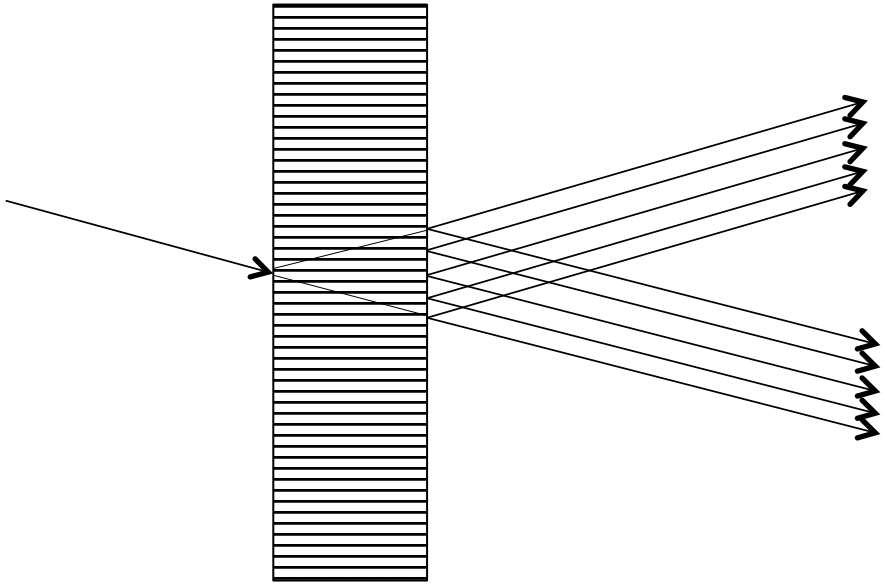

Energy flows within the Borrman fan inside crystal
Reflected and transmitted beams are blurred.

Practical issues: Choice of scintillator

Table 2. A survey of characteristics of selected single crystal scintillators [5, 13, 128, 136, 143].

Crystal	Density ($g\ cm^{-3}$)	Light yield (photon MeV^{-1})	Dominant scintillation decay time (ns)	Emission maximum (nm)	$\Delta E/E$ at 662 keV (%)
CsI:Tl	4.51	66 000	800	550	6.6
NaI:Tl	3.67	41 000	230	410	5.6
$LaBr_3$:Ce	5.3	61 000	35	358	2.9
K_2LaI_5:Ce	4.4	55 000	24	420	4.5
BaF_2 (only cross luminescence)	4.88	1 500	0.6–0.8	180–220	7.7
$Bi_4Ge_3O_{12}$	7.1	8 600	300	480	9.0
$PbWO_4$	8.28	300	2–3	410	30–40
$CdWO_4$	7.9	20 000	5 000	495	6.8
$YAlO_3$:Ce	5.6	21 000	20–30	360	4.6
$LuAlO_3$:Ce	8.34	12 000	18	365	~15
$Y_3Al_5O_{12}$:Ce	4.56	24 000	90–120	550	7.3
$Lu_3Al_5O_{12}$:Ce	6.67	12 500	55	530	11
Gd_2SiO_5:Ce	6.7	8 000	60	420	7.8
Lu_2SiO_5:Ce	7.4	26 000	30	390	7.9

Desire High High Low Matched to camera

Other issues: Availability, environment

Martin Nikl, Meas. Sci. Tech. 2006

pco.edge 4.2

scientific CMOS camera

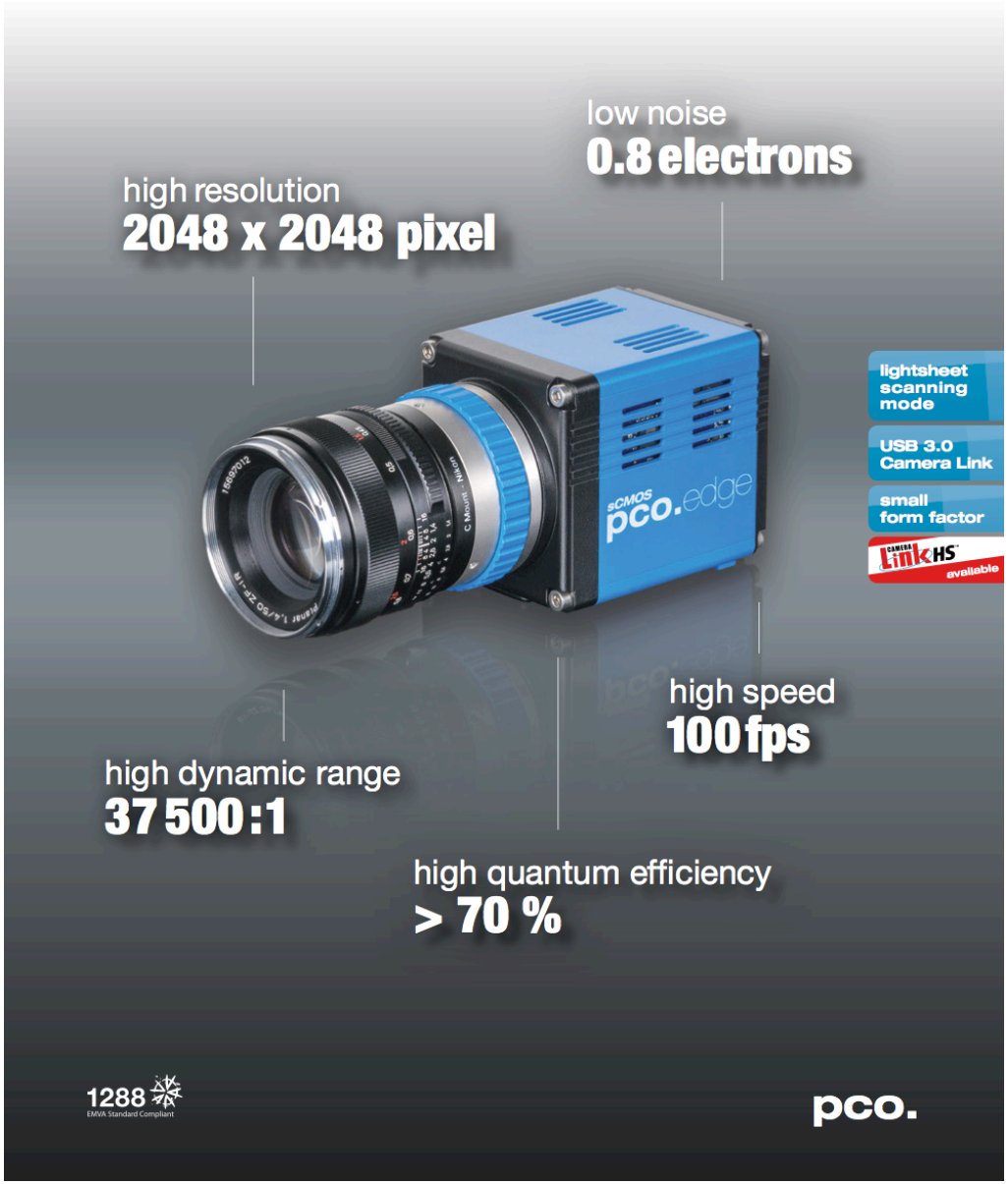

technical data Camera Link

image sensor

type of sensor	scientific CMOS (sCMOS)
image sensor	CIS2020
resolution (h x v)	2048 x 2048 active pixel
pixel size (h x v)	6.5 µm x 6.5 µm
sensor format / diagonal	13.3 mm x 13.3 mm / 18.8 mm
shutter modes	rolling shutter (RS) with free selectable readout modes, lightsheet scanning mode[1]
MTF	76.9 lp/mm (theoretical)
fullwell capacity (typ.)	30 000 e⁻
readout noise[2]	0.9med /1.4rms e- @ slow scan 1.0med /1.5rms e- @ fast scan
dynamic range (typ.)	33 000 : 1 (90.4 dB) slow scan
quantum efficiency	> 70 % @ peak
spectral range	370 nm .. 1100 nm
dark current (typ.)	< 0.5 e⁻/pixel/s @ 5 °C
DSNU	< 1.0 e⁻ rms
PRNU	< 0.5 %
anti blooming factor	> 10 000

frame rate table[3]

typical examples	fast scan	slow scan
2048 x 2048	100 fps	35 fps
2048 x 1024	200 fps	70 fps
2048 x 512	400 fps	140 fps
2048 x 256	800 fps	281 fps
2048 x 128	1600 fps	562 fps
1920 x 1080	189 fps	66 fps
1600 x 1200	170 fps	60 fps
1280 x 1024	200 fps	70 fps
640 x 480	426 fps	150 fps
320 x 240	853 fps	300 fps

frame rate table extended readout mode[4]

typical examples	fast scan	slow scan
2048 + 12 x 2048	100 fps	35 fps
2048 + 12 x 1024	200 fps	70 fps

[1] Selectable via SDK (software development kit).
[2] The readout noise values are given as median (med) and root mean square (rms) values, due to the different noise models, which can be used for evaluation. All values are raw data without any filtering.
[3] Max. fps with centered ROI.
[4] Extended readout mode with 12 columns of black reference pixel.
[5] The high dynamic signal is simultaneously converted at high and low gain by two 11 bit A/D converters and the two 11 bit values are sophistically merged into one 16 bit value.

camera

frame rate	100 fps @ 2048 x 2048 pixel, fast scan
exposure / shutter time	100 µs .. 10 s
dynamic range A/D[5]	16 bit
A/D conversion factor	0.46 e⁻/count
pixel scan rate	272.3 MHz fast scan 95.3 MHz slow scan
pixel data rate	544.6 Mpixel/s 190.7 Mpixel/s
binning horizontal	x1, x2, x4
binning vertical	x1, x2, x4
region of interest (ROI)	horizontal: steps of 1 pixel vertical: steps of 1 pixel
non linearity	< 1 %
cooling method	+ 5 °C stabilized selectable: peltier with forced air (fan) or water cooling (both up to 27°C ambient)
trigger input signals	frame trigger, sequence trigger, programmable input (SMA connectors)
trigger output signals	exposure, busy, line, programmable output (SMA connectors)
data interface	Camera Link Full (10 taps, 85 MHz)
time stamp	in image (1 µs resolution)

general

power supply	12 .. 24 VDC (+/- 10 %)
power consumption	20 W max. (typ. 10 W @ 20 °C)
weight	700 g
operating temperature	+ 10 °C .. + 40 °C
operating humidity range	10 % .. 80 % (non-condensing)
storage temperature range	- 10 °C .. + 60 °C
optical interface	F-mount & C-mount
CE / FCC certified	yes

pco.

technical data

quantum efficiency

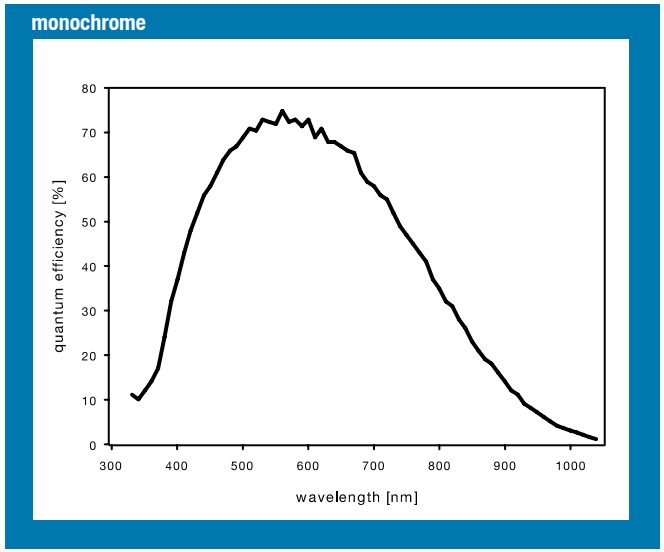

camera views

USB 3.0

Camera Link

Want to match peak camera spectral response to scintillator peak spectral output

Detective Quantum Efficiency (DQE)

$$DQE \equiv \frac{SNR_{out}^2}{SNR_{in}^2}$$

SNR = signal to noise ratio

For a transparent scintilllator/lens/camera system:

$$DQE = \eta_{abs}\left[1 + \frac{1 + 1/\eta_{v/e}}{\eta_{col}(E_x / E_v)\eta_{x/v}}\right]^{-1}$$

η_{abs} = X-ray absorption efficiency of scintillator screen (depends on x-ray wavelength)

$\eta_{v/e}$ = Camera quantum efficiency (light to electrons; depends on wavelength of light)

$\eta_{x/v}$ = Conversion efficiency from x-ray to visible light of scintillator screen

$\eta_{col} = (NA/n)^2/4$ *NA* = NA of light objective; *n* = refractive index of scintillator

E_x = X-ray energy

E_v = Visible light energy

Koch et al, JOSA A15, 1998
Thierry & Koch, JSR 13, 2006.

Generally, scintillator/lens systems in the 1-10 μm resolution range have DQE between 1-10%.

DQE example

A typical image SNR requirement is 'Rose criteria': SNR = 5

In Poisson statistics, noise = sqrt(N); so, SNR = N/sqrt(N) = sqrt(N) where N is counts

So, you want SNR(out) = 5. Neglect sample absorption for this exercise.

SNR(in) = sqrt(SNR^2(out)/DQE)

If DQE = 1% , this means that you need a SNR(in) of sqrt(5^2/0.01) = 50

Assuming Poisson statistics, you need 50^2 = 2500 x-rays per pixel to achieve SNR(out) = 5.

Assume each demagnified pixel is 1 um x 1 um and the field of view is 1 mm x 1 mm, then the x-ray photon density you need is at least 2500 photons/pixel x 10^6 pixels/mm^2 = 2.5 x 10^9 ph/mm^2 per image.

Conservative ball-park estimate: need 10^{10} ph/mm^2 for um-resolution imaging with scintillator/lens coupling setup per image

Outline

Part 1: Key concepts for imaging
Part 2: Practical issues and instruments
Part 3: Imaging techniques and examples
Part 4: Current frontiers

Absorption contrast

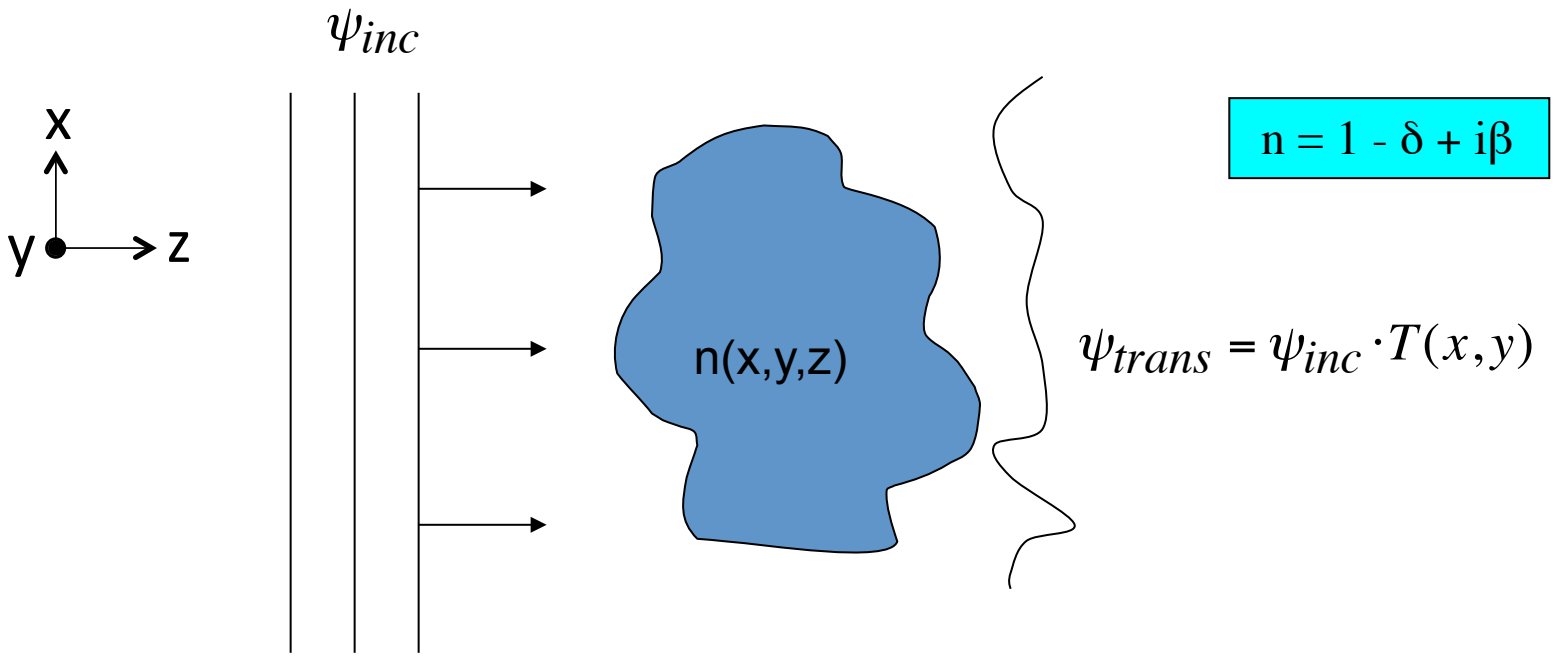

$$T(x,y) = e^{ik\int n(x,y,z)dz} = e^{-k\int \beta(x,y,z)dz}\, e^{-ik\int \delta(x,y,z)dz} = A(x,y)\, e^{i\phi(x,y)}$$

If you place a detector *immediately* after the sample, you would measure:

$$I(x,y) = \left|\psi_{trans}\right|^2 = \left|I_0\right|\left|T(x,y)\right|^2 = I_0 \cdot \left|A\right|^2$$

Information about β only

Most common form of absorption contrast imaging:

http://40.media.tumblr.com/
tumblr_lqd2n3KRWE1qzcf71o1_1280.jpg

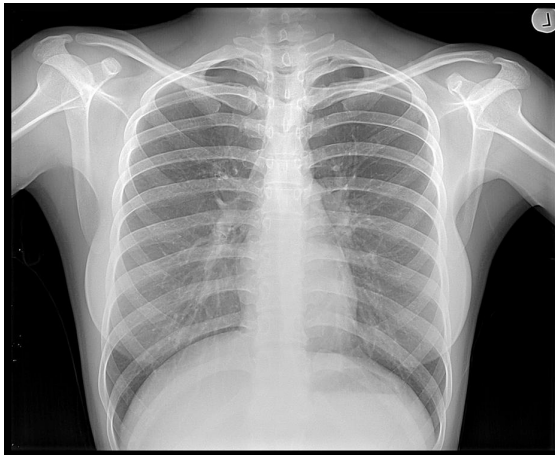

Detector as close to sample as possible
Minimize blurring due to source
Minimize any propagation effects

In absorption, you measure:

$$\beta \propto \lambda^4$$

$$\mu = \frac{4\pi\beta}{\lambda} \quad \propto \quad \lambda^3$$

$$I(x,y) = \left|\psi_{trans}\right|^2 = \left|I_0\right|\left|T(x,y)\right|^2 = I_0 \cdot \left|A\right|^2 = I_0\, e^{-\int \mu(x,y,z)dz}$$

$$I(x,y) = I_0\, e^{-\int \mu(x,y,z)dz}$$

$$-\ln\left[\frac{I(x,y)}{I_0(x,y)}\right] = \int \mu(x,y,z)\,dz$$

Negative logarithm of the intensity ratio is a line integral of a local function of the sample.
It is suitable for tomography: Can obtain 3D information by recording different projections.

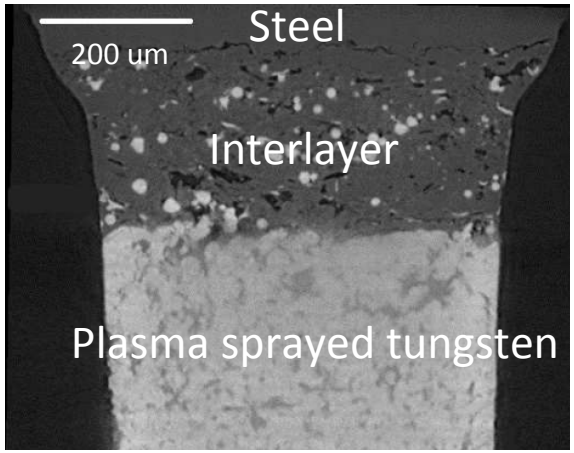

Plasma sprayed tungsten on steel substrate

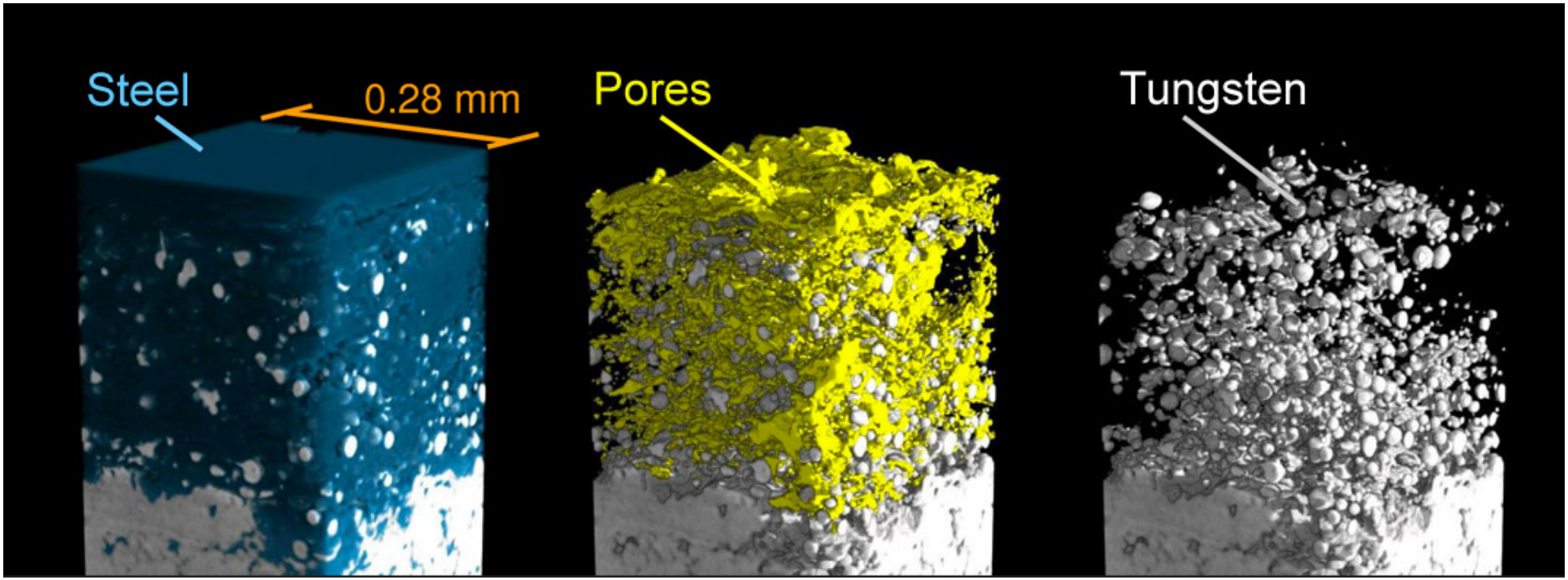

Zivelonghi et al, ESRF

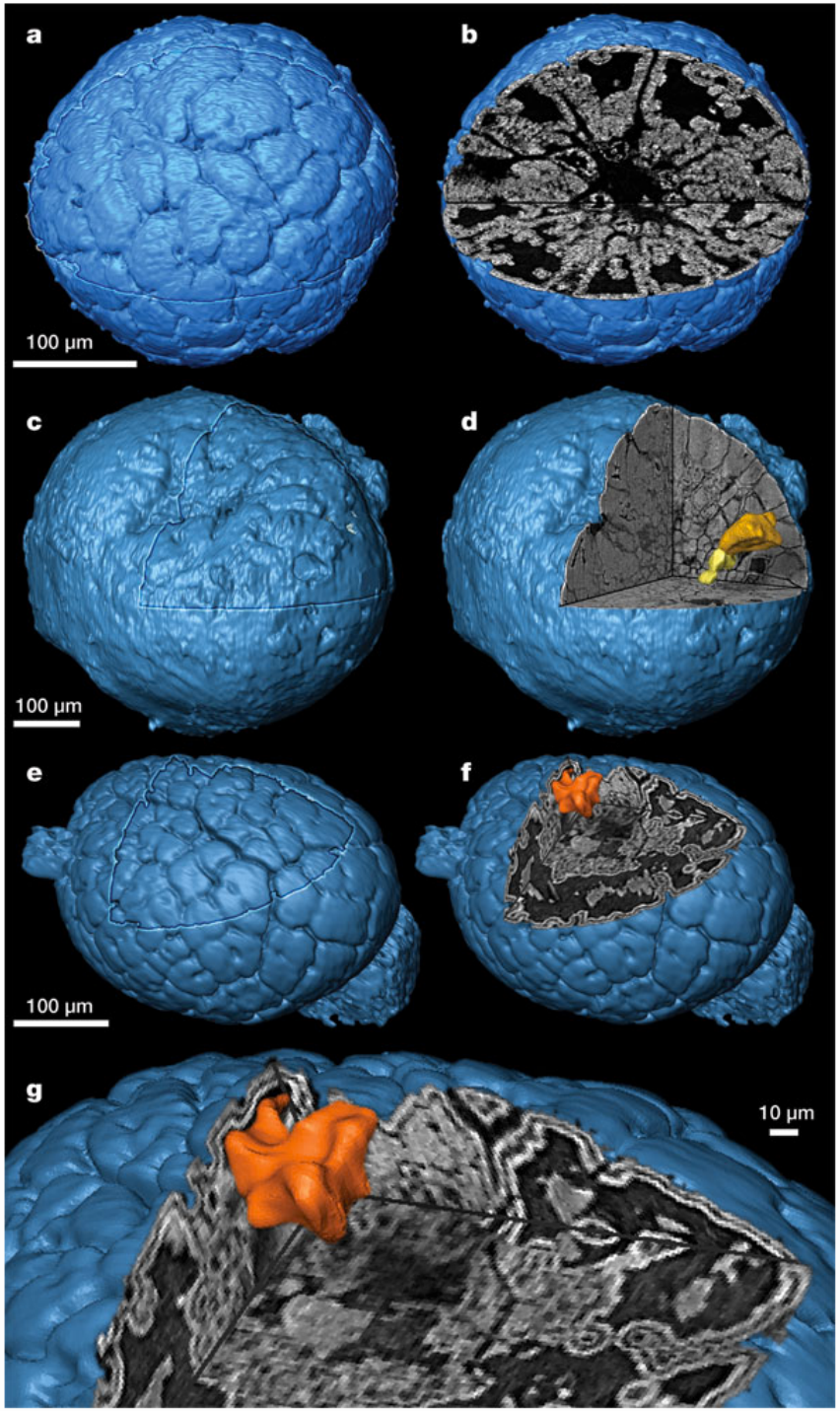

Divisions between adjacent blastomeres variably preserved on the surface and within. a, b, Museum of Earth Science, Institute of Geology, Chinese Academy of Geological Sciences (MESIG) 20061. Divisions between some, but not all, blastomeres are preserved internally. c, d, MESIG 20062. Divisions between all, or nearly all, blastomeres are preserved to their full extent; the orange and yellow structures are renderings of the morphology of a column of blastomeres. e–g, Geological Museum of Peking University (GMPKU) 2204. Divisions between blastomeres are generally not preserved, and instead the core of the embryo is characterized by the centrifugal addition of diagenetic crust layers (easily distinguished from edge artefacts through their absence from some of the objects seen in the slices); orange structure represents a rendering of one of the cavities within the diagenetic infilling.

Donoghue et al, Nature 442 2006.

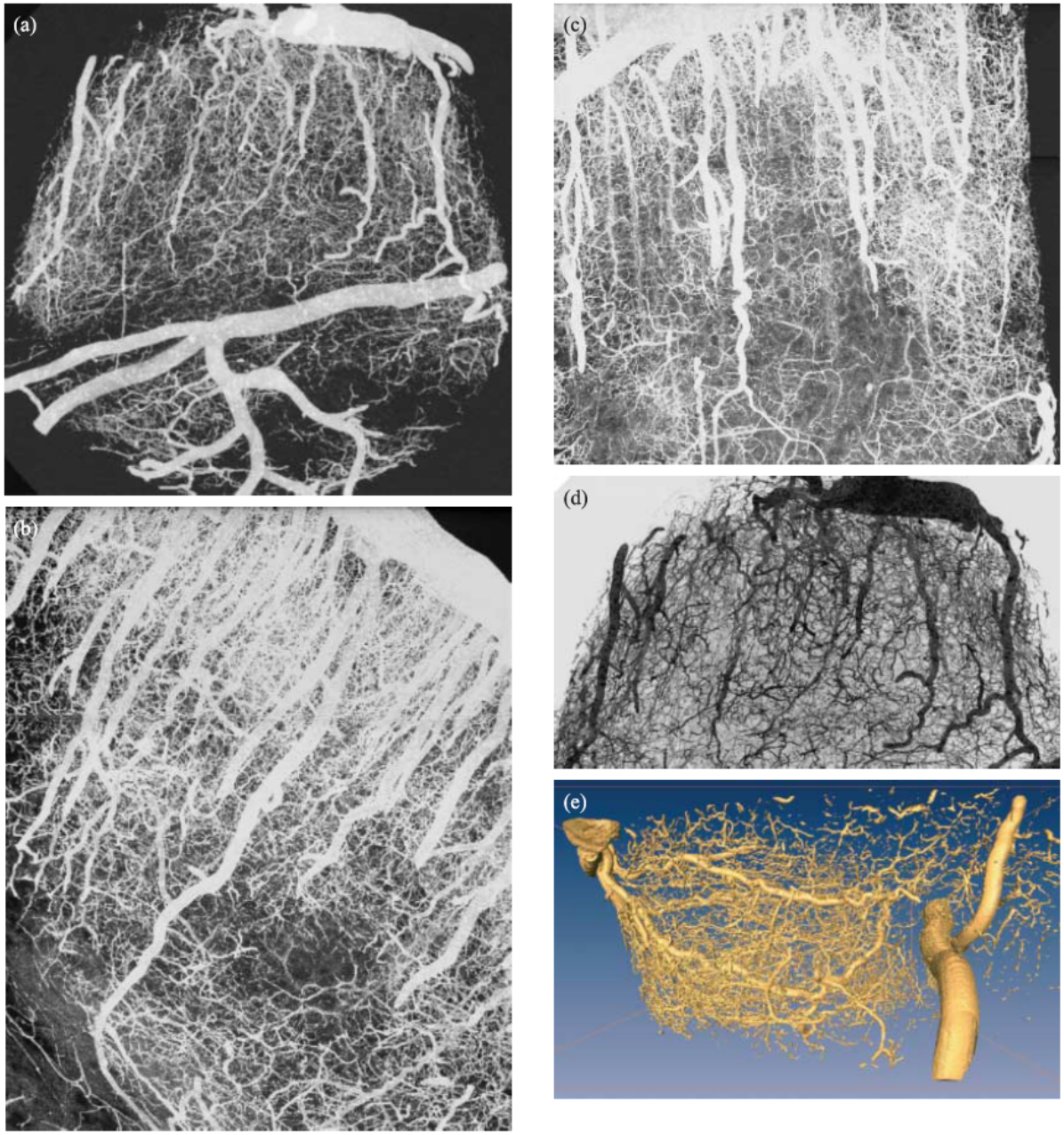

Fig. 5. Volume renderings of a sample injected with barium (600 mg mL^{-1}), obtained at 20 keV in absorption mode with a voxel size equal to 1.4 µm. The images correspond to different samples extracted from different cortical regions of the same rat. Maximum intensity projections have been performed for volumes with a size equal to $\Delta x = 1.5$ mm, $\Delta y = 1.5$ mm, $\Delta z = 1$ mm: (a) Projection in the x–y plane of a sample extracted from the fronto-central region; (b) projection in the y–z plane of a sample extracted from the frontal cortex; (c) x–z projection of the same sample as in (b); (d) close-up view on the x–y plane projection of (a), using an in-depth coding in grey levels; (e) 3D iso-surface view of sample (a) in the z–y plane.

Plouraboue et al, J. Microscopy 215, 2004

Take advantage of energy tunability

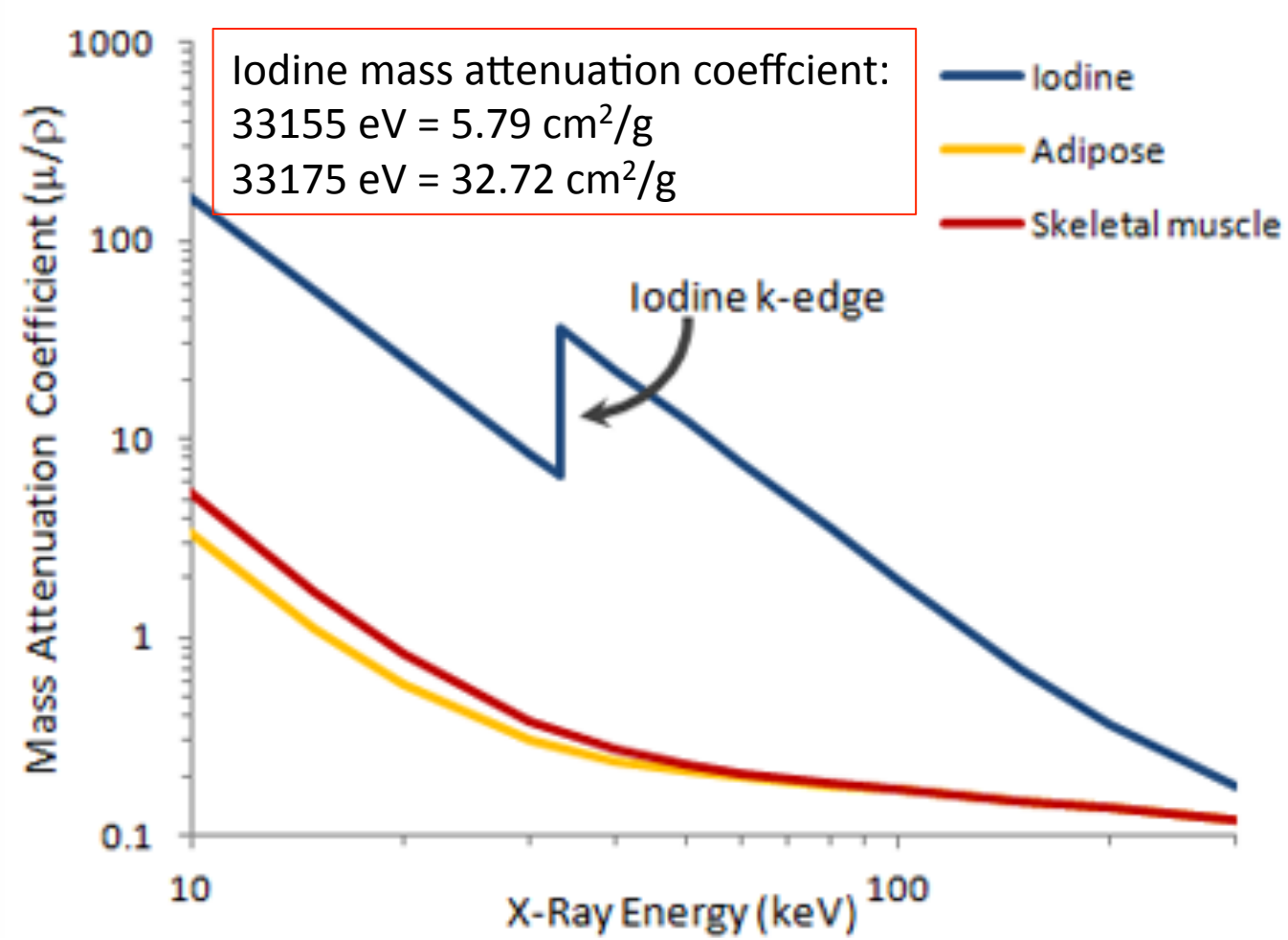

Take images above and below absorption edge. Divide (or subtract) images. Result will isolate iodine.

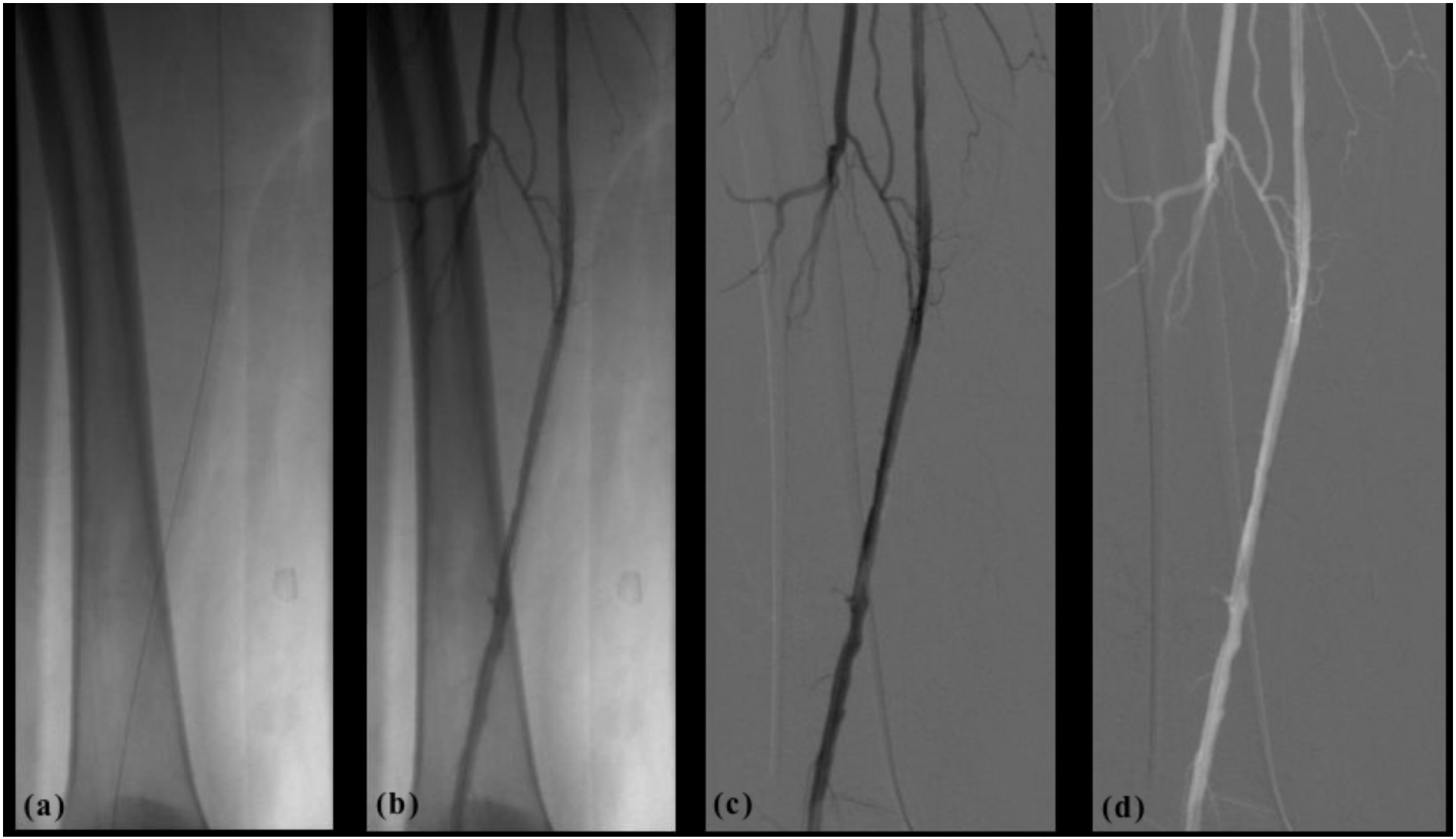

Before iodine After iodine Before - After After - Before

Angiography

wikibooks.org

Phase contrast imaging

$$T(x,y)=e^{ik\int n(x,y,z)dz}=e^{-k\int \beta(x,y,z)dz}e^{-ik\int \delta(x,y,z)dz}=A(x,y)e^{i\phi(x,y)}$$

$A(x,y)$ *is the wave amplitude*

$\phi(x,y)$ *is the accumulated phase difference*

How to measure $\phi(x,y)$ or how to be sensitive to $\phi(x,y)$

‘Conventional’ interferometry

$$\psi = A e^{i\phi}$$

Wave function we want to measure

$$\psi_{ref} = A_{ref} e^{i\phi_{ref}}$$

Reference wave function

$$\left|\psi + \psi_{ref}\right|^2 = \left[A e^{i\phi} + A_{ref} e^{i\phi_{ref}}\right]\left[A e^{-i\phi} + A_{ref} e^{-i\phi_{ref}}\right]$$

$$\left|\psi + \psi_{ref}\right|^2 = A^2 + A_{ref}^2 + 2AA_{ref}\cos(\phi_{ref} - \phi)$$

Measured intensity

Need a reference wave: reference wave must be coherent

Need to be able to ‘add’ or ‘overlay’ ψ and ψ_{ref} coherently

For quantitative phase, need more work to yield true ϕ

Need to ‘unwrap’ the phase (modulo 2π) to yield true ϕ

Phase imaging with Laue-Laue-Laue interferometer

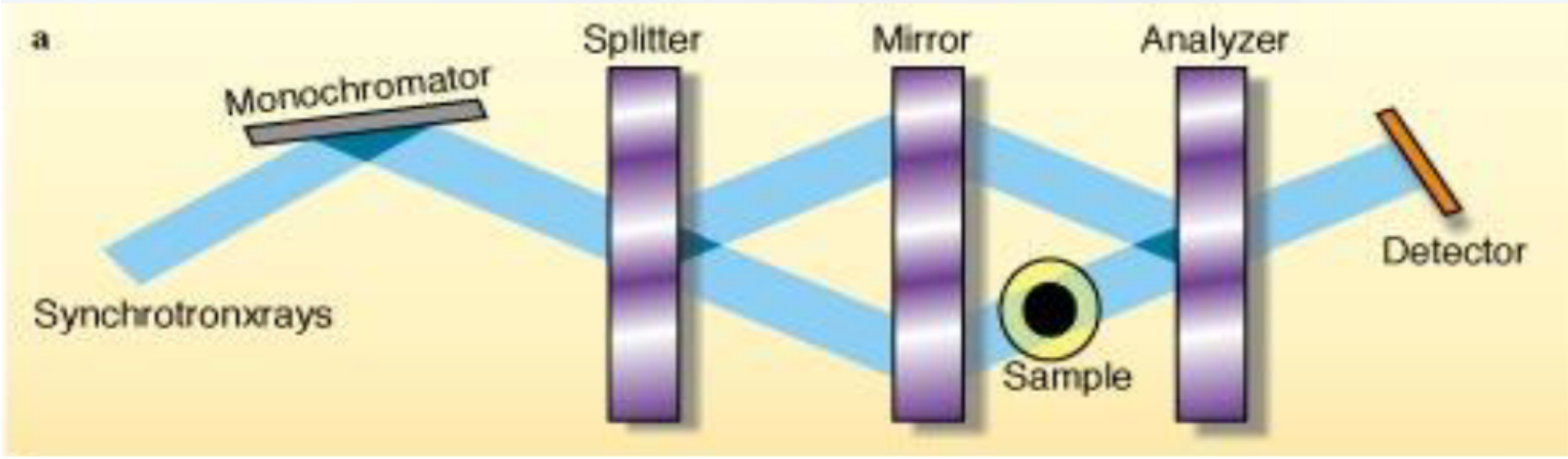

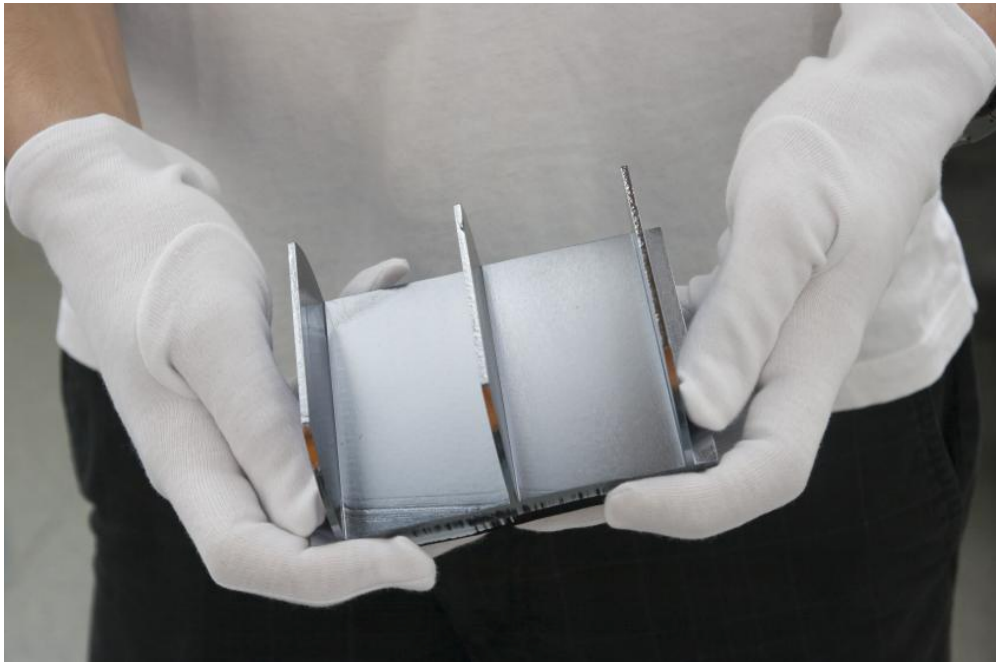

Neutron interferometer, www.physics.org

The two beams overlap at the analyzer.

Moire pattern formed with angstrom level spacing.

How the Moire pattern overlays on the atomic planes in the analyzer determines the transmitted beam.

A schematic view of the positioning system for the skew-symmetric two-crystal X-ray interferometer. The S2 and tilt tables control the θ and ϕ rotation of the crystal blocks relative to each other. The ...

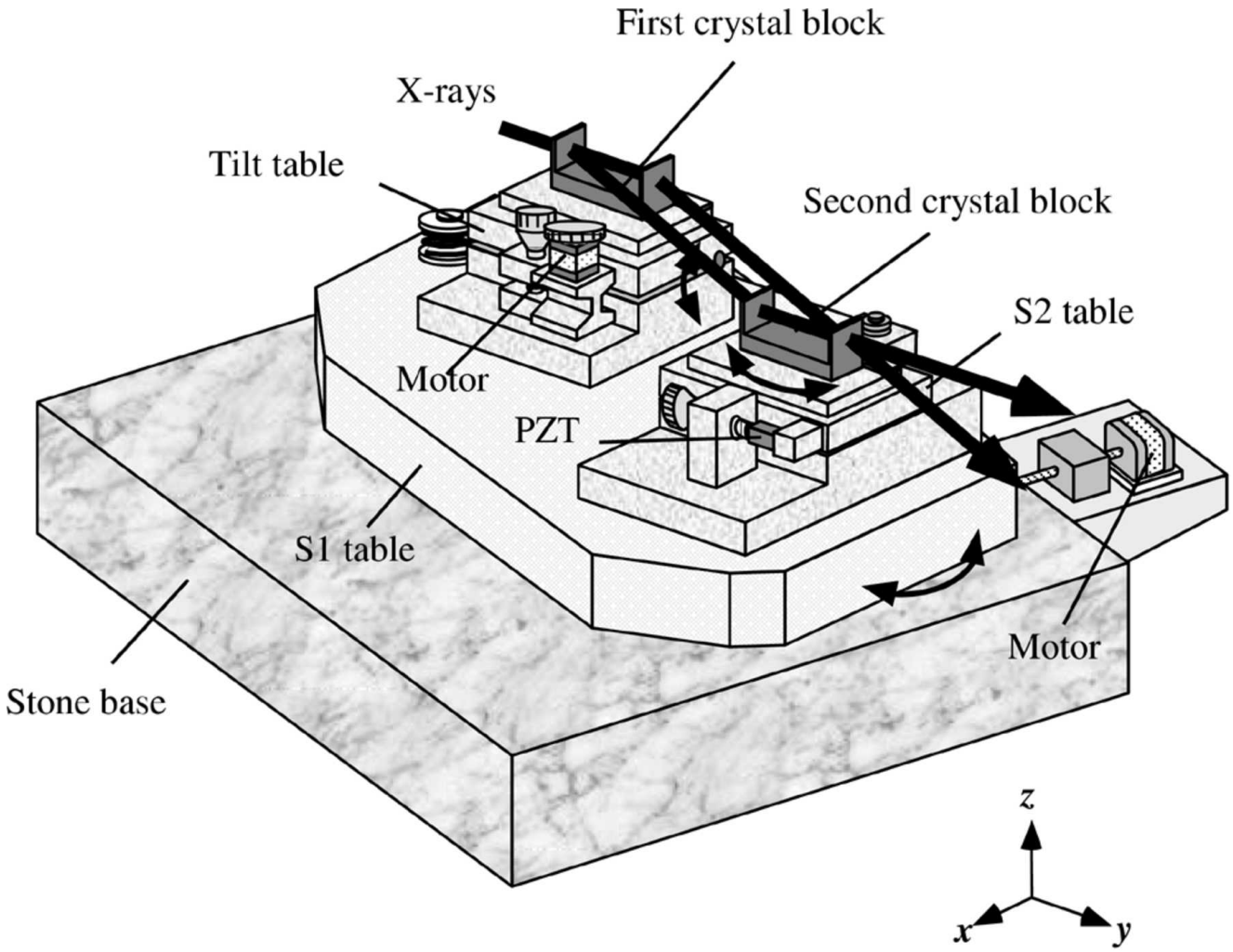

JOURNAL OF SYNCHROTRON RADIATION

Yoneyama *et al.*

Volume 9 | **Part 5** | September 2002 | Pages 277–281 | 10.1107/S090904950201350X

Example of LLL imaging

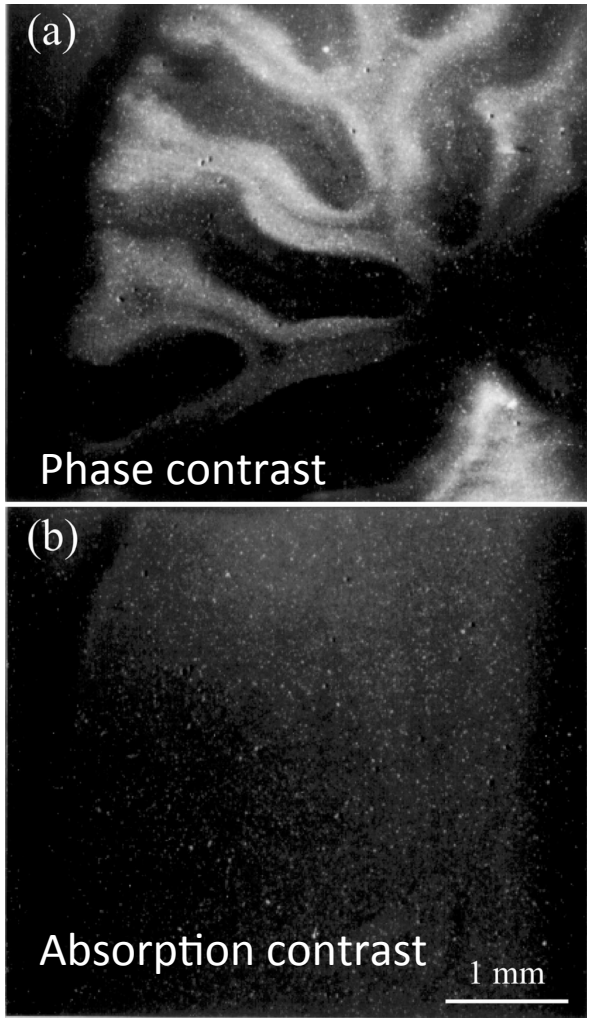

Slice of rat cerebellum

Momose et al, JSR 9, 136-142, 2002.

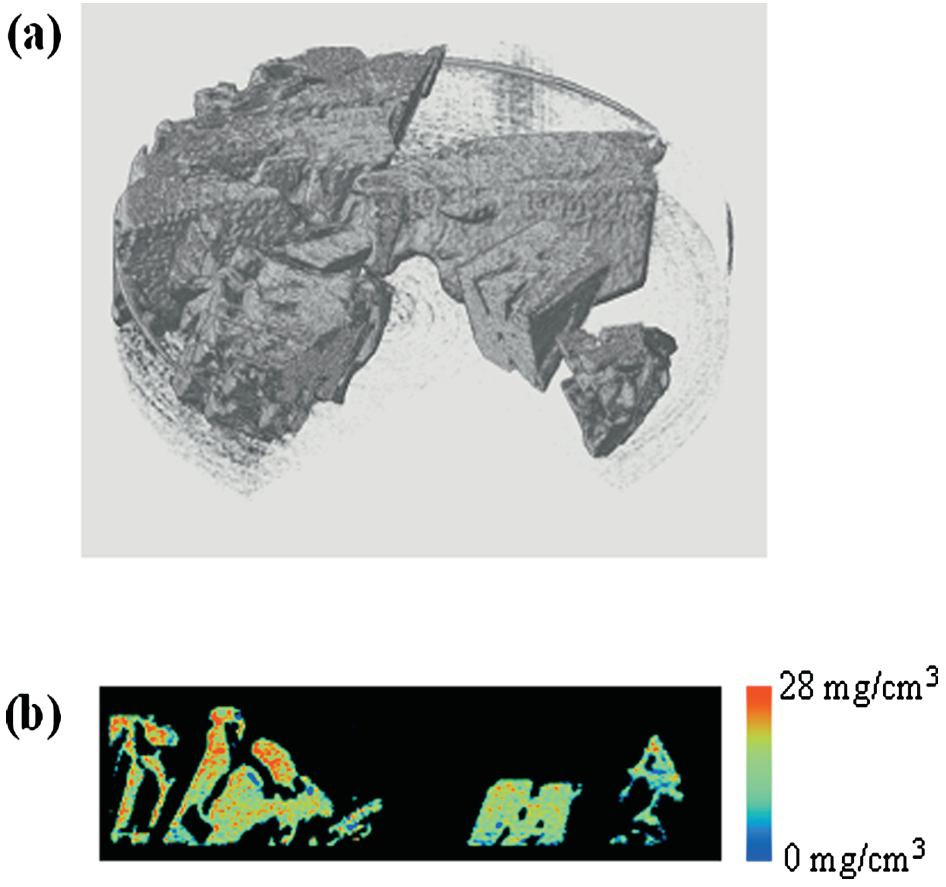

Tetrahydrofuran hydrate crystal

Takeya et al, APL 90, 081920 (2007).

Advantages of interferometry:

- Measures phase $\phi(x,y)$. Only technique that directly measures phase.
- Quantification of the phase possible.
- Sensitivity down to 1-2 mg/cm^3.
- X-ray source does not need to be coherent – crystal does the work of making two coherent beams.

Disadvantages of interferometry:

- Extremely challenging to maintain stability of Splitter, Mirror and Analyzer. These need to be stable at the level of the crystal lattice spacing. Usually made as a singular piece (Splitter, Mirror and Analyzer) from an ingot. Extremely sensitive to temperature – need mK stability over interferometer.
- Limited space for sample and stability requirement limits sample environment cells.
- Spatial resolution limited by Laue analyzer.

Analyzer-based phase-contrast imaging: crystals

Detect the beam deflection angle due to the phase gradient

Known by a variety of names: diffraction enhanced imaging (DEI), refraction contrast imaging, Schlieren imaging, phase-dispersive imaging.

Requires an 'analyzer crystal' that is sensitive to the small beam deflection angles

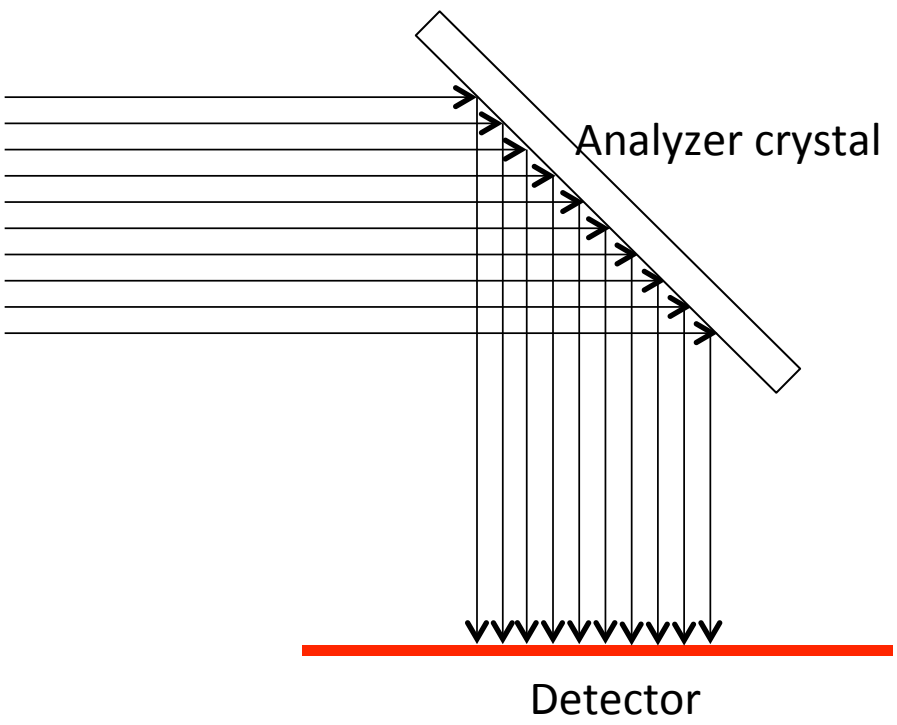

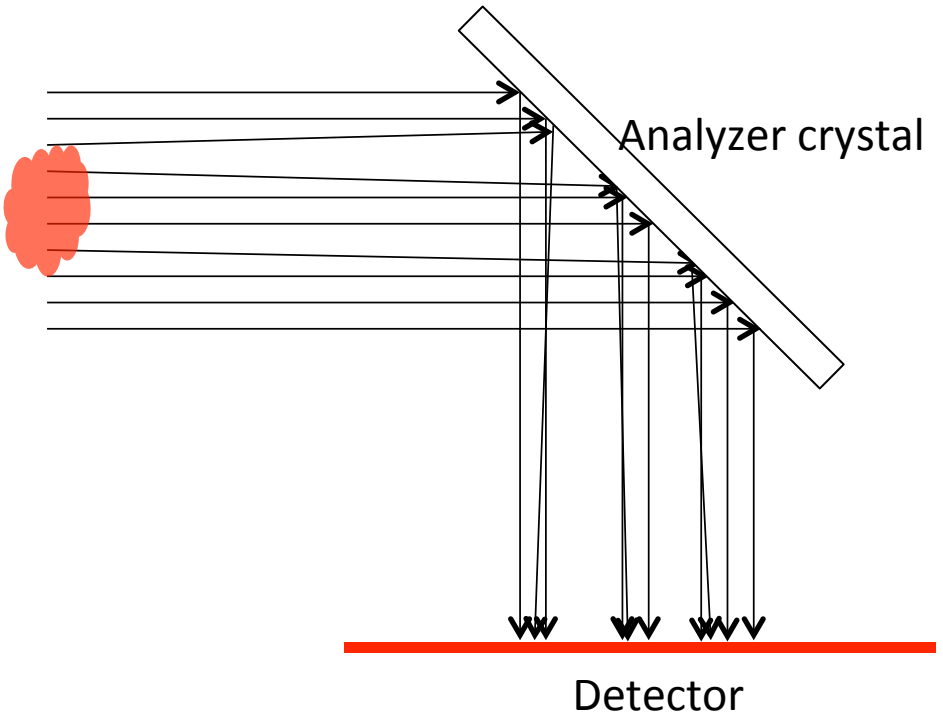

This technique is sensitive to $\nabla\phi(x,y)$

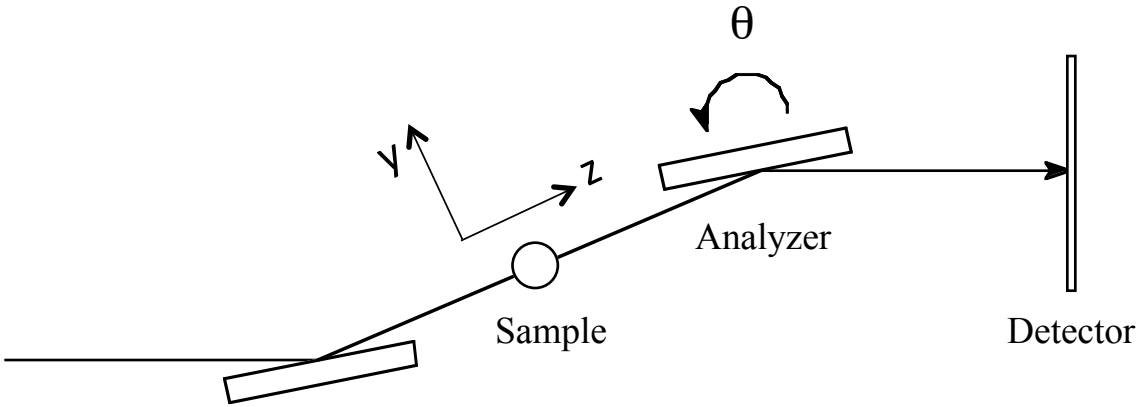

$$I_{abs} = \frac{I_L S_H + I_H S_L}{R_L S_H + R_H S_L}$$

$$I_{refr} = \frac{I_H R_L - I_L R_H}{I_L S_H + I_H S_L}$$

Rocking curve width: Convolution of two Darwin widths

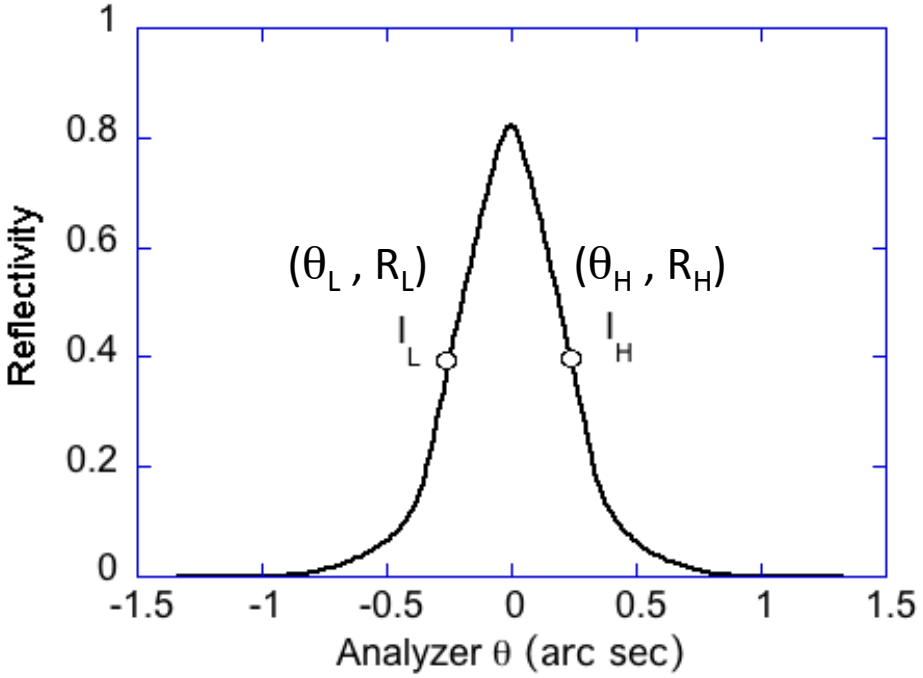

I_L = Image taken at θ_L
I_R = Image taken at θ_H

R_L = Reflectivity at θ_L
R_H = Reflectivity at θ_H

S_L = |Slope at θ_L|
S_H = |Slope at θ_H|

$$I_{refr} = \int \frac{\partial \delta(x,y,z)}{\partial y}\, dz$$

Refraction contrast in Nylon fiber

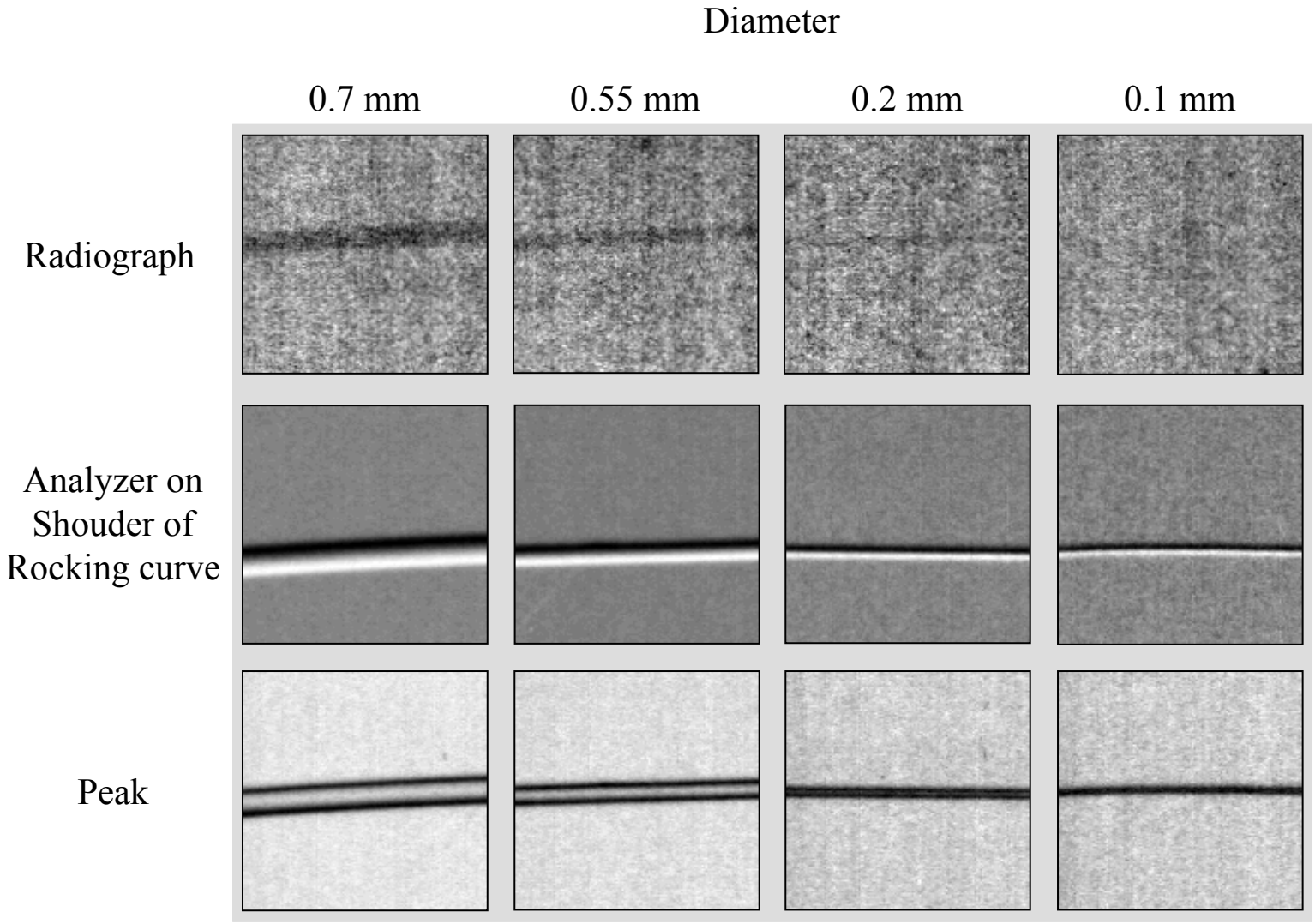

Nylon fiber simulates density variation in soft tissue

From Zhong Zhong, BNL

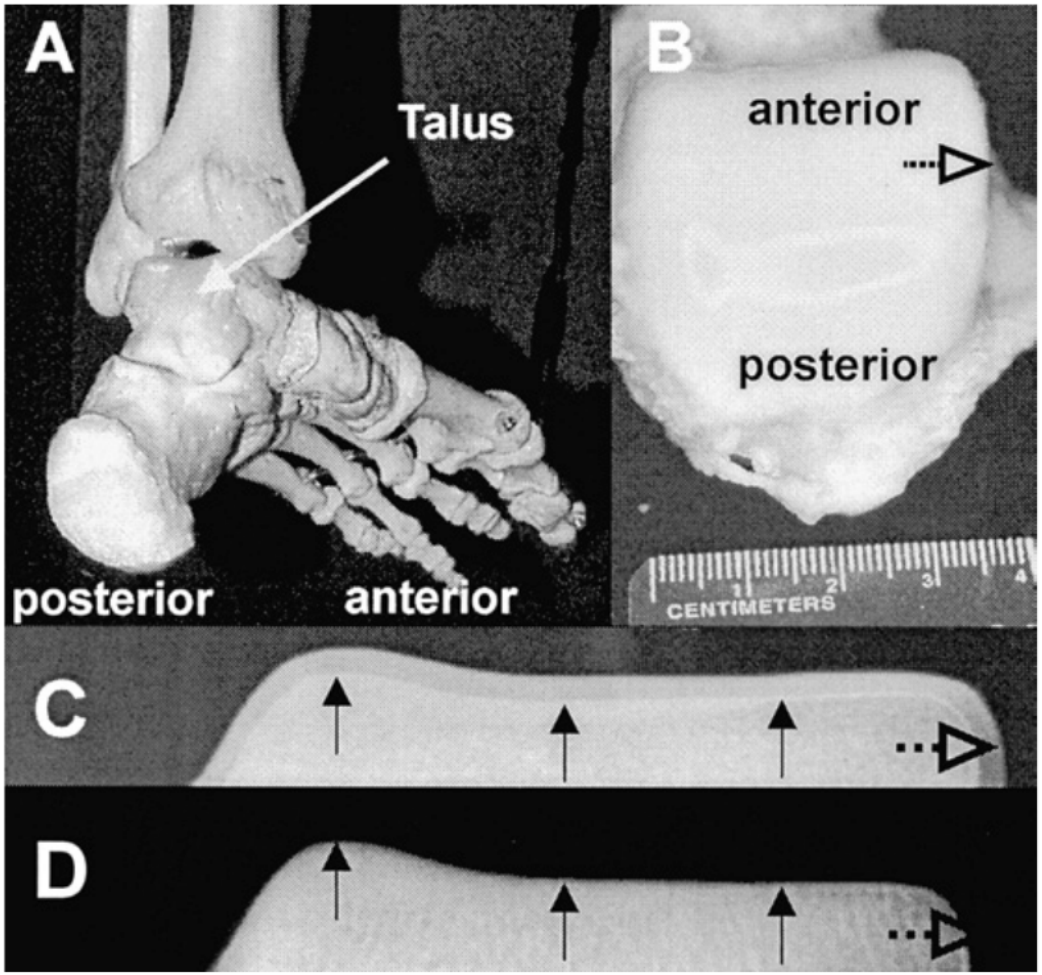

Fig. 2. The ankle joint: an overview. (a) Medial aspect of the ankle joint from a left foot of a human skeleton. This joint is formed by the tibia and fibula articulating with the talus (arrow) to form the talocrural (ankle) joint. (b) The photograph shows the superior surface of the talus. The arrow indicates the orientation of the talus in relation to (c). (c) A DE image at 30 keV, with the X-ray beam parallel to the articular surface from posterior to anterior. The fine arrows indicate the bone/cartilage interface, with the cartilage (approx. 1.5 mm in height) as the less bright layer. The large arrow indicates the orientation of the DE image relative to the macroscopic image in (b). The actual resolution of the DE image is approximately 100 μm and the image is approximately three-fold magnified as compared to the proportions of the talus. (d) Synchrotron radiograph of the same specimen as shown in (c).

Mollenhauer et al, Osteoarthritis and Cartilage 10, 2002.

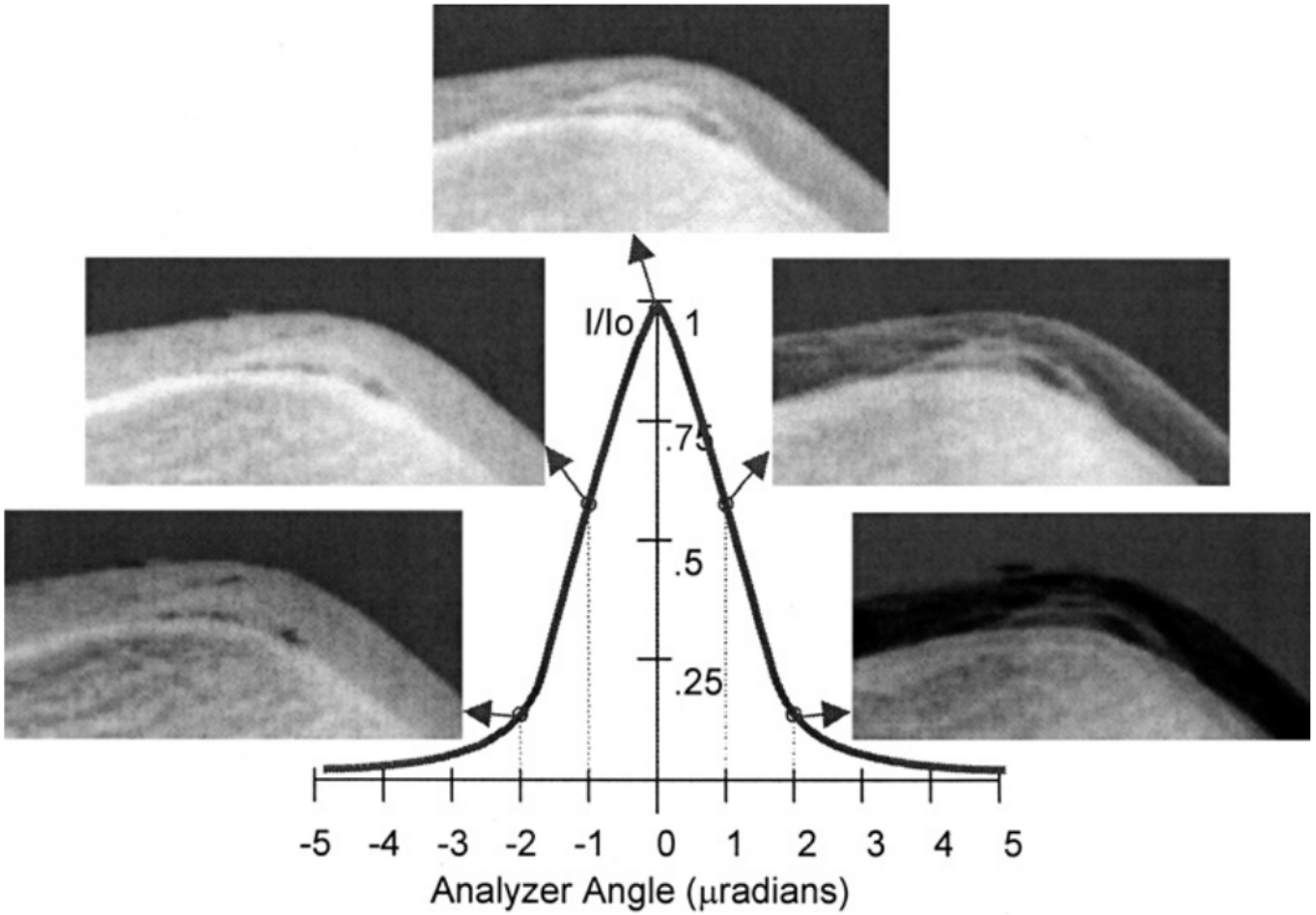

Fig. 3. DEI images of articular cartilage along the rocking curve. An illustration showing the alterations in image appearance from articular cartilage as the analyser setting is taken through the rocking curve at 30 keV. The locations at which the images are taken are indicated on the rocking curve. Note the heterogeneities in contrast within the cartilage tissue whose appearance change at various points in the rocking curve.

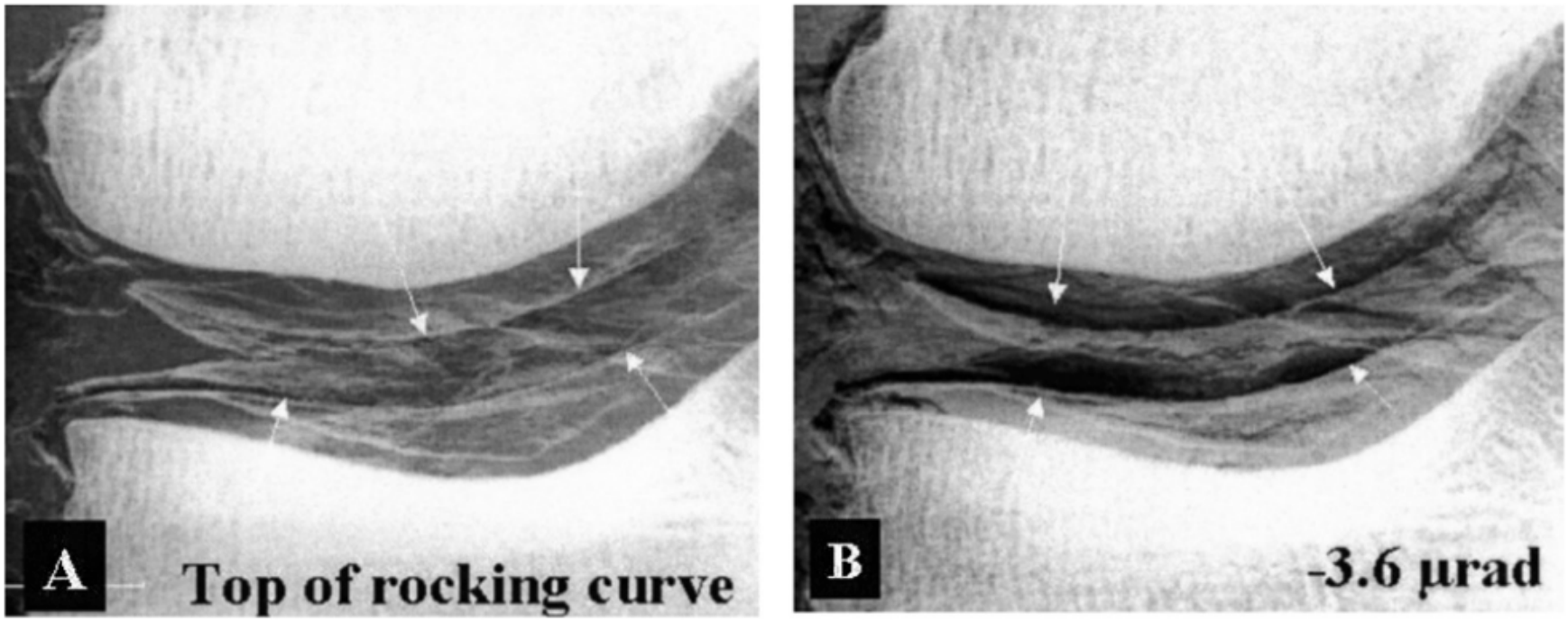

Fig. 7. DE images of the medial condyle of an intact knee joint at the top of the rocking curve (a) and at −3.6 µrad (b). The image was taken with all surrounding soft tissue, except the skin, in place. Note that the articular hyaline cartilage (whose borders can be seen at arrows) and menisci are visible even through the surrounding connective tissues.

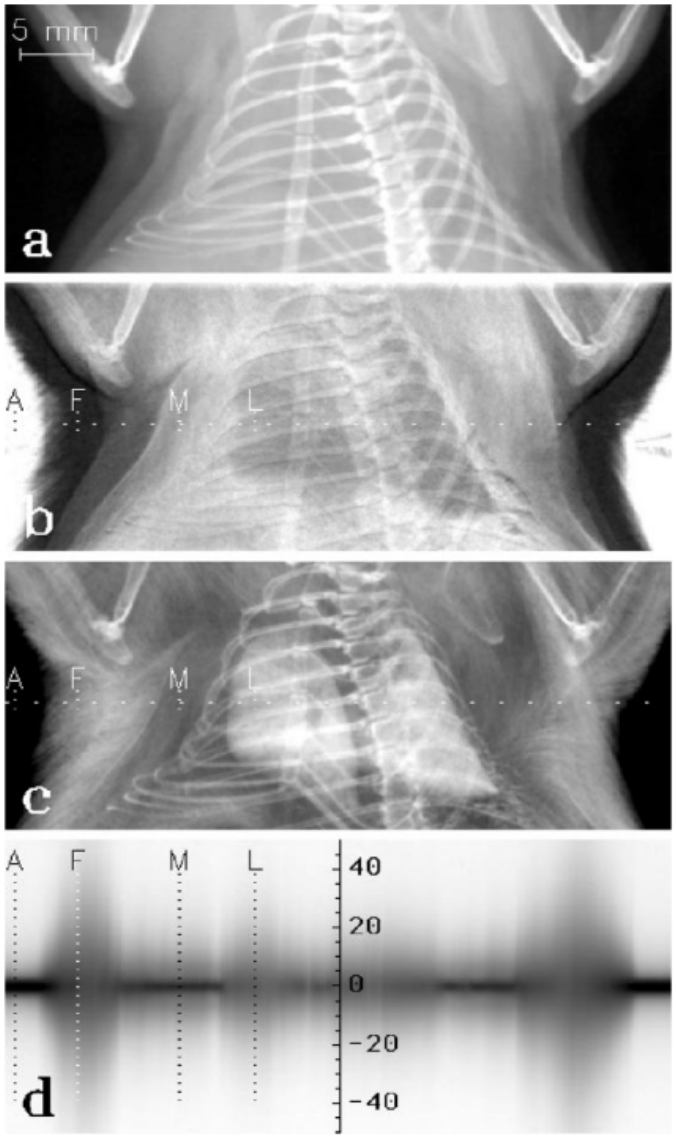

Fig. 10. (a) Normal radiograph of a mouse at 18 keV. Darker color represents greater X-ray intensity. (b,c) DEI images with the analyzer at − 10 and 0 μrad, respectively. Refer to text for explanations of A, F, M and L regions. (d) Rocking-curve scan through the middle of the lung, indicated by the horizontal dashed lines in the images above; Vertical axis corresponds to changing analyzer angle from − 50 to 50 μrad.

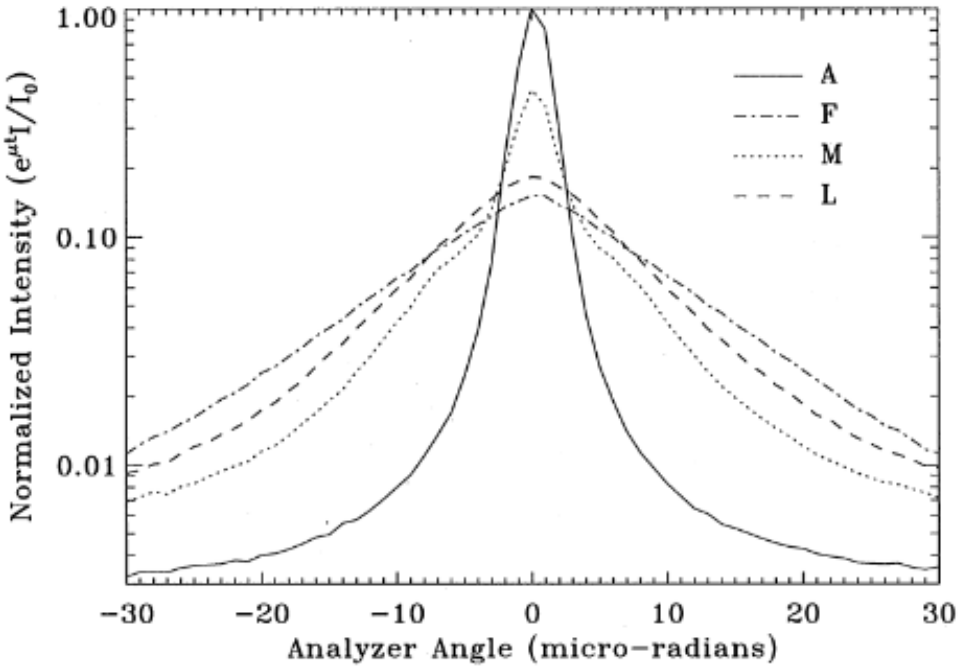

Fig. 11. Normalized analyzer rocking curves through the air (A), fur (F), lung (L), and muscle (M) regions.

Analyzer crystal can reject small angle scattering

Zhong et al, NIM A450, 2002.

Extensions: Dark field imaging, SAXS imaging, USAXS imaging

Set analyzer crystal OUTSIDE of the reflectivity range
Only x-rays that have been scattered significantly will be detected.
Additional reflections to ensure low tails of reflectivity curve.

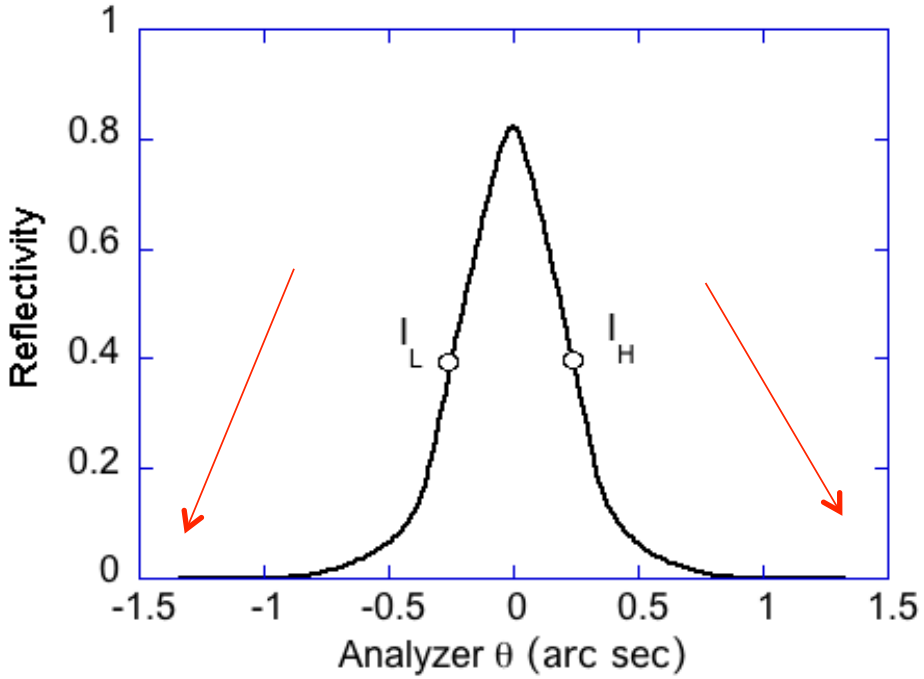

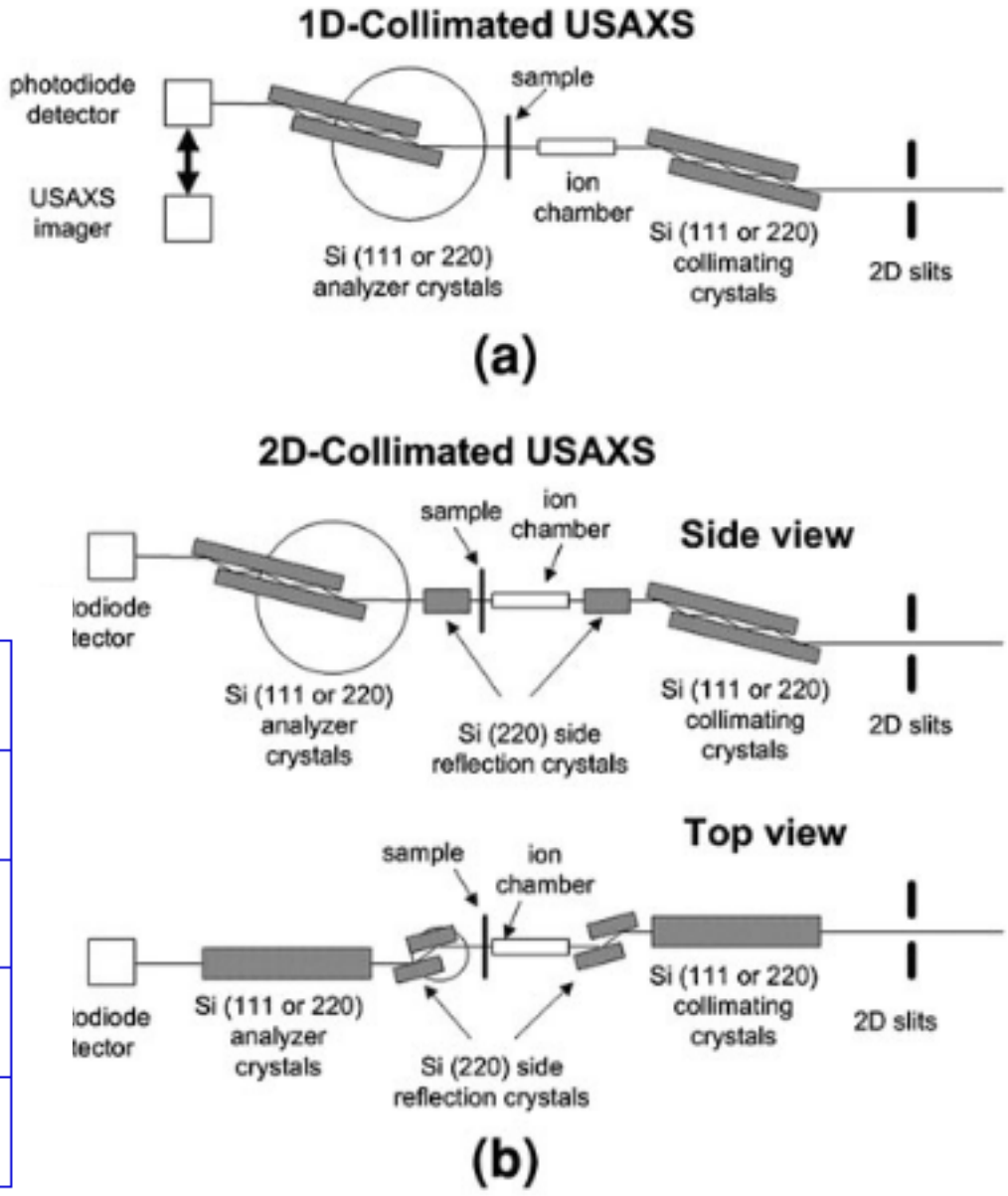

Ilavsky et al, Metall. and Materials Transactions, 2013.

USAXS imaging enables an additional contrast mechanism: ultras-small angle scattering

Good for identifying materials with similar density but with different microstructures.

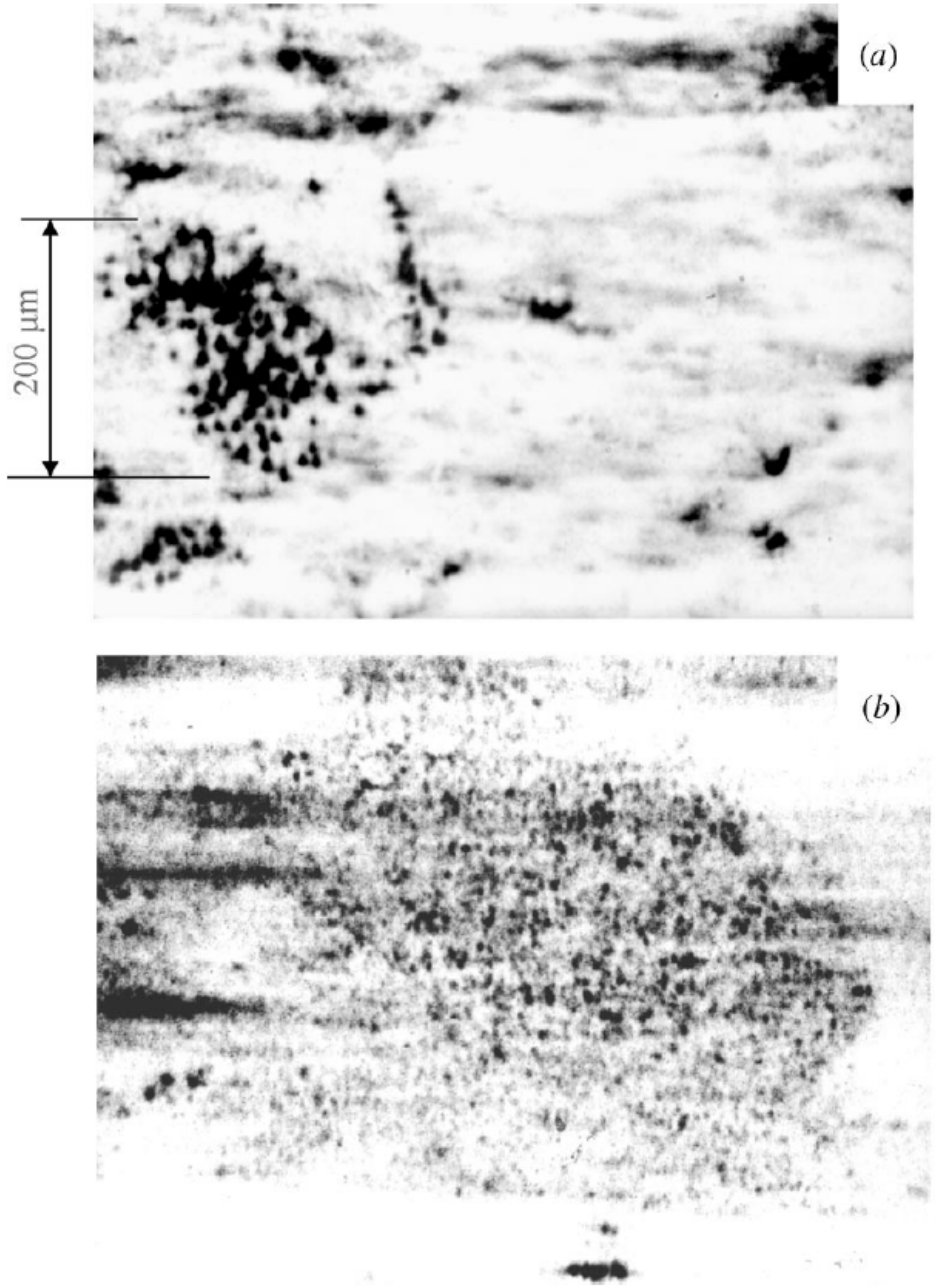

Figure 6
USAXS images of the same region of the sample taken with (*a*) $q = 1.3 \times 10^{-4}$ Å^{-1} and (*b*) $q = 7.5 \times 10^{-4}$ Å^{-1}.

Levine & Long, JAC, 2004.
Sample: Deformed polycrystalline Cu

Analyzer-based phase-contrast imaging: gratings

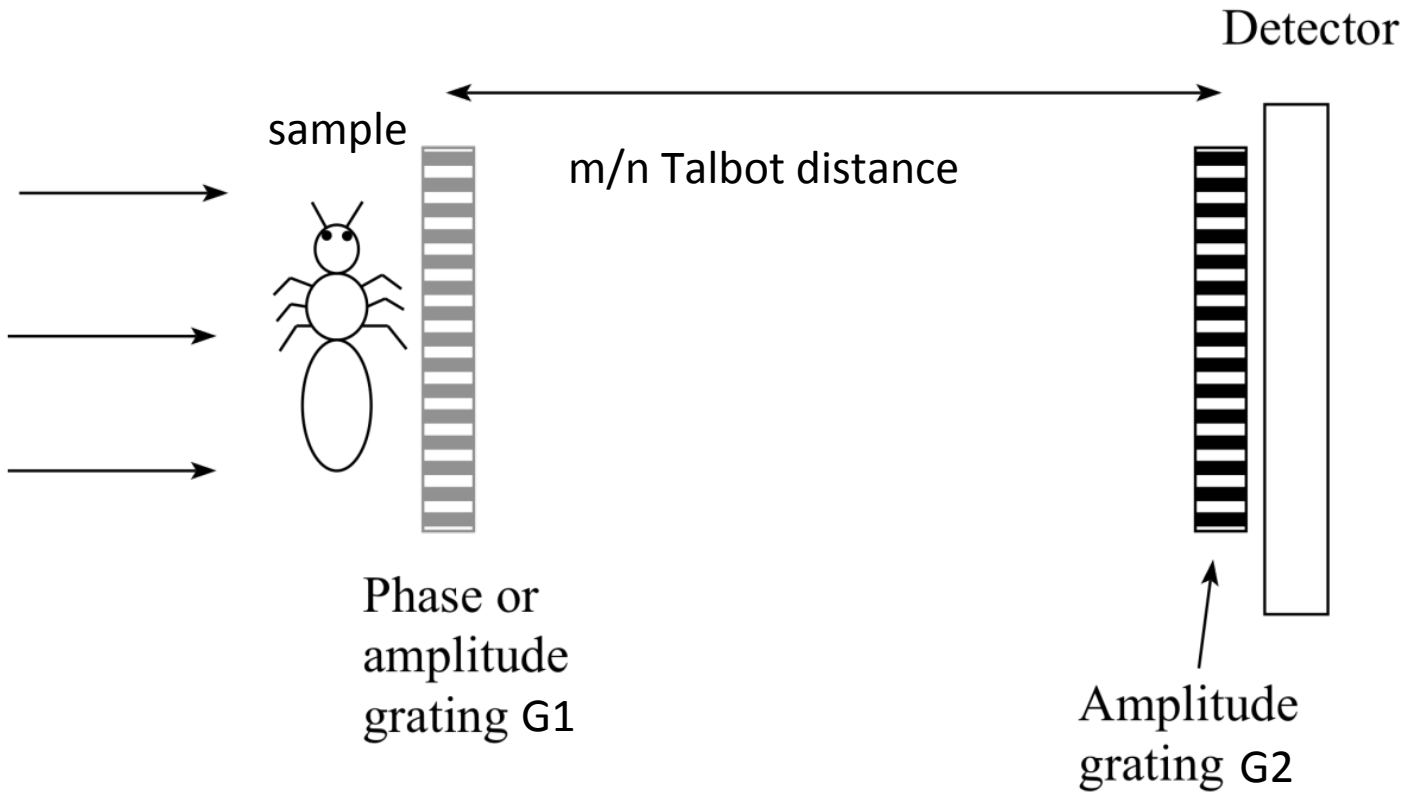

Talbot or Fractional Talbot effect creates a *related image* of G1 at the G2 position.
G2 made to have same periodicity at the G1 *related image*.

Fabrication of amplitude grating is a challenge at high energies – need high aspect ratio for high spatial resolution and thick enough to stop high energy x-rays.

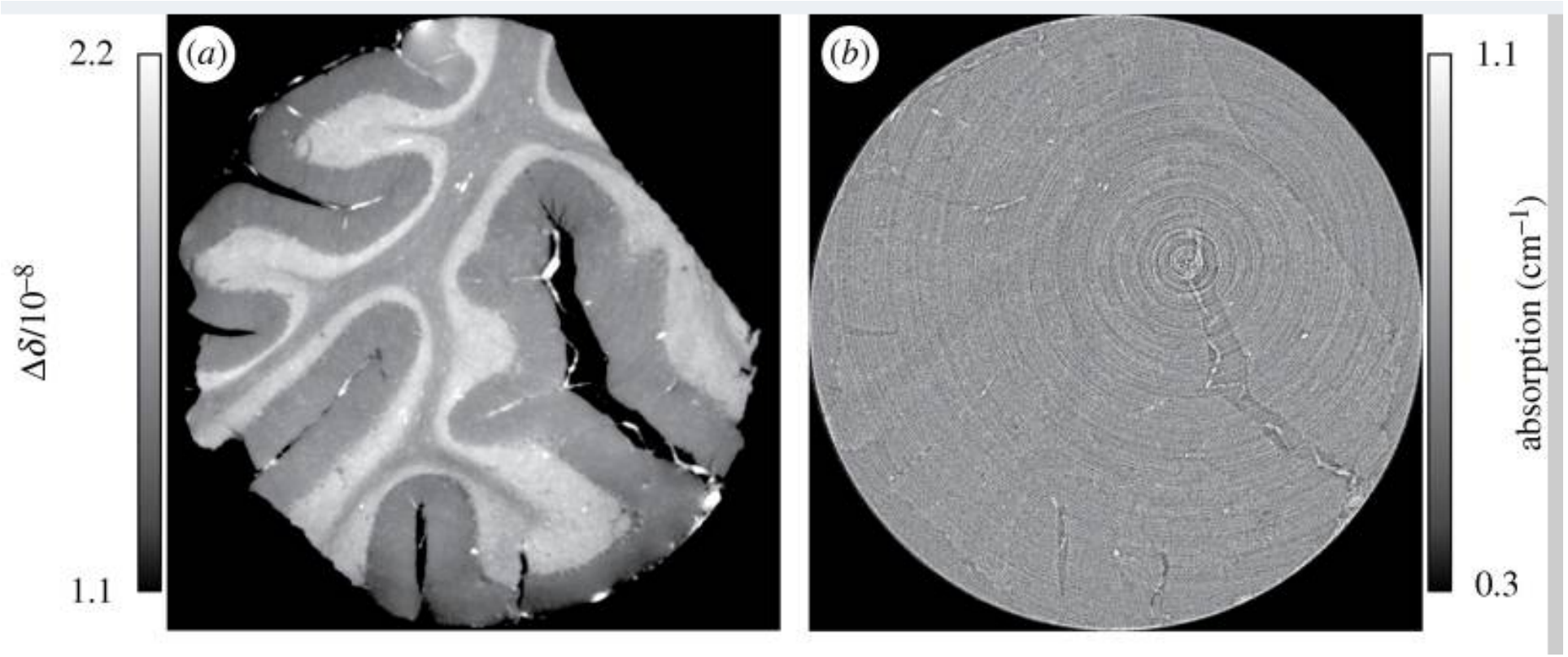

Phase image

Absorption image

Chunk of human cerebellum. 3D measurement. Above is one computer slice.

Schulz et al, JRSoc Interface 2010

General advantages of analyzer based imaging:

- Outstanding angular discrimination – ability to isolate small angle scattered x-rays
- Lots of interest in medical community – medical samples tend to have a lot of scatter and generally composed of slowly varying phases (ie, smoothly varying phase).
- X-ray source coherence not required. Crystals do the angular discrimination for you. For grating analyzer, a 'source grating' can be used.
- Grating based imaging attracting much attention because it accommodates broad bandwidth radiation, unlike the crystal analyzer. Better suited for lab source.

Disadvantages of analyzer based imaging:

- Spatial resolution limited by crystal extinction length or grating period.
- Mostly 1D phase sensitivity in the scattering plane. 2D implementation more challenging – requires another set of crystals or grating that scatter in the other orthogonal plane. For gratings – a '2D diffraction grating' is possible.
- High angular discrimination implies a lower overall photon efficiency.

Propagation phase contrast

$$\psi_L(x) = \psi_0(x) \otimes P_L(x)$$

$$\tilde{\psi}_L(f) = \tilde{\psi}_0(f).\tilde{P}_L(f)$$

Convolution in real space is equivalent to multiplication of the Fourier transforms

$$P_L(x) = \frac{e^{ikL}}{i\lambda L}\exp\left[\frac{i\pi x^2}{\lambda L}\right] \quad \rightarrow \quad \tilde{P}(f) = \exp[-i\pi\lambda L f^2]$$

In 1-D

For $\pi\lambda L f^2 << 1$ $\qquad \tilde{P}(f) \approx 1 - i\pi\lambda L f^2$

$$\tilde{\psi}_L(f) = \tilde{\psi}_0(f).\tilde{P}_L(f) = \tilde{\psi}_0(f)\,[1 - i\pi\lambda L f^2]$$

$$\tilde{\psi}_L(f) = \tilde{\psi}_0(f) - i\pi\lambda L f^2 \tilde{\psi}_0(f)$$

$$I(x) = |\psi_L(x)|^2 = |\psi_0(x)|^2\left[1 - \frac{L\lambda}{2\pi}\nabla^2\phi(x)\right]$$

Image is sensitive to the Laplacian (second derivative) of the phase.
Depends on distance from sample, L.

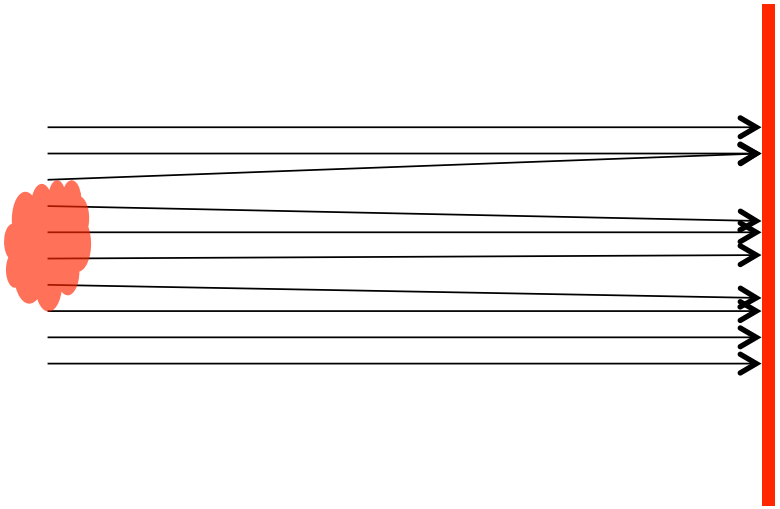

Small angular deviations of the beam after the sample should show up as intensity variations some distance downstream of the sample.

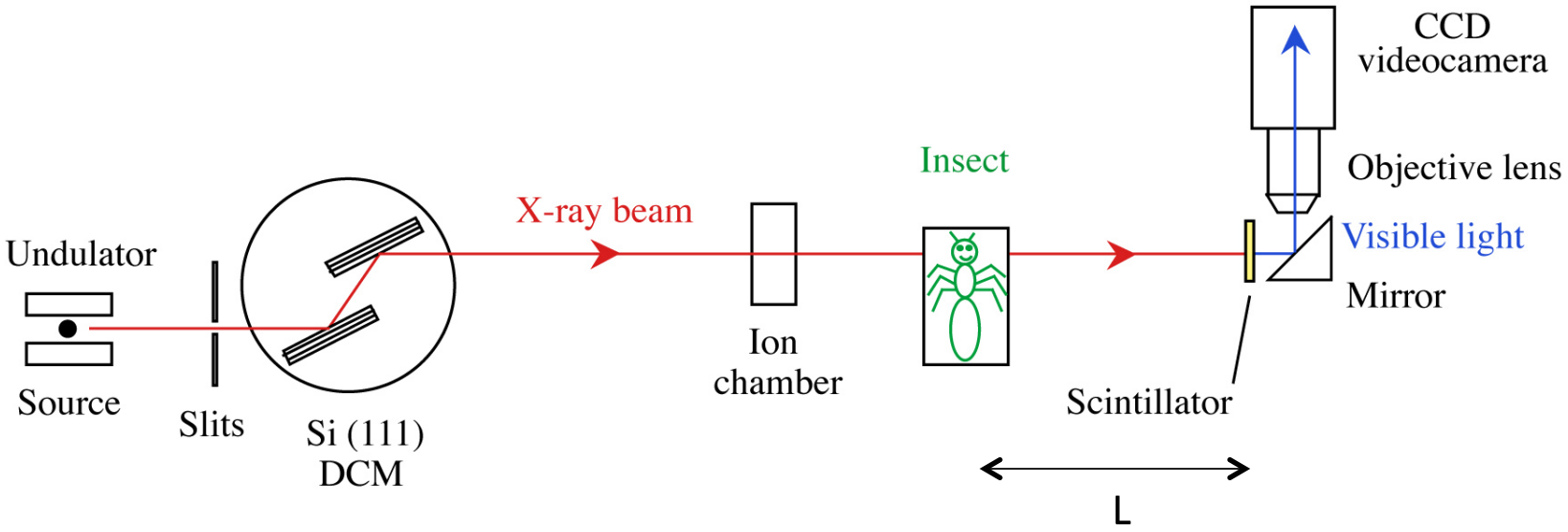

Ant head

Absorption contrast

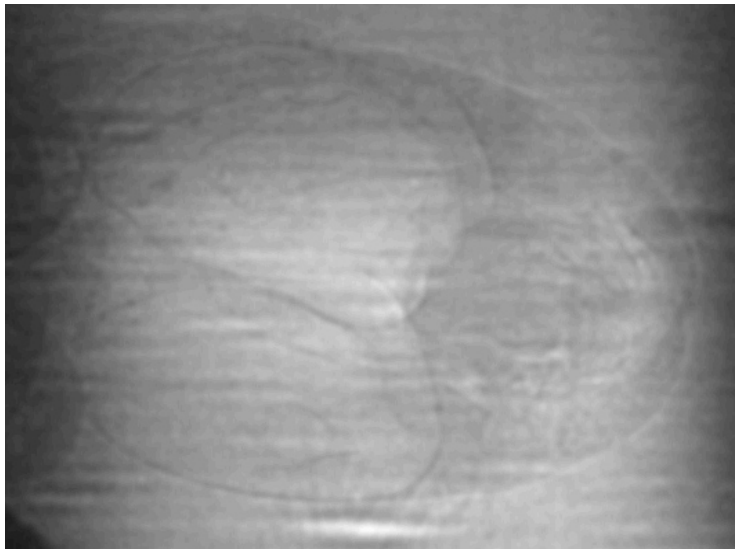

Phase enhanced contrast

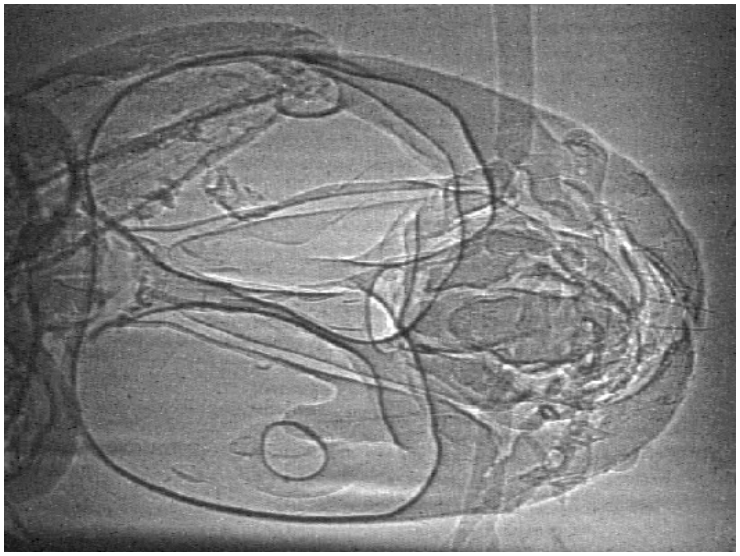

Same spatial resolution ~ 2 μm

Westneat et al, Science 299, 2003

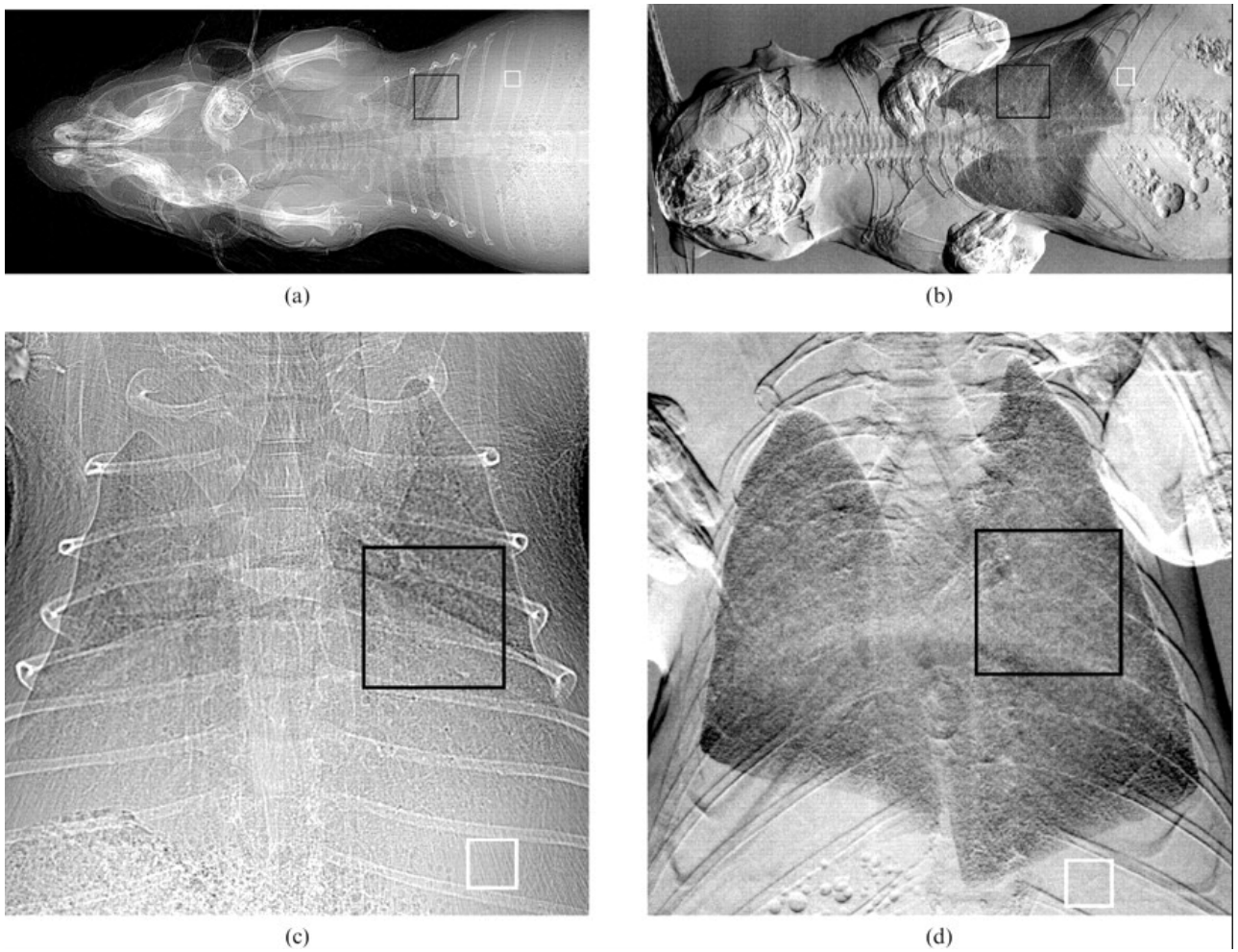

Figure 6. Phase contrast images of a 1-month-old male mouse imaged at 33 keV. (a) Propagation-based imaging (PBI) with l2=4.26 m. Image size: 95.93 mm × 32.22 mm. Black region of interest (ROI): 300 × 300 pixels. White ROI: 100 × 100 pixels. Exposure time: 5.0 s. Surface entrance dose: 8.6±0.3 mGy. (b) Analyser-based imaging (ABI) image of the same mouse. Image size: 47.16 mm × 20.00 mm. Black ROI: 300 × 300 pixels. White ROI: 100 × 100 pixels. Exposure time: 0.5 s. Surface entrance dose: 0.91±0.03 mGy. (c, d) Magnified segments of the lung from (a) and (b), respectively.

Kitchen et al, British Journal Radiology 78, 2005.

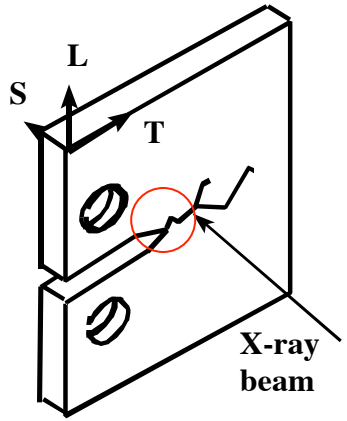

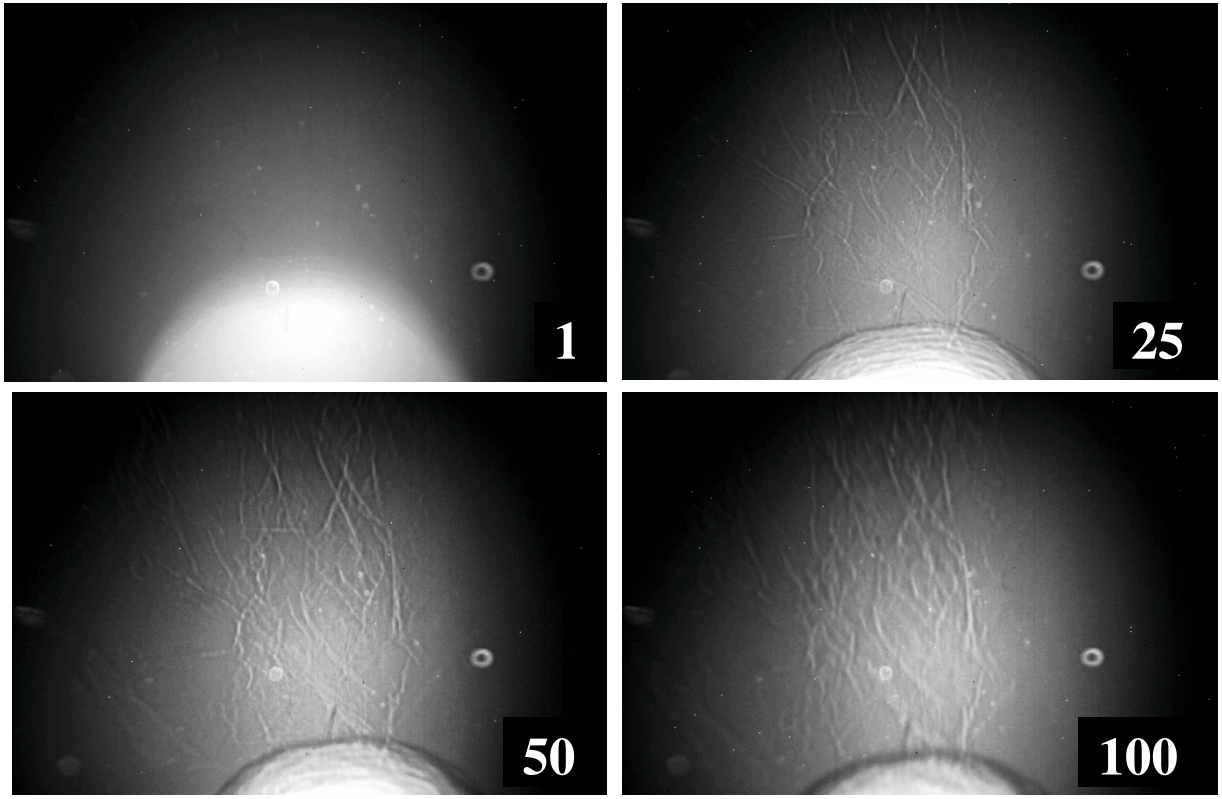

Sample: 2 mm Al, stress-induced cracks
Energy: 30 keV

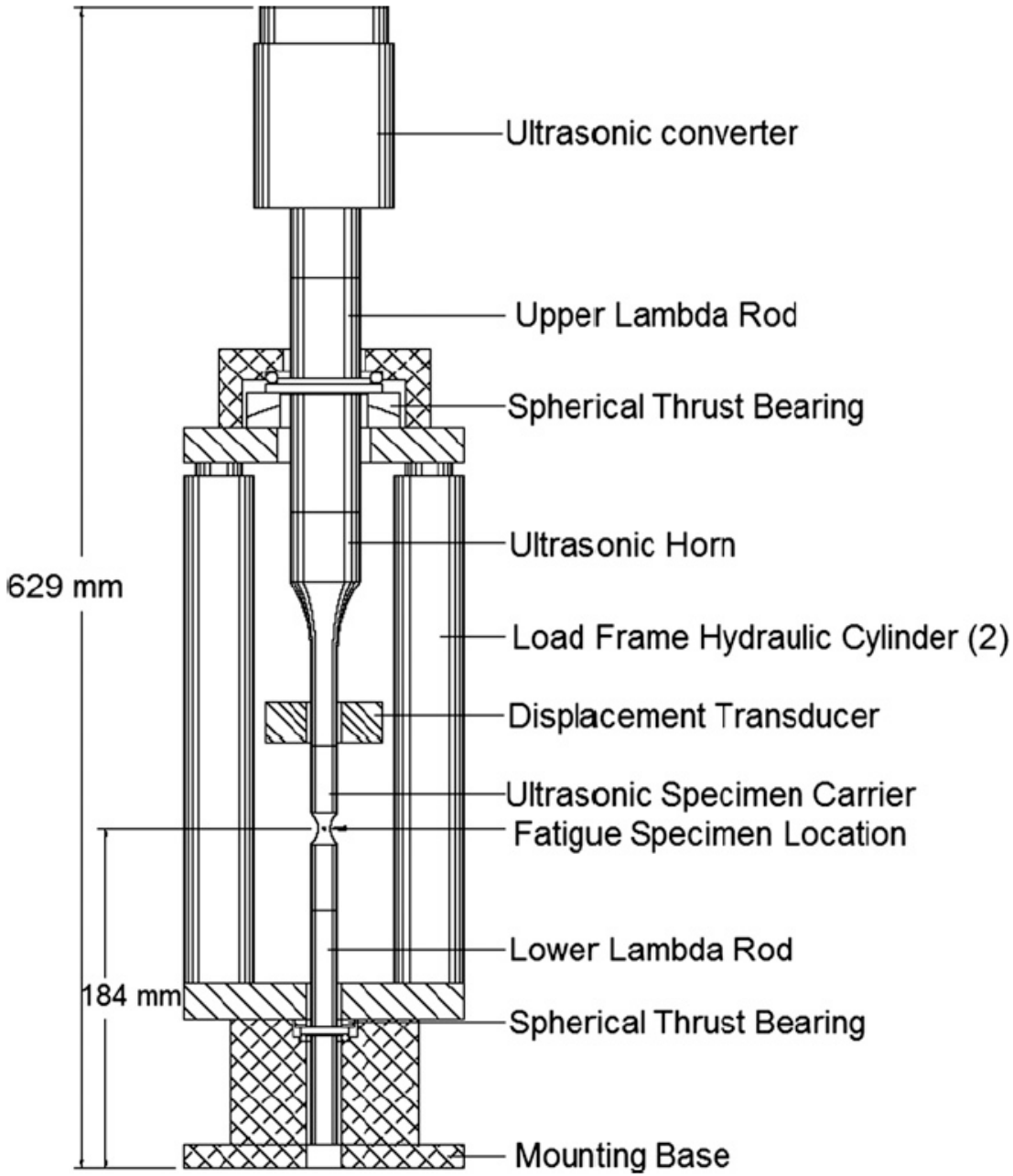

Fig. 1a. Schematic of portable ultrasonic fatigue system.

Liu et al, Acta Materialia (2011)

23 keV, 0.15-0.2 mm thick samples

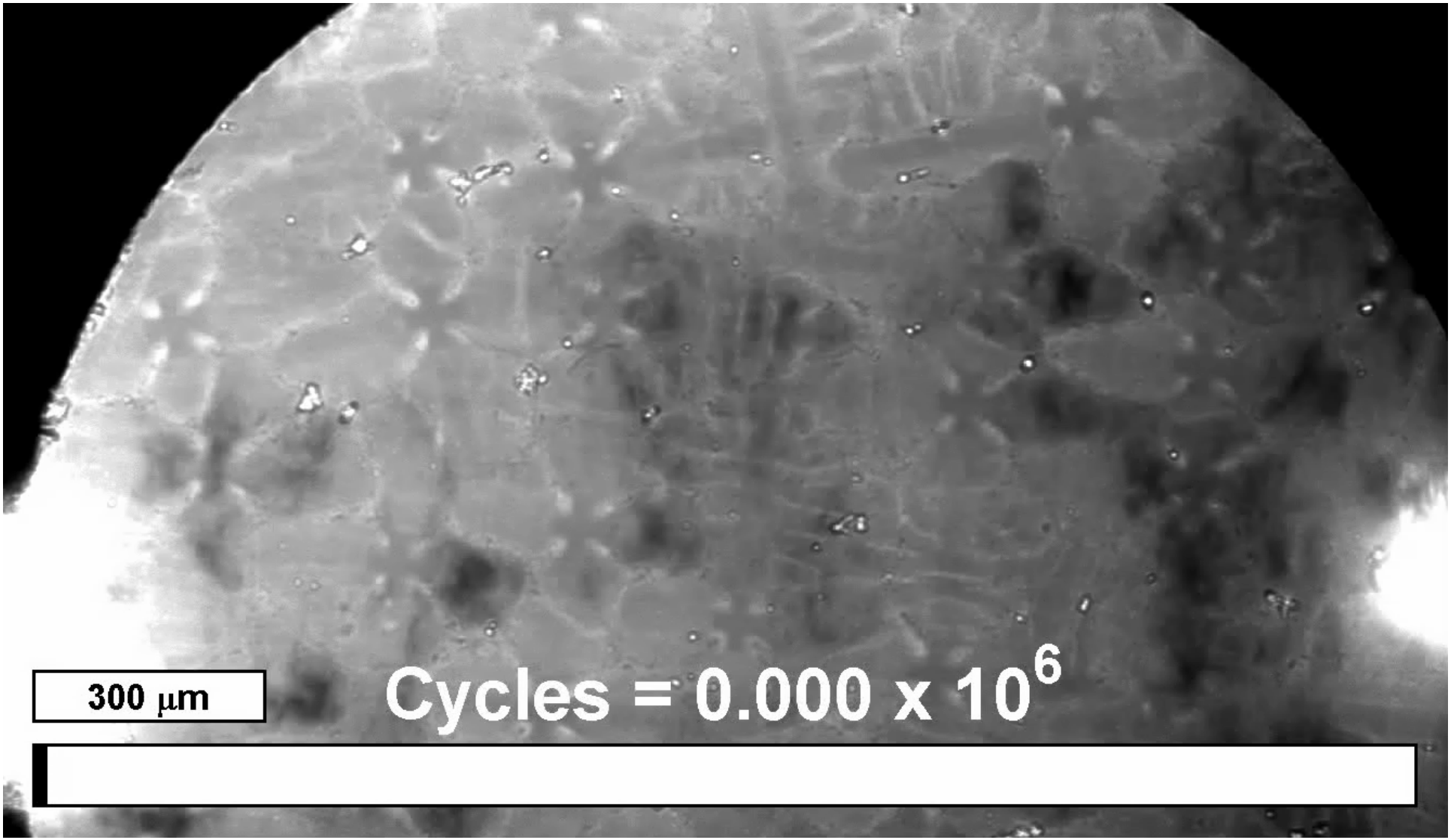

In-situ real time tracking of crack formation and propagation in nickel superalloy

High pressure diesel injector

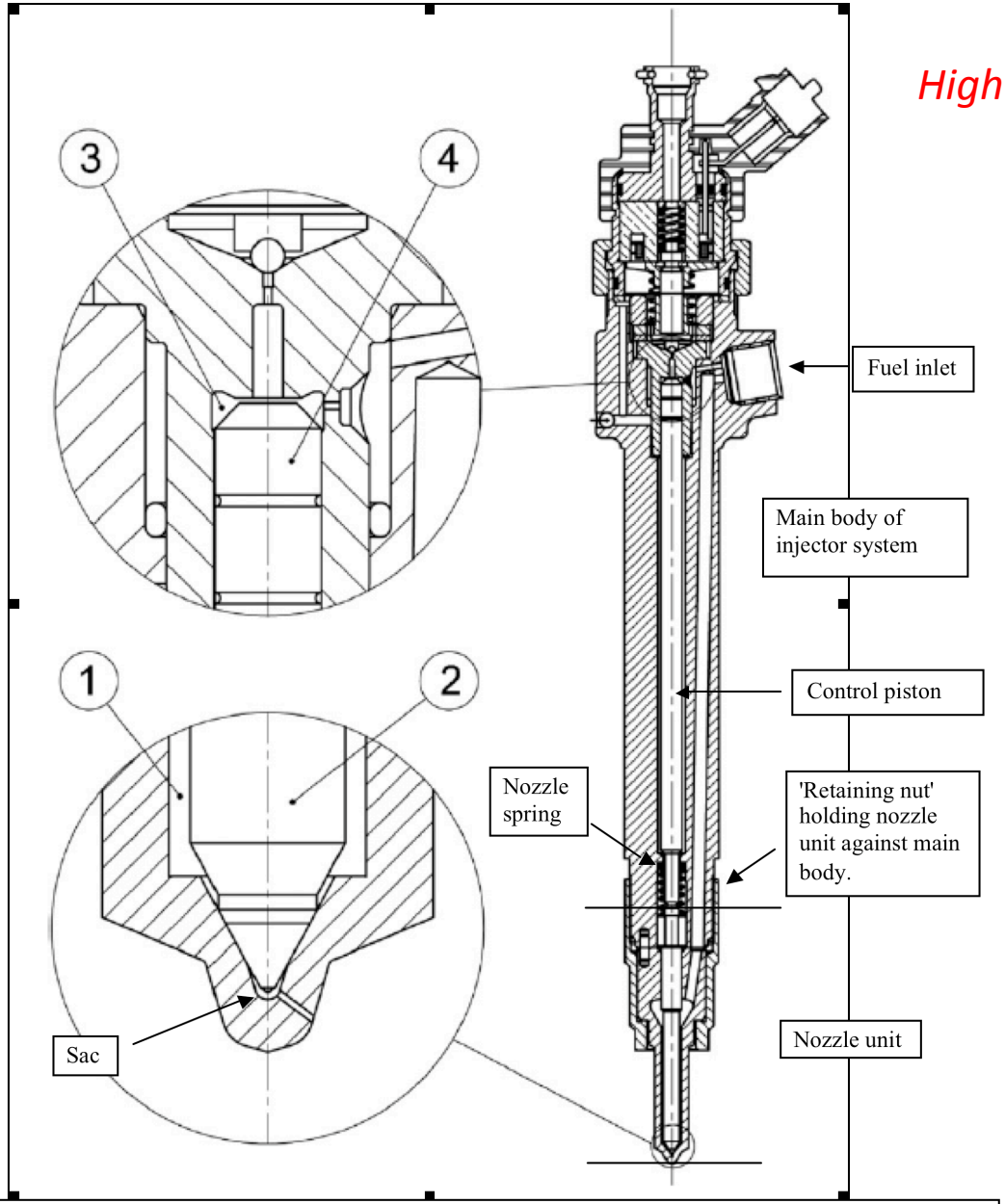

(2) is the needle valve.
Control piston motion detection devices are located near the fuel inlet.
Note that in this illustration, the exit hole is off-center.

Taken from Coppo et al, Sensors and Actuators A134, 366-373, 2007.

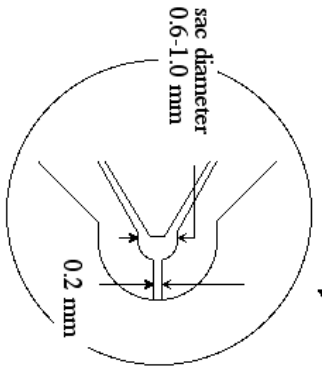

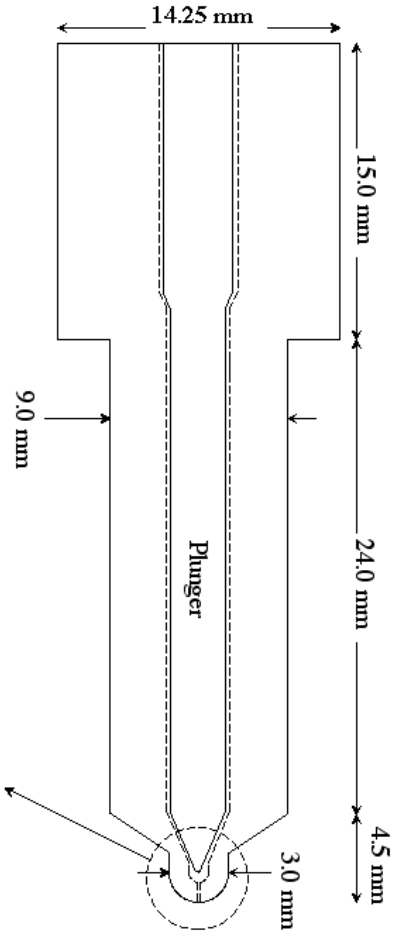

- *Fuel injectors are high pressure (1000 bars) systems, typically made of steel. Injection cycle is ~ 1 ms.*
- *Dynamics of the pintle (which only moves ~ 200 μm) within the steel body has never been directly visualized.*
- *To understand spray, you need to know what happens inside the nozzle.*
- *Highly nonlinear and transient processes.*
- *Scaled up and transparent models do not necessarily reflect the actual system.*
- *Capacitance measurements made far away (> 200 mm) do not reflect actual motion at the sac.*

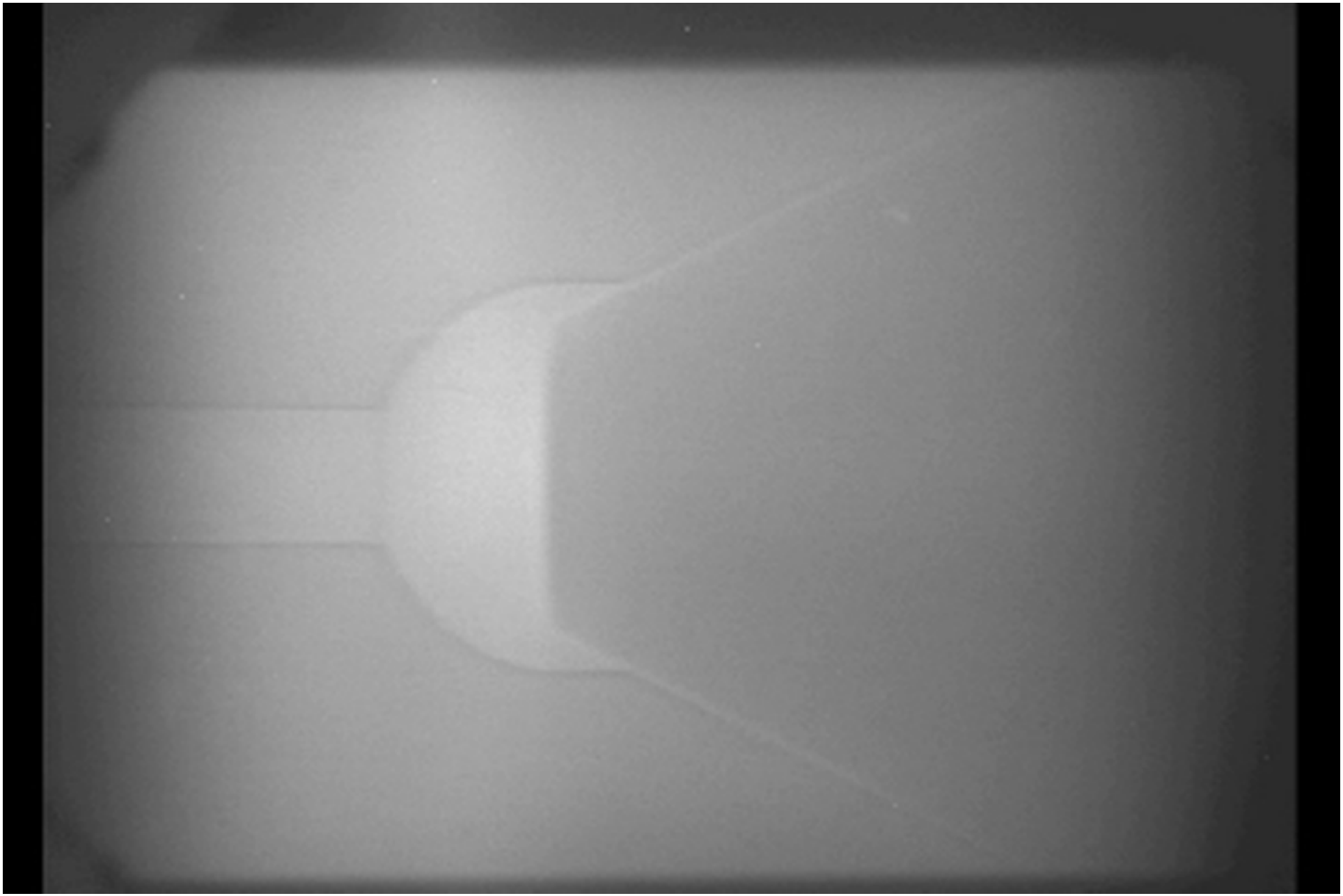

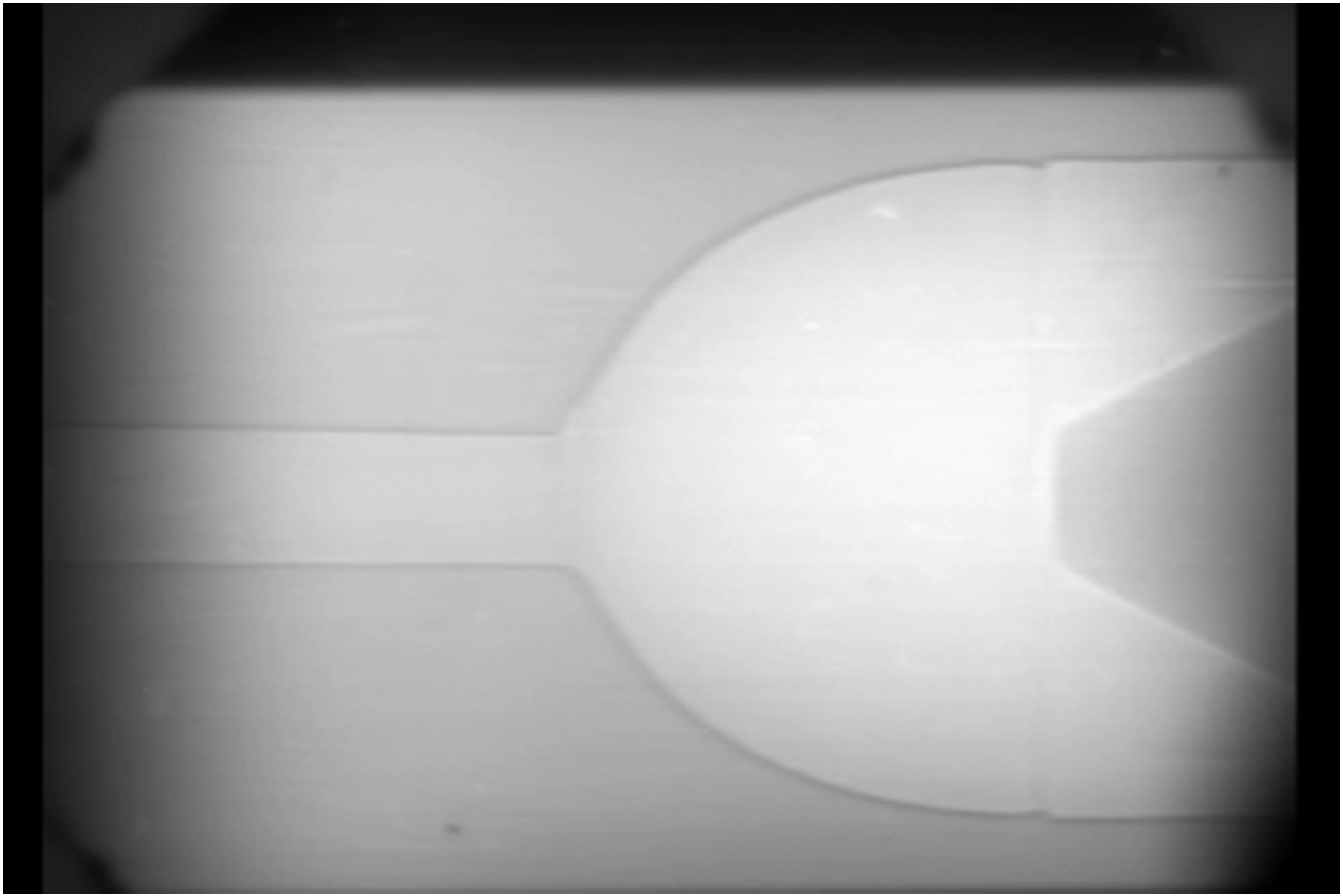

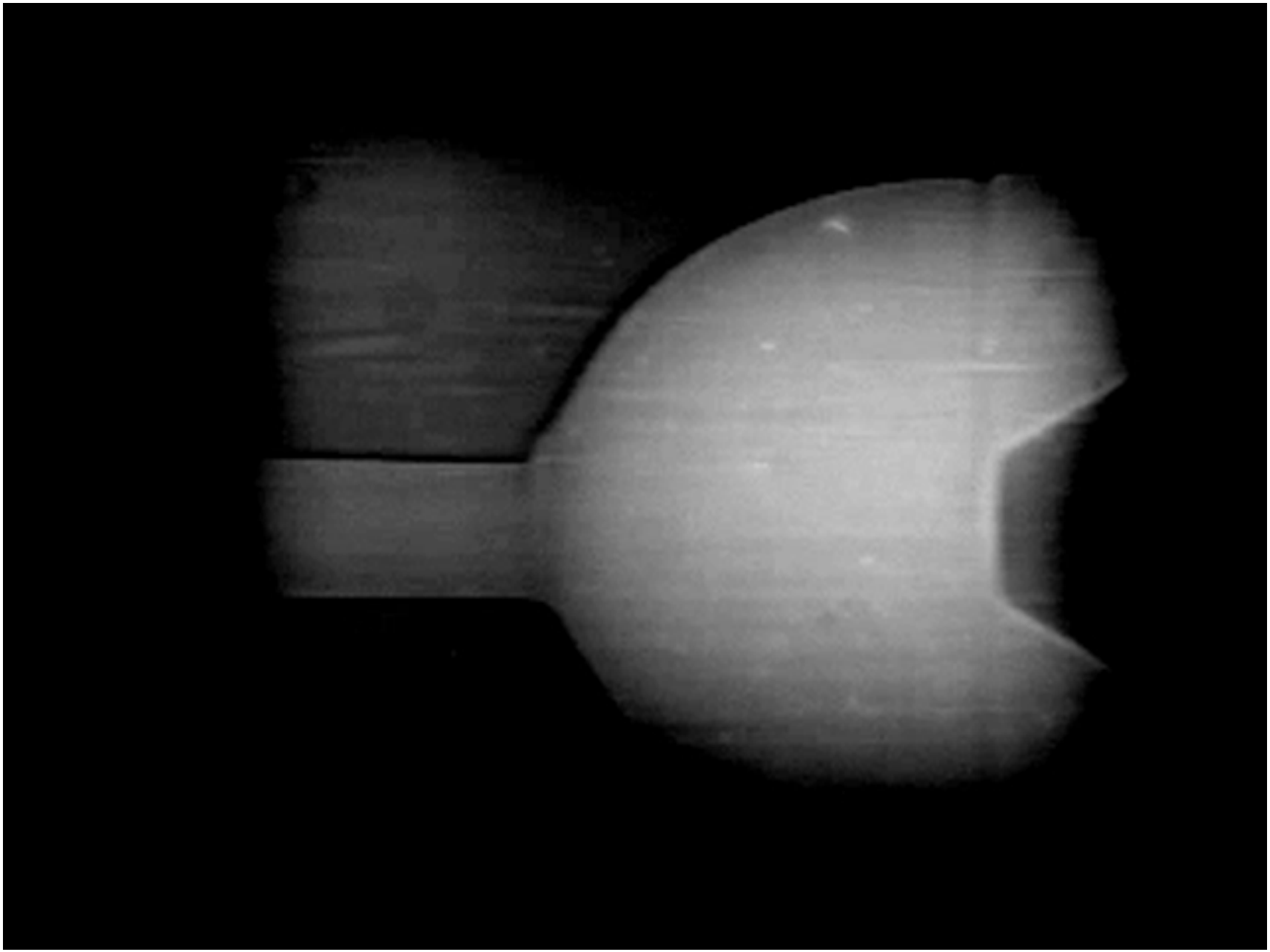

18 keV 0.02 s exposure
for radiography
1 mm diameter
samples (mostly Al)

For tomography, 1 Hz
rotation. 250
projections in 0.5 s.

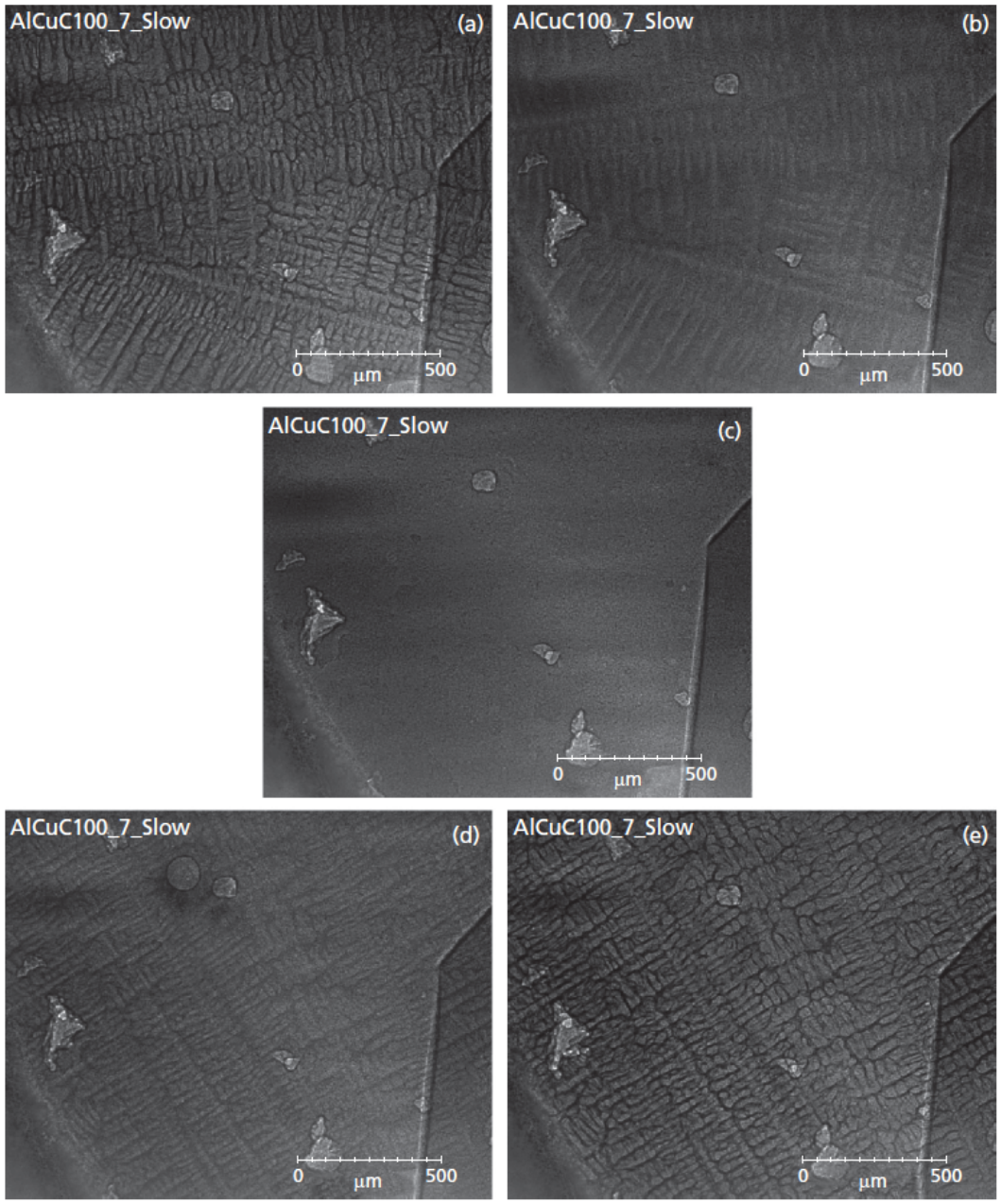

Figure 1. X-ray images obtained using synchrotron x-ray radiography during Al-7at.%Cu (a–c) melting and (d–e) slow continuous cooling. The angular feature on the right in each image is associated with the quartz.

Amy Clarke et al, EMR2, 2013

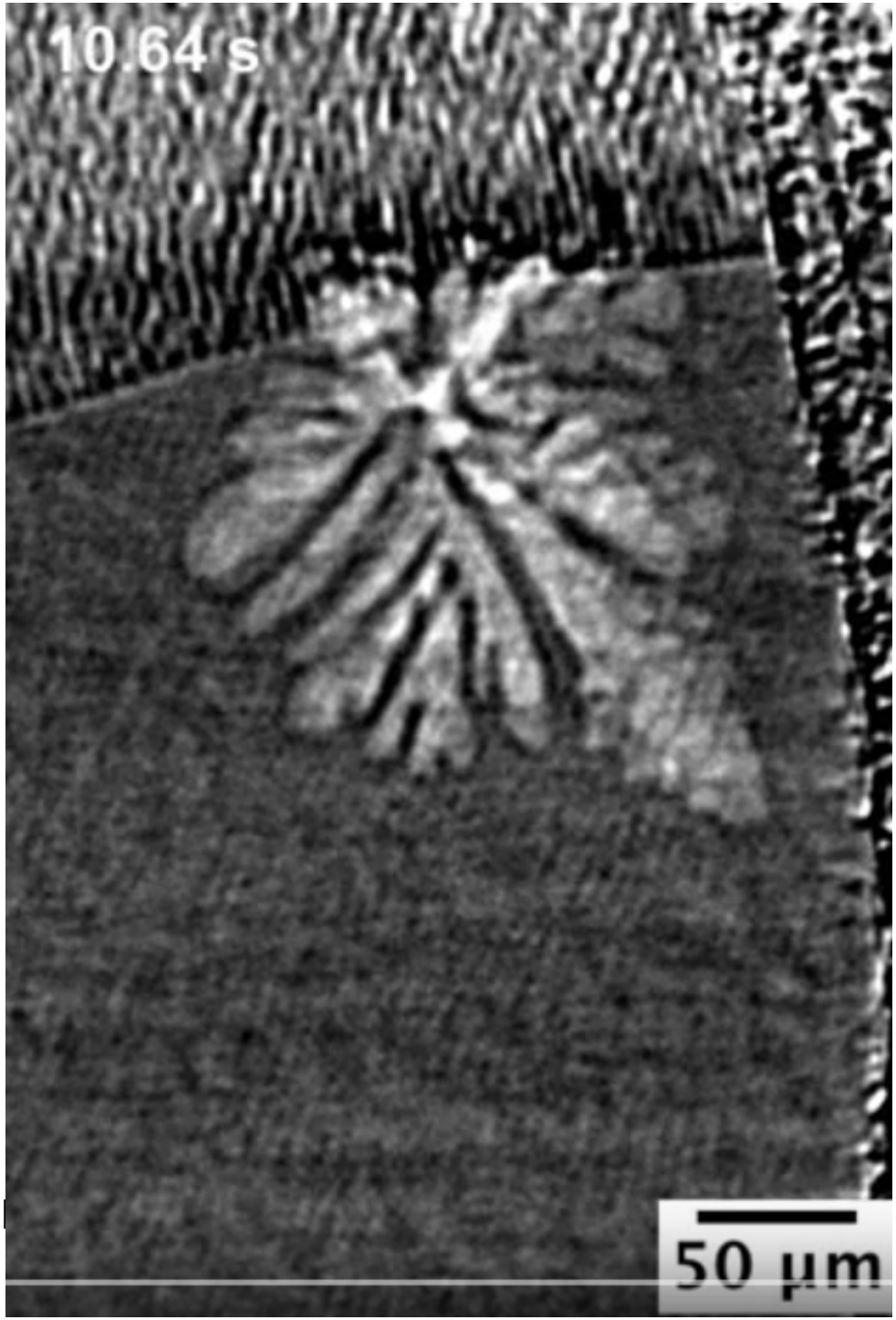

Aluminum rich crystal

Amy Clarke, LANL.

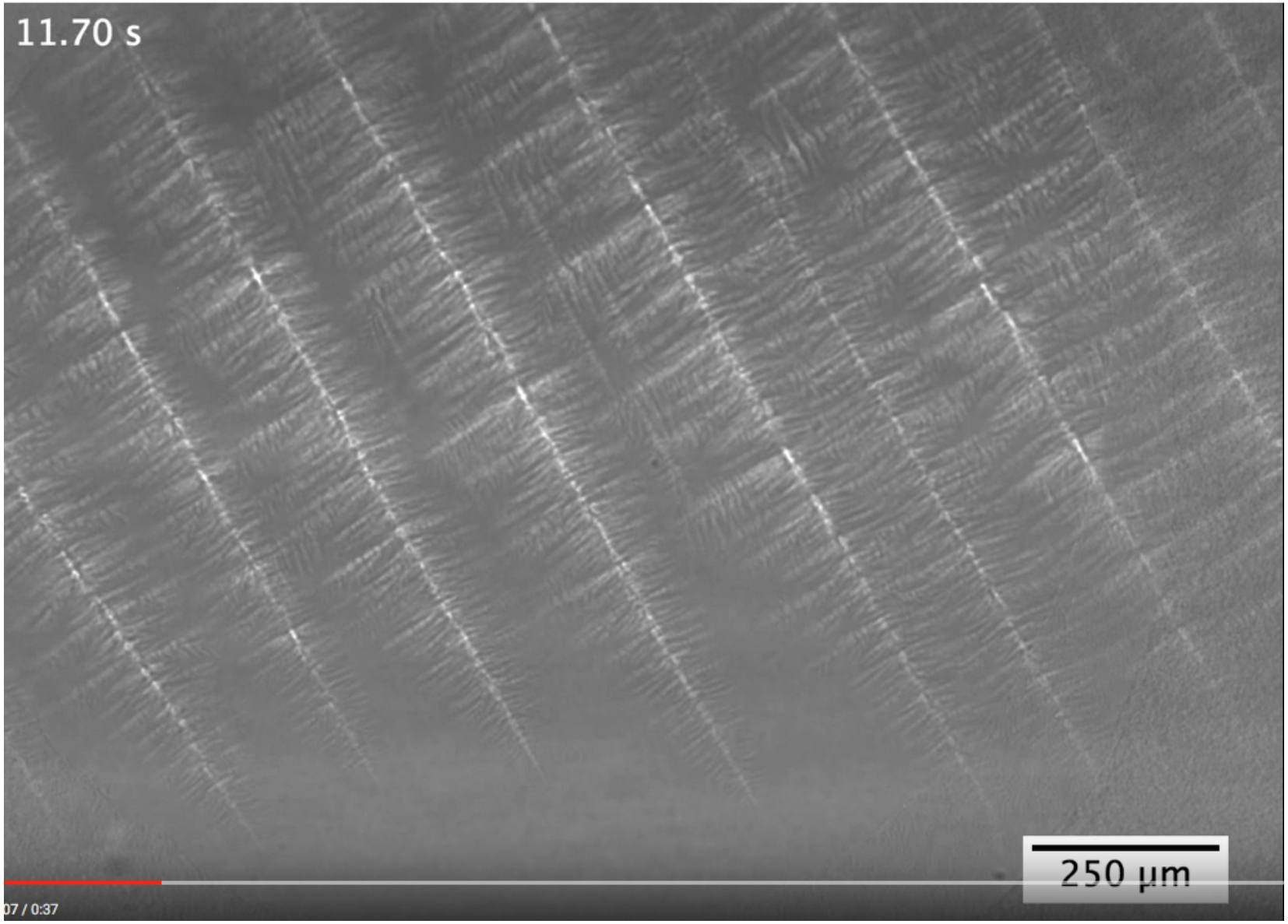

Dendritic growth in Al-Cu alloy

Amy Clarke, LANL

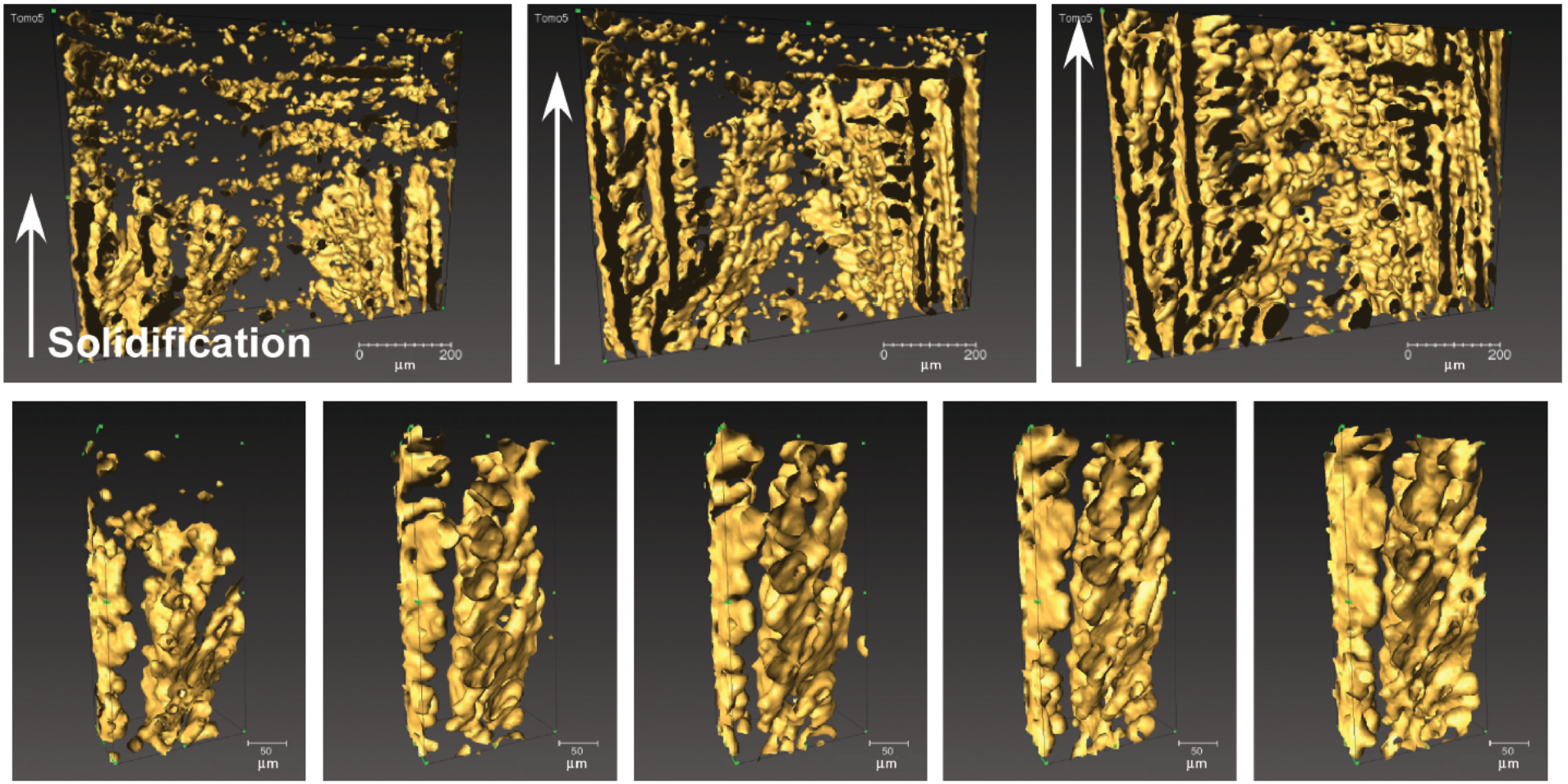

Figure 5. Preliminary synchrotron X-ray tomography of 3D dendritic growth and coarsening in Al-7at.%Cu during solidification. The lower series of images depicts the evolution of a smaller volume of liquid and solid present in the upper series of images. Note that time increases from left to right for both image series.

Clarke et al, Emerging Materials Research (2013)

Quantitative phase contrast imaging – Holotomography

Sketch of the experimental setup for quantitative phase tomography: a multilayer monochromator selects the photons with an energy close to 21 keV from the synchrotron radiation emitted by an insertion device.

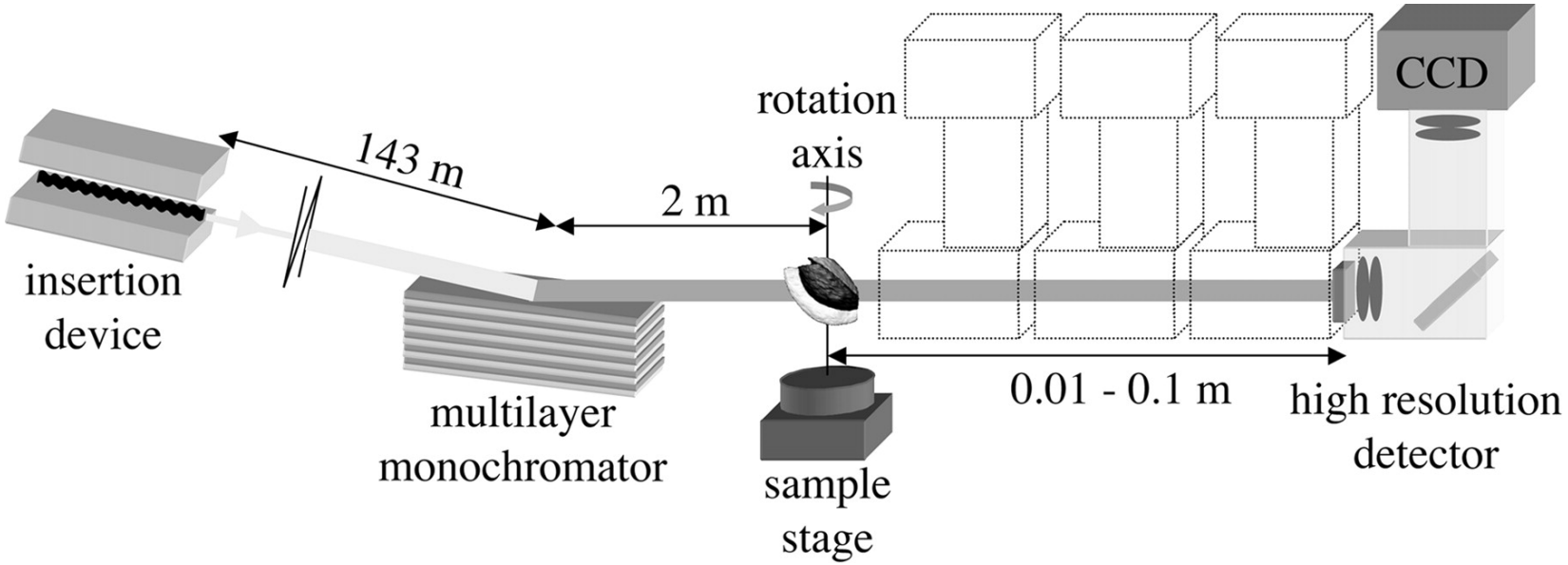

Peter Cloetens et al. PNAS 2006;103:14626-14630

Architecture of an Arabidopsis seed.

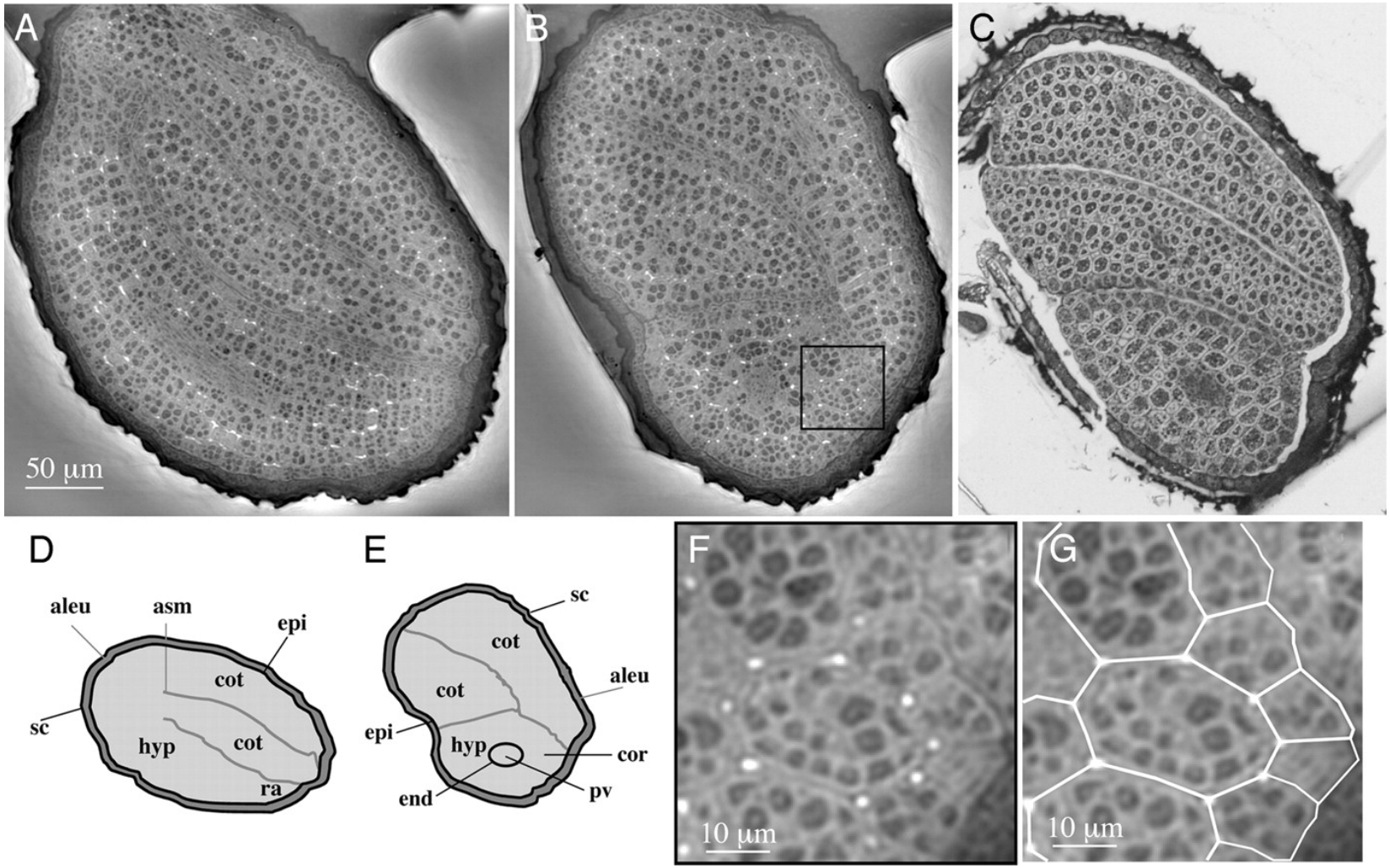

Peter Cloetens et al. PNAS 2006;103:14626-14630

3D rendering of intercellular air space in the hypocotyl (A) and in a cotyledon (B) and air space in cotyledon at higher magnification (C).

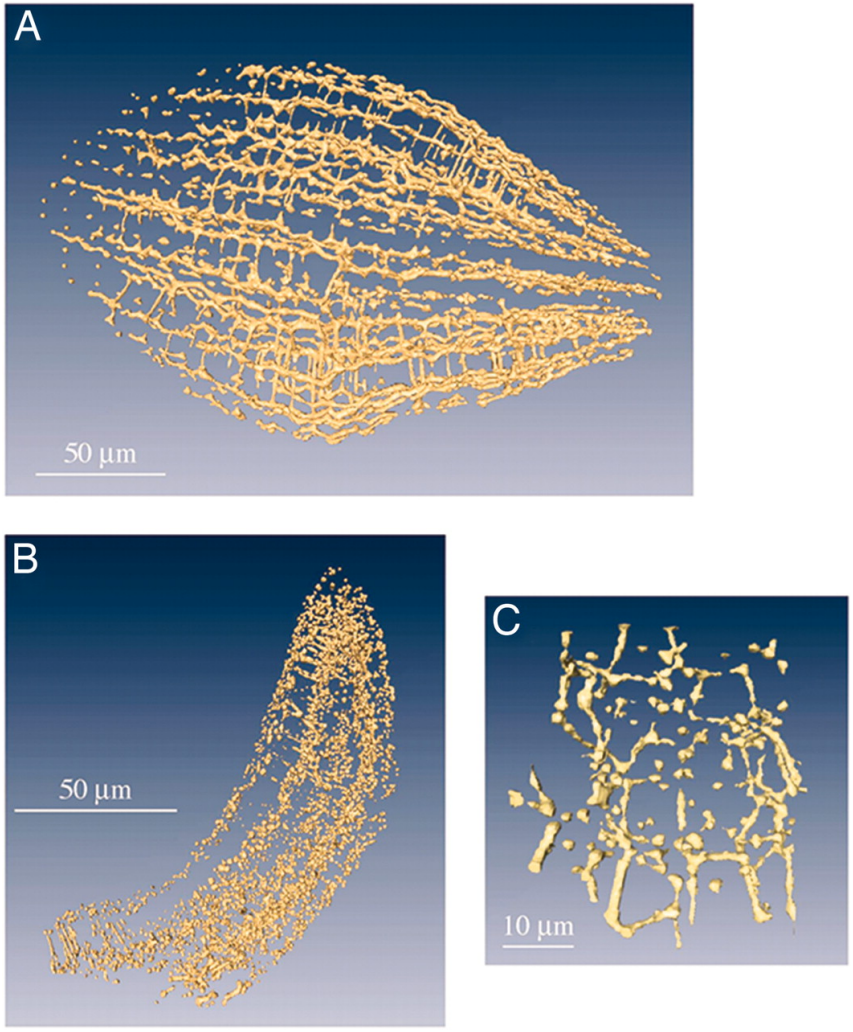

Peter Cloetens et al. PNAS 2006;103:14626-14630

Braincase anatomy and exceptional brain preservation in a sibyrhynchid iniopterygian from the Pennsylvanian of Kansas.

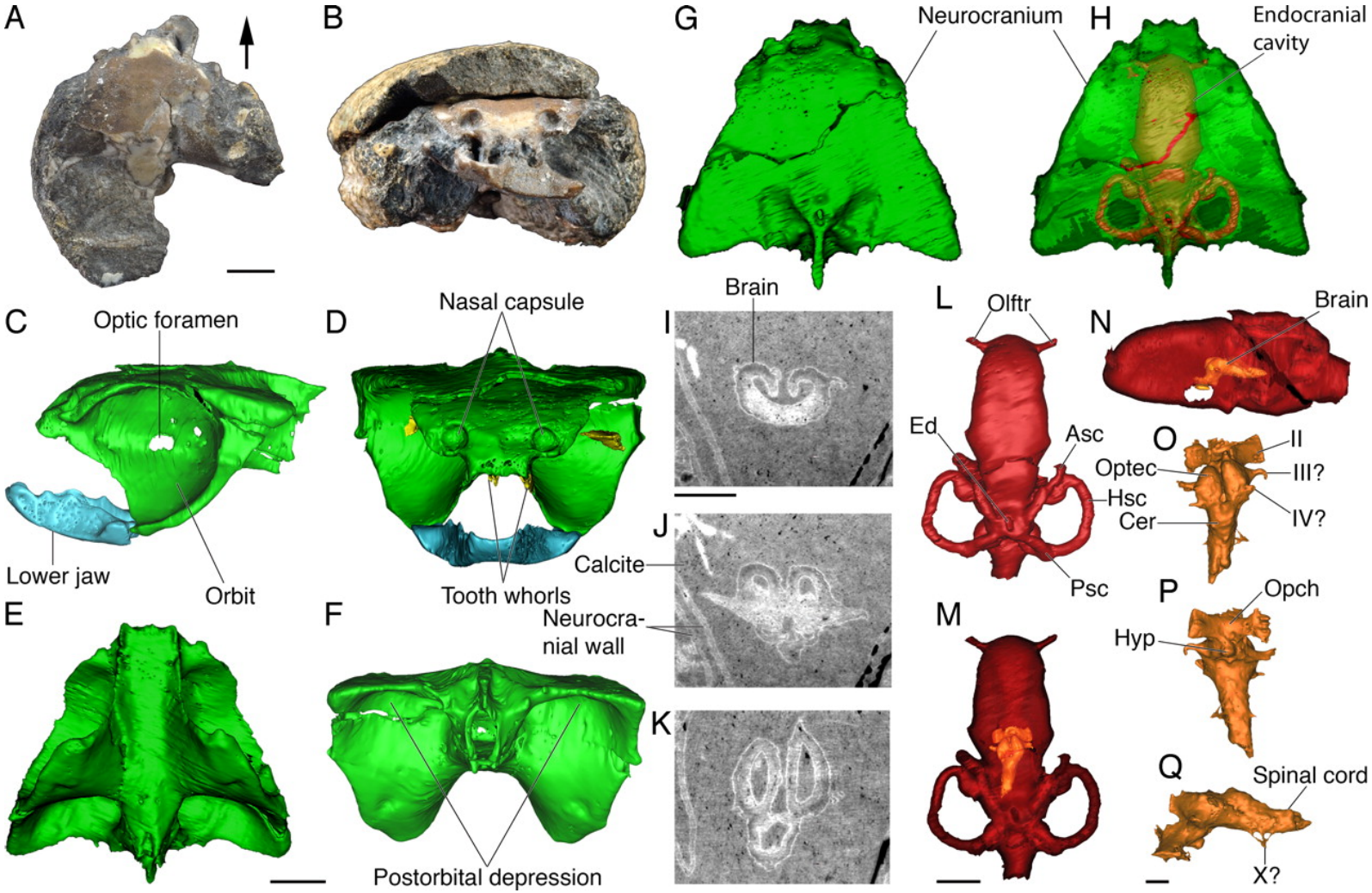

Alan Pradel et al. PNAS 2009;106:5224-5228

Stereo imaging

For tracking particles motion in 3D.

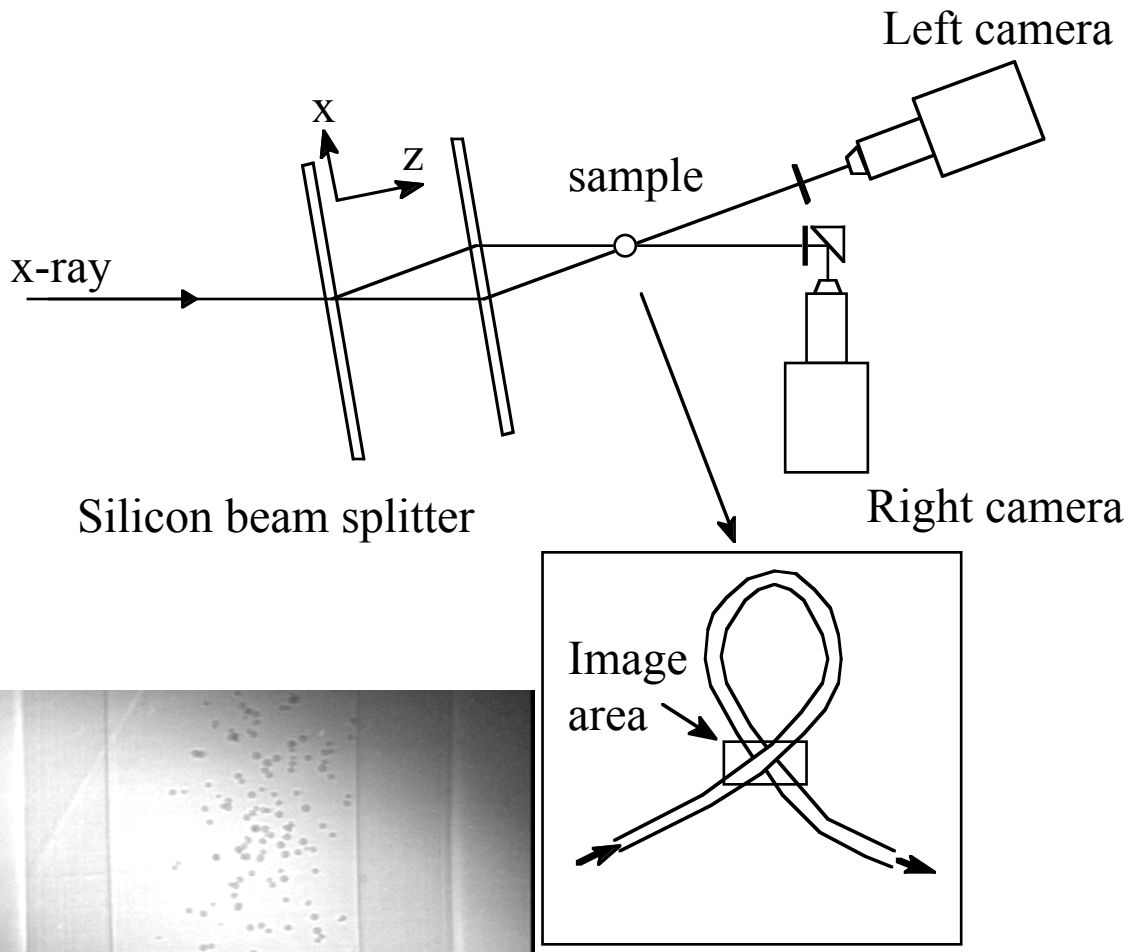

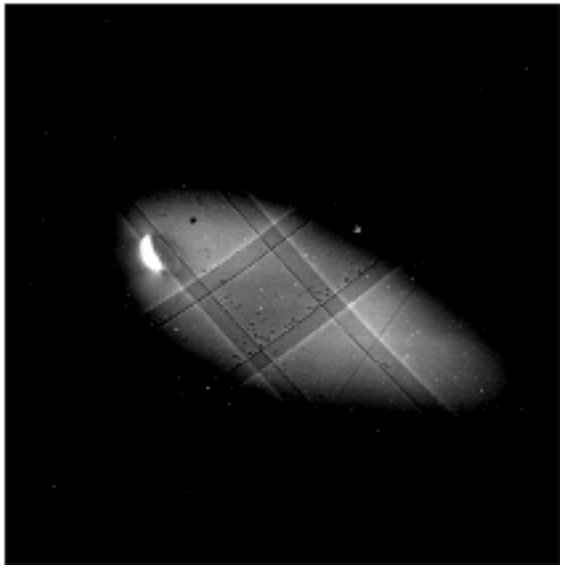

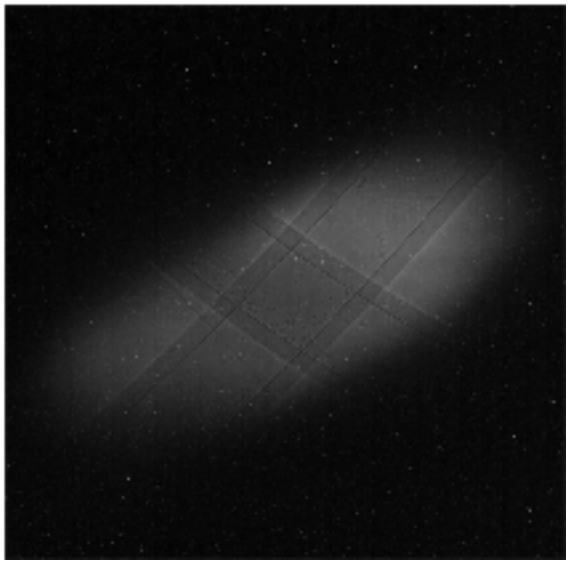

Video of straight section of tube

Lee et al, JSR 18, 2011

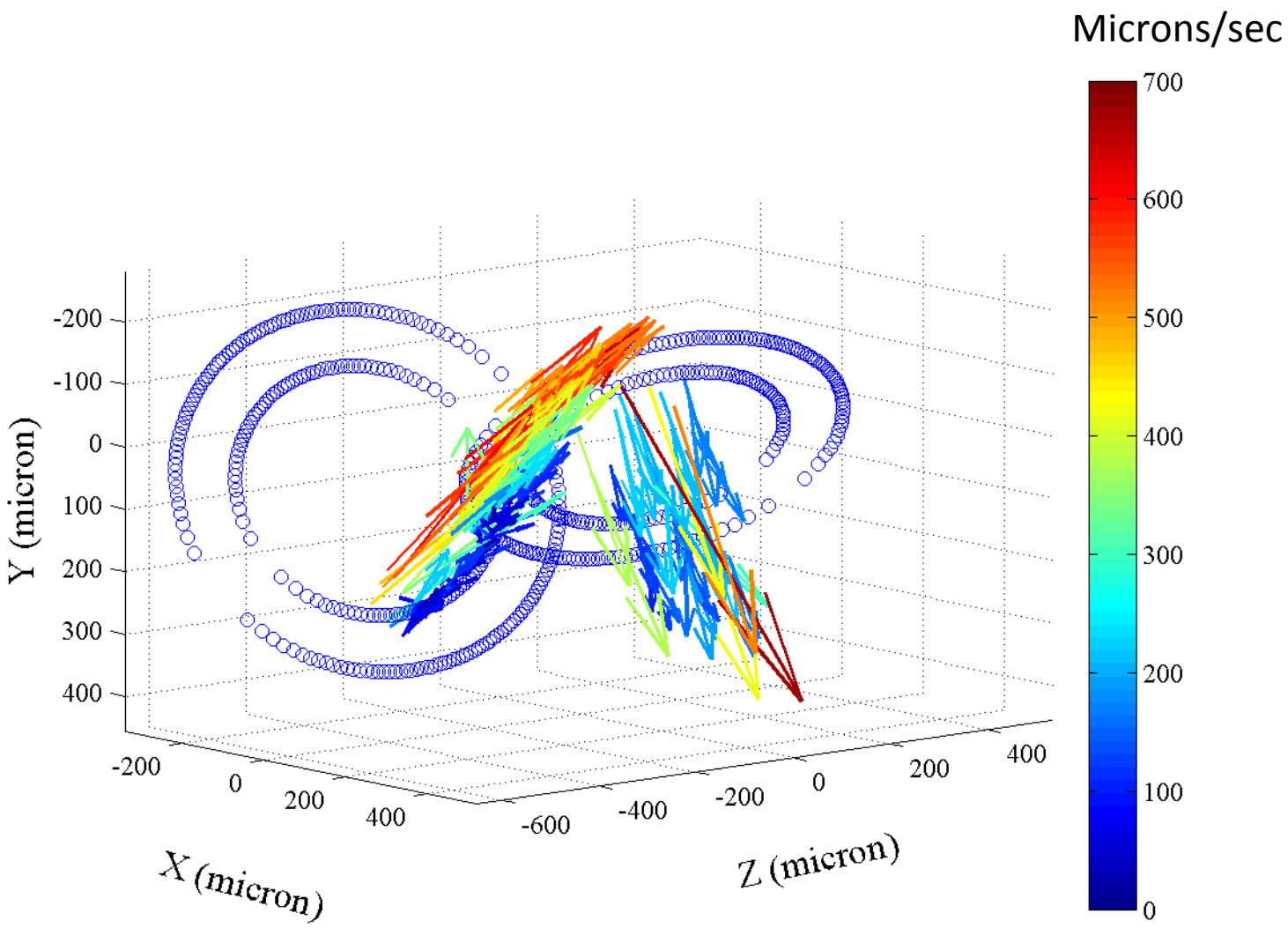
Microns/sec
700
600
500
400
300
200
100
0
Y (micron)
-200
-100
0
100
200
300
400
X (micron)
-200
0
200
400
Z (micron)
-600
-400
-200
0
200
400

Lens based imaging: Transmission x-ray microscope

An exact x-ray analog of the optical microscope
X-ray condenser: Single bounce capillary or zone plate
X-ray objective: Zone plate

see slides XX

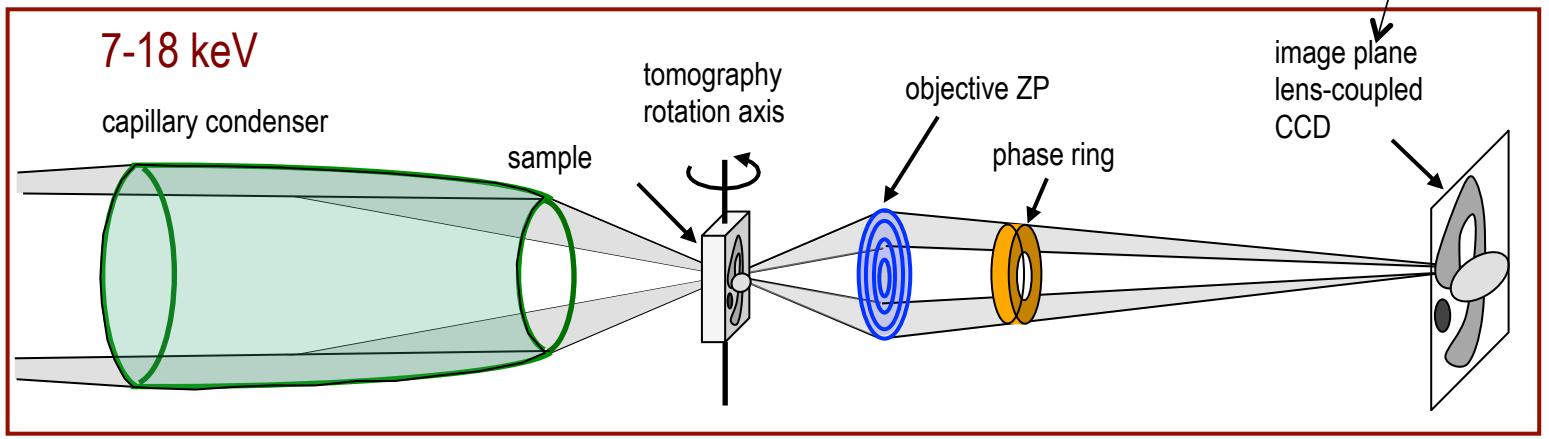

Magnification occurs in two stages:

X-ray stage ~ 80

Visible light stage ~ 10

ZP efficiency ~ <10%

Resources: www.microscopyu.com

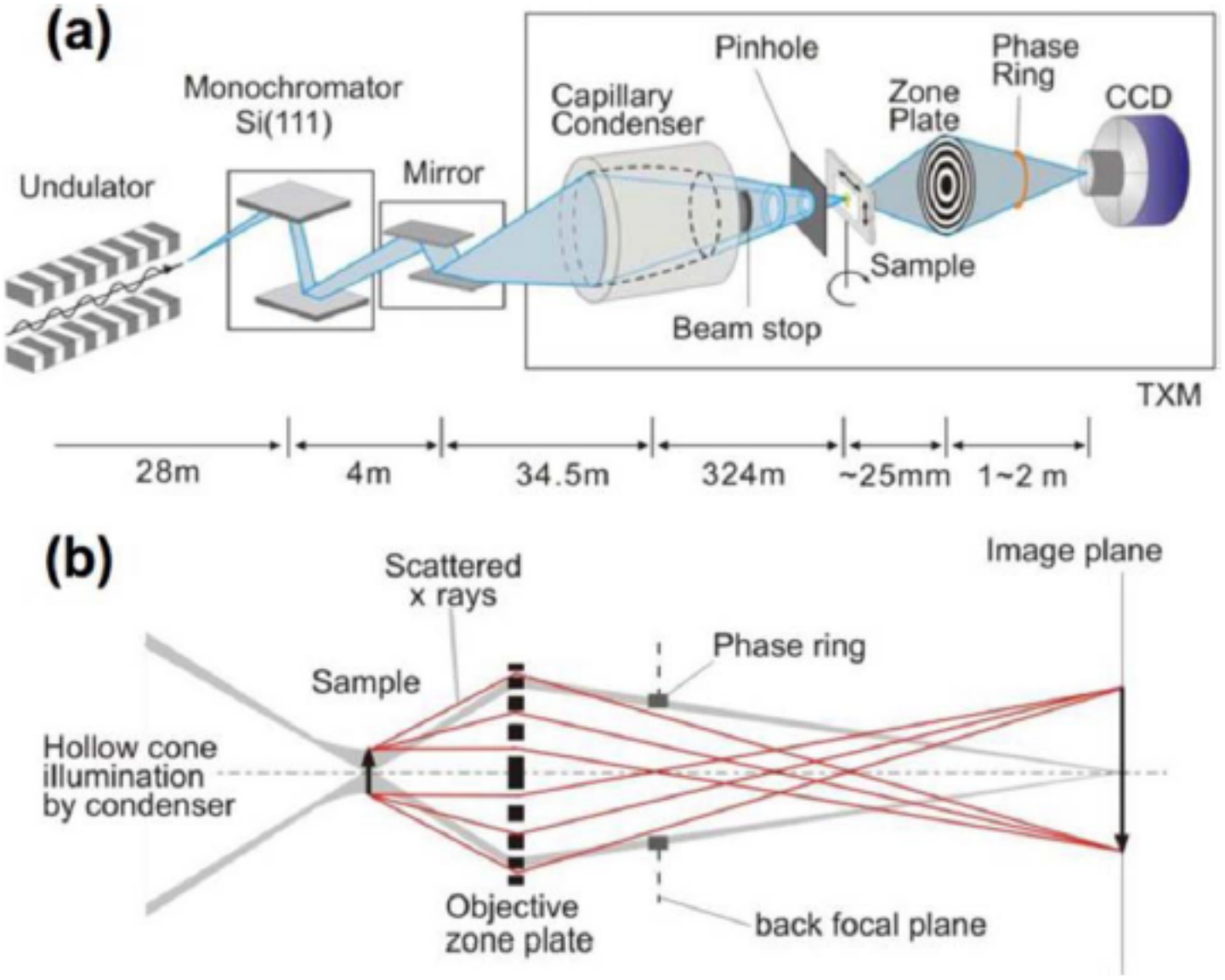

Fig. 2. (Color online) (a) Layout of the transmission x-ray microscope (TXM). (b) Geometry for the Zernike phase contrast.

Chen et al, Optics Letters, 2011

Real Time Nano-Imaging of Electrochemical Growth

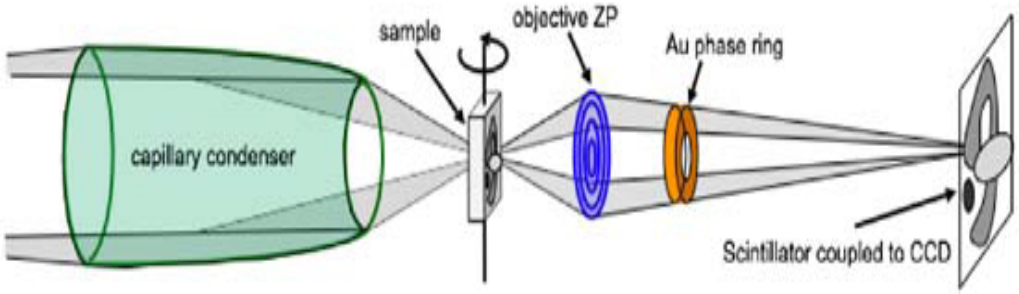

- Modern x-ray lenses (Fresnel zone plates) and bright x-ray sources enable x-ray microscopic imaging at nano-scale spatial resolutions
- Example: In-situ studies of dendritic growth of Cu in $CuSO_4$ solution by electrical potential (APS 32-ID, 8 keV)
  - Frame rate: 100 msec/frame
  - TXM FOV: 22 μm

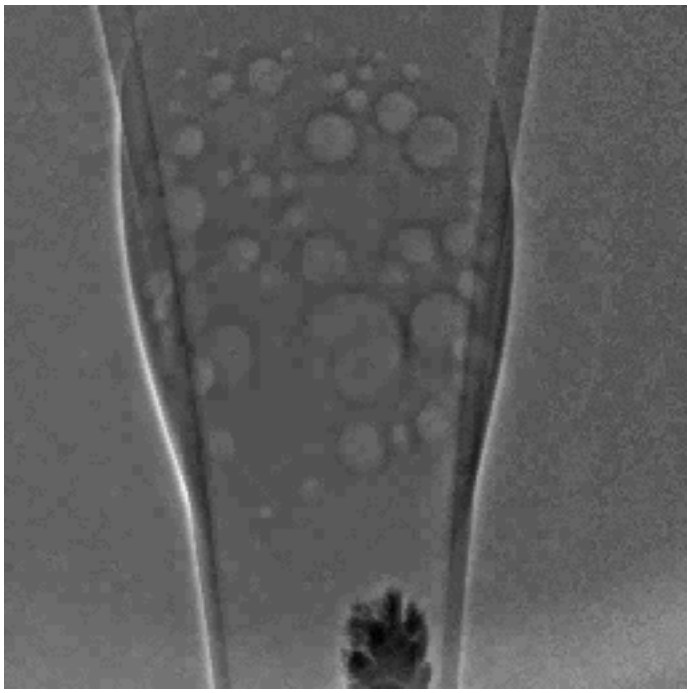

J. Yi, S. Wang (ANL), Y-K. Hwu (Acad. Sinica, Taiwan), J. H. Je (POSTECH, Korea), Y. S. Chu (NSLS-II, BNL)

*APPLIED PHYSICS LETTERS **97**, 033101 (2010)*

In situ 3D morphological changes in Li-ion battery tin electrode

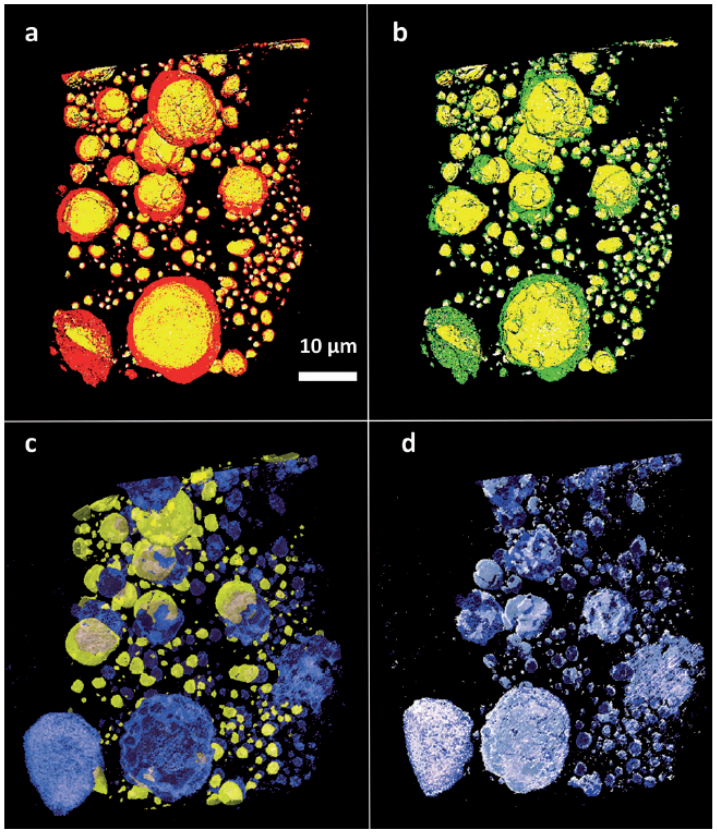

Figure 2. Overlaid 3D views of the sample during the first two cycles. a) The fresh electrode (yellow) and the electrode after the first lithiation (red). b) The fresh electrode (yellow) and the electrode after the first delithiation (green). c) The fresh electrode (yellow) and the electrode after the second lithiation (purple). d) The electrode after the second lithiation (purple) and the electrode after the second delithiation (gray).

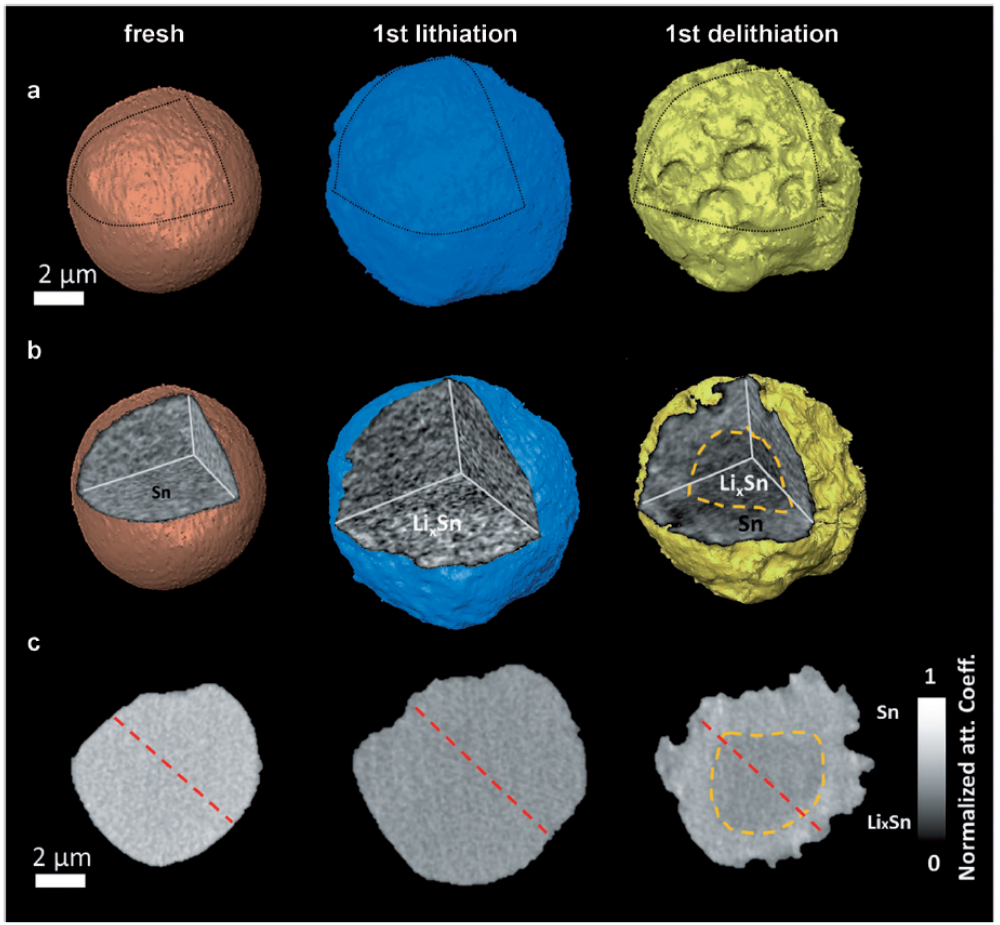

4 hours per 3D scan

X8C

J. Wang et al, Angewandte Communications 53, 2014

Zernike phase contrast

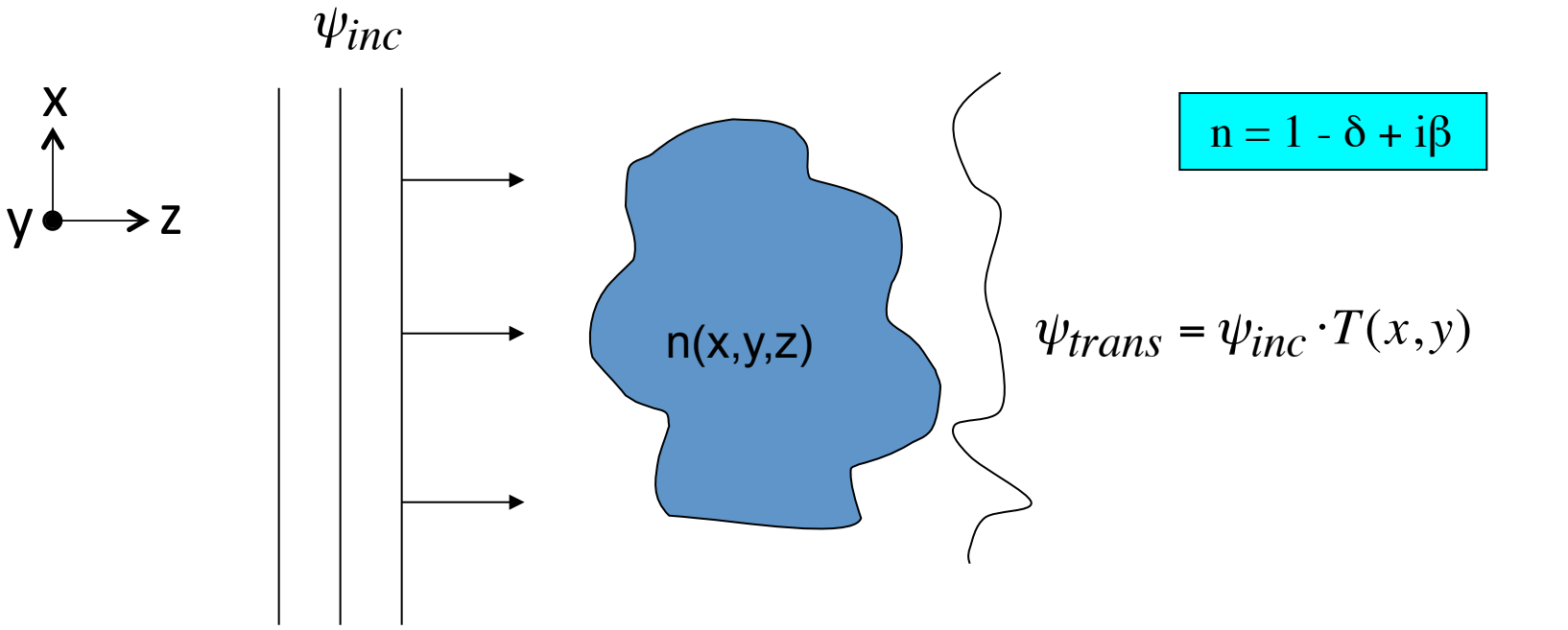

$$T(x,y) = e^{ik\int n(x,y,z)dz} = e^{-k\int \beta(x,y,z)dz}\, e^{-ik\int \delta(x,y,z)dz} = A(x,y)\, e^{i\phi(x,y)}$$

For small ϕ(x,y), $T(x,y) \approx A(x,y)\left[1 + i\phi(x,y)\right]$

If you can change the '1' to 'i' then:

$$I(x,y) = \left|\psi_{trans}\right|^2 = \left|I_0\right|\left|T(x,y)\right|^2 = I_0 \cdot \left|A\right|^2 \cdot \left[1 + 2\phi(x,y)\right]$$

Now, I(x,y) is sensitive to the phase term!

Zernike phase contrast

$$T(x,y) \approx \left[1 + i\phi(x,y)\right]$$

How to change the '1' to a '+/- i' ???

$$\tilde{T}(f_x,f_y) \approx \left[\delta(f_x,f_y) + i\tilde{\phi}(f_x,f_y)\right]$$

The '1' term is associated with the fx = fy =0 ('q'=0) term in frequency space. This beam passes through the sample without direction change.

To change from a '1' to a 'i', you introduce a phase change.
Recall: exp(i π/2) = i

So, to change the '1' to a 'i' you need to introduce a π/2 phase shift in the 'q=0' beam. (Odd multiples of π/2 will also work).

But how to do this??

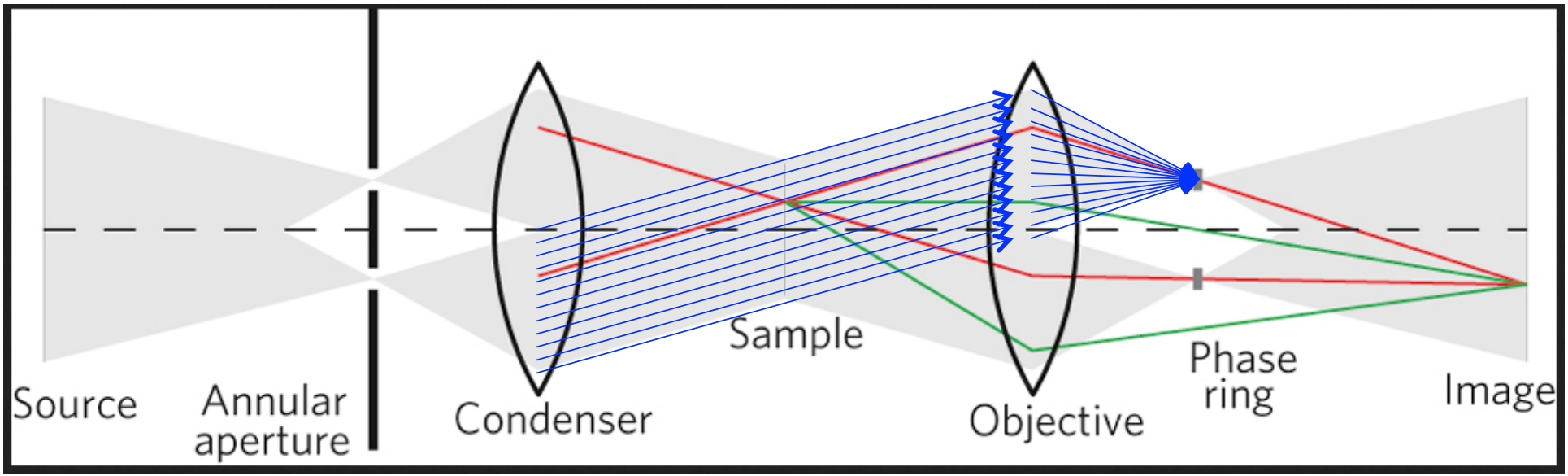

Because the q=0 rays are spatially separated at the back focal plane of the objective, it is possible to change its phase without affecting all the other frequencies

Challenge: In practice, it is inevitable that you also change the phase of q != 0 because of finite size of phase ring width. Image will have artifacts.

Holzner et al, Nature Physics 6, 2010.

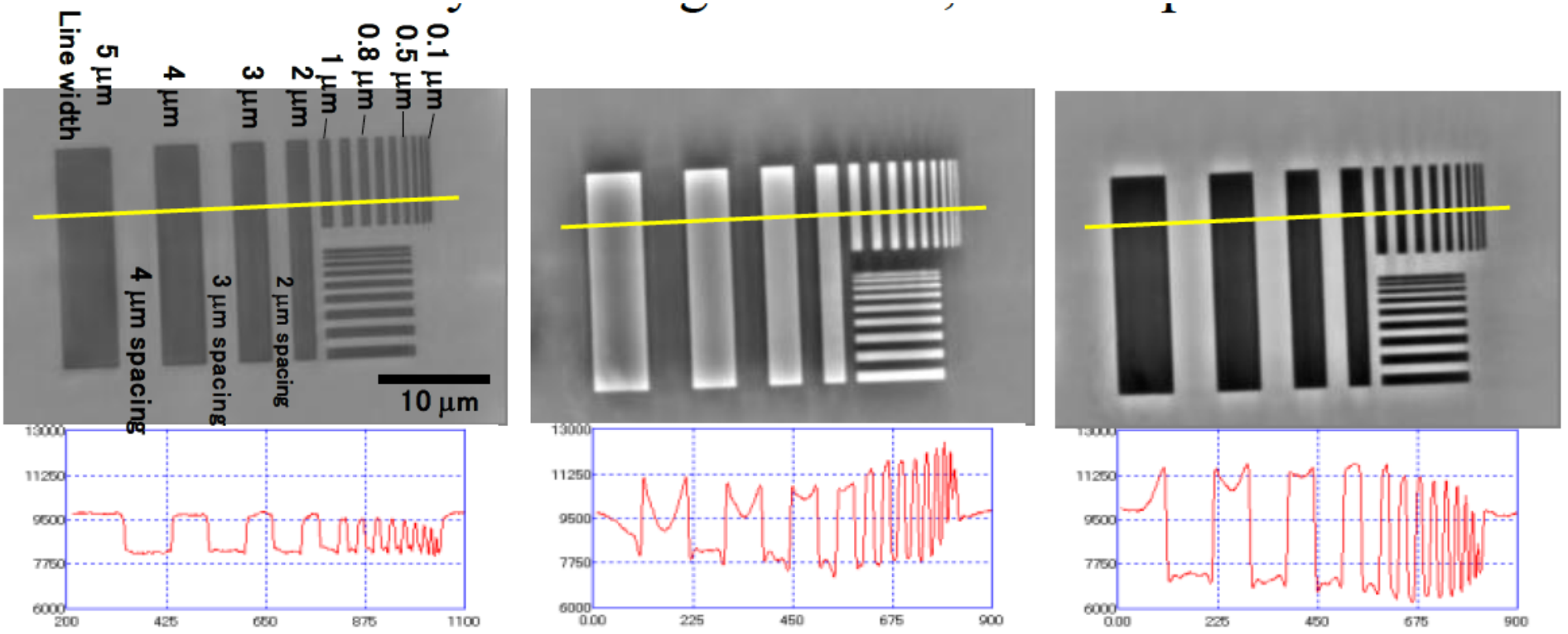

(a) **(b)** **(c)**

Figure 6. X-ray images and intensity profiles of tantalum test pattern (thickness: 0.5 µm), (a) TXM image, (b) ZXM bright phase contrast, and (c) ZXM dark phase contrast image. Beamline: BL47XU, x-ray energy: 8 keV, exposure time: 0.15 sec, pixel size: 47 nm.

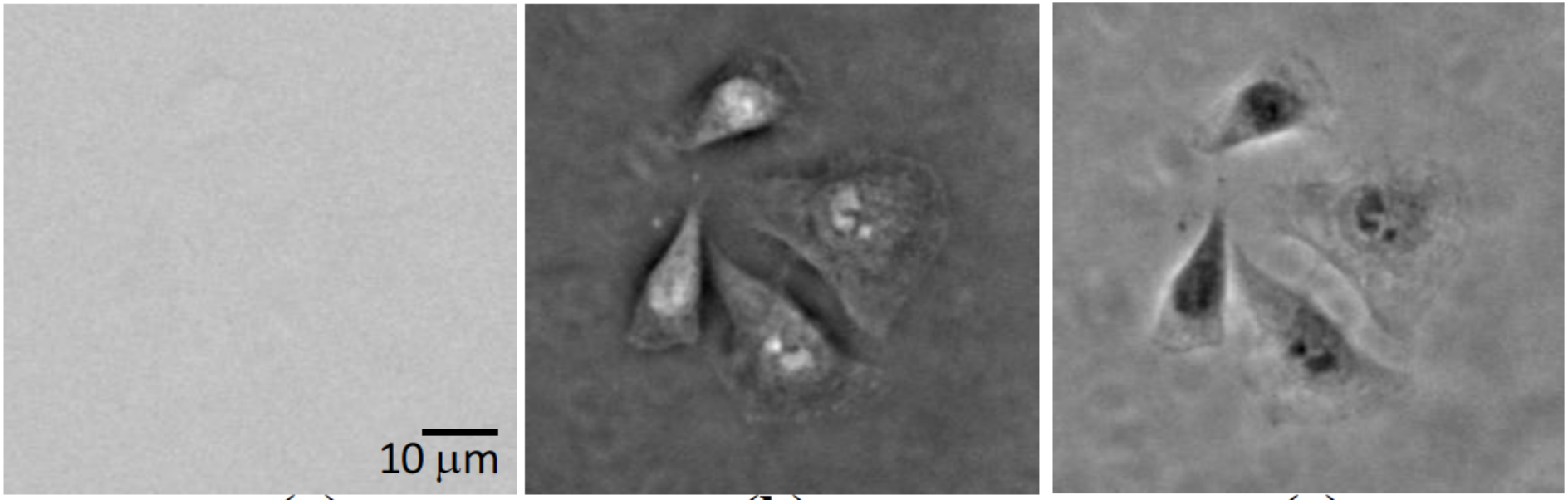

Figure 7. X-ray images of human cervical cancer HeLa cells (dry), (a) TXM image, (b) ZXM bright phase contrast, and (c) ZXM dark phase contrast image. Beamline: BL20XU, x-ray energy: 8 keV, exposure time: 30 sec, pixel size: 130 nm.

Terminology: Dark field imaging is when the 'q=0' beam is NOT captured. Only the scattered beam contributes. Eg, SAXS and USAXS imaging are dark field techniques.

Takeuchi et al, J of Physics, Conf. Series 186, 2009.

Outline

Part 1: Key concepts for imaging
Part 2: Practical issues and instruments
Part 3: Imaging techniques and examples
Part 4: Current frontiers

Current frontiers:

- Faster – more emphasis on looking at dynamics
- Quantitative techniques – especially phase retrieval
- Diffraction contrast – 3D grain structure
- 3D image analysis – how to extract useful quantities? Eg porosity, tortuosity, tracking dynamics.
- Alternate 3D reconstruction algorithms – fewer angular projections (lower dose, faster)
- Forward-backward simulations to take into account x-ray/material interactions not included in refractive index eg, scattering.
- All leading to f(x,y,z,E,t,q,….) where f can be β, δ, fluorescence, scattering intensity, etc.

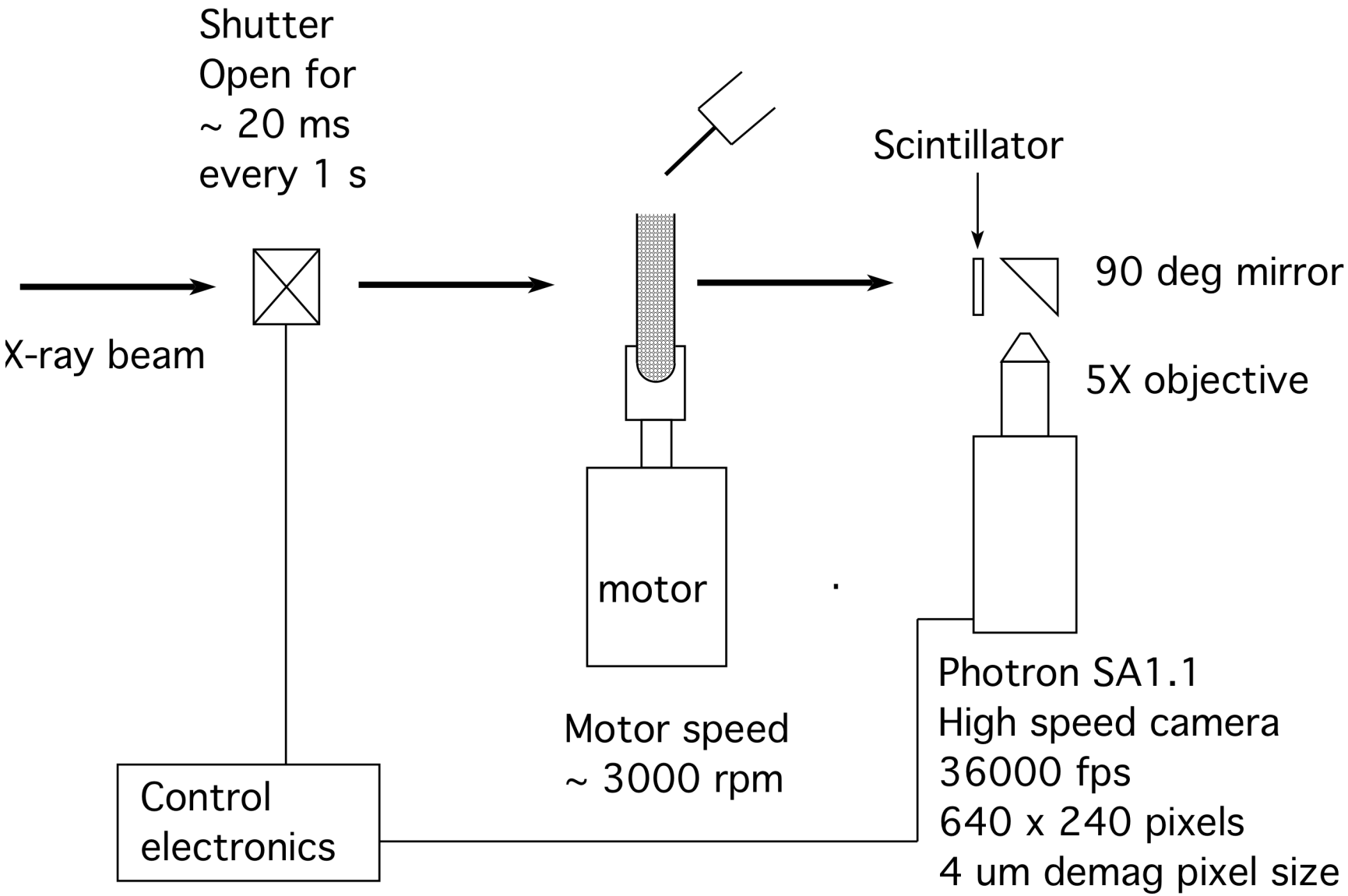

Sample: 1- 2 mm diameter uncompacted sand column

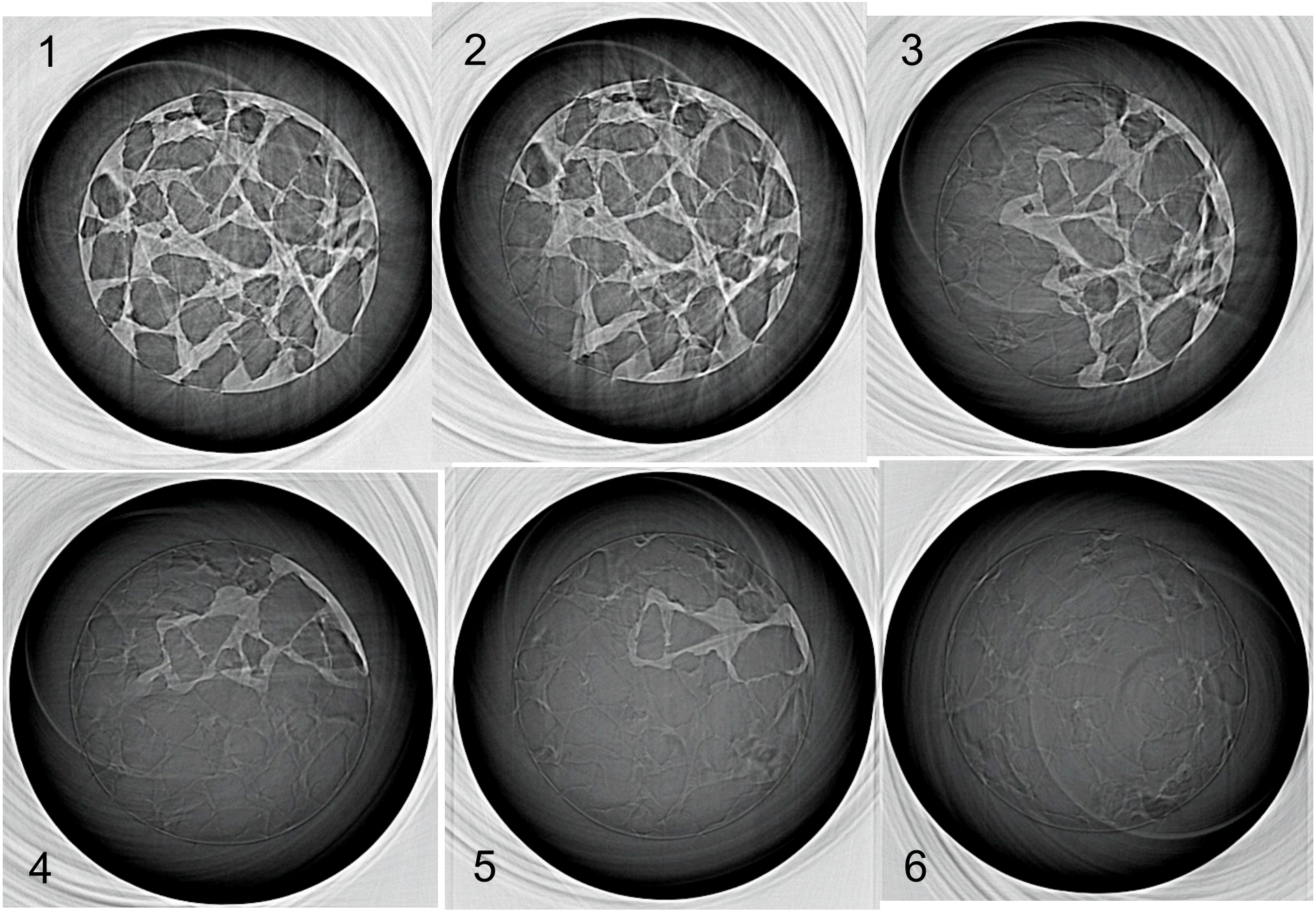

Cross sections separated by 1 s

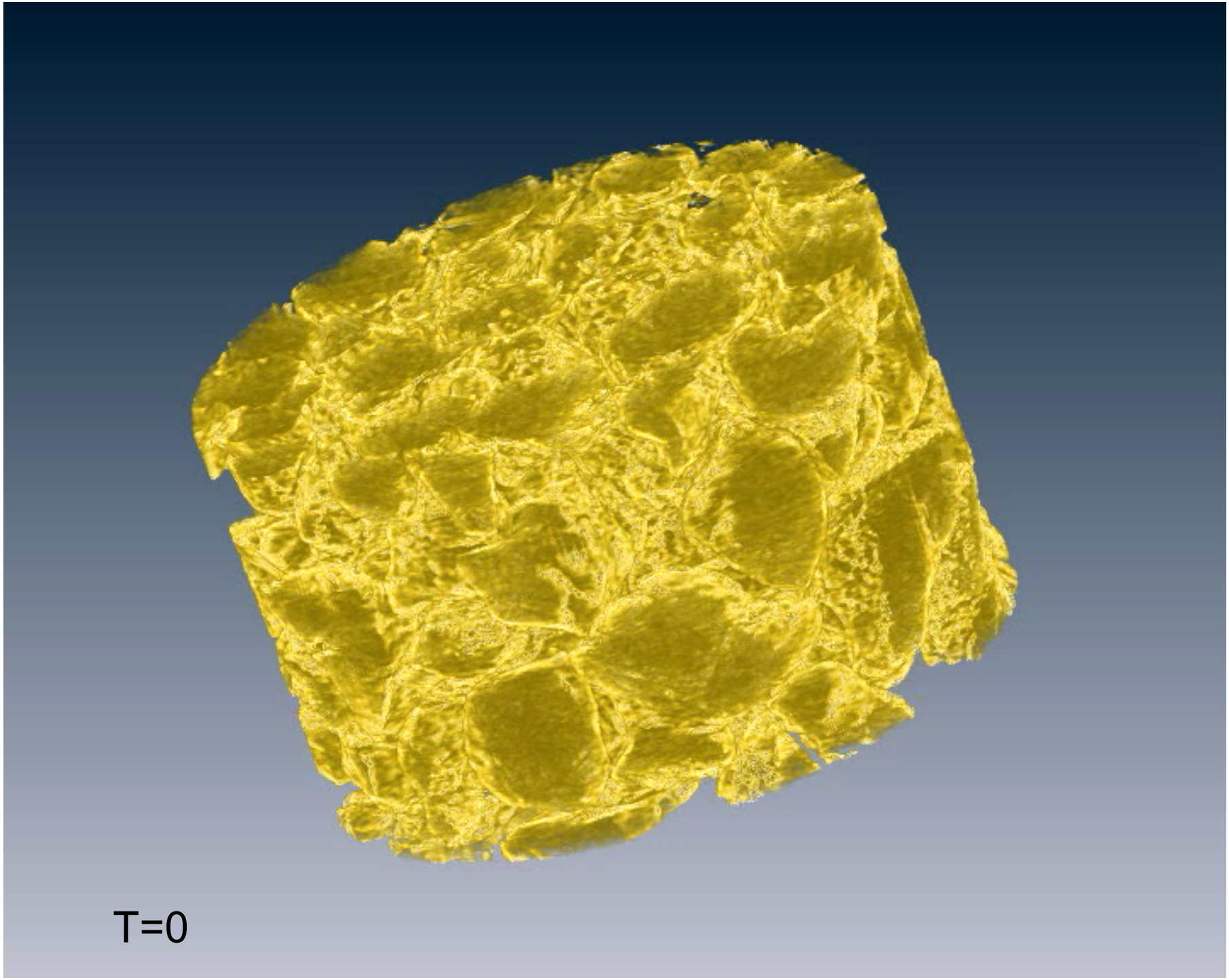
T=0

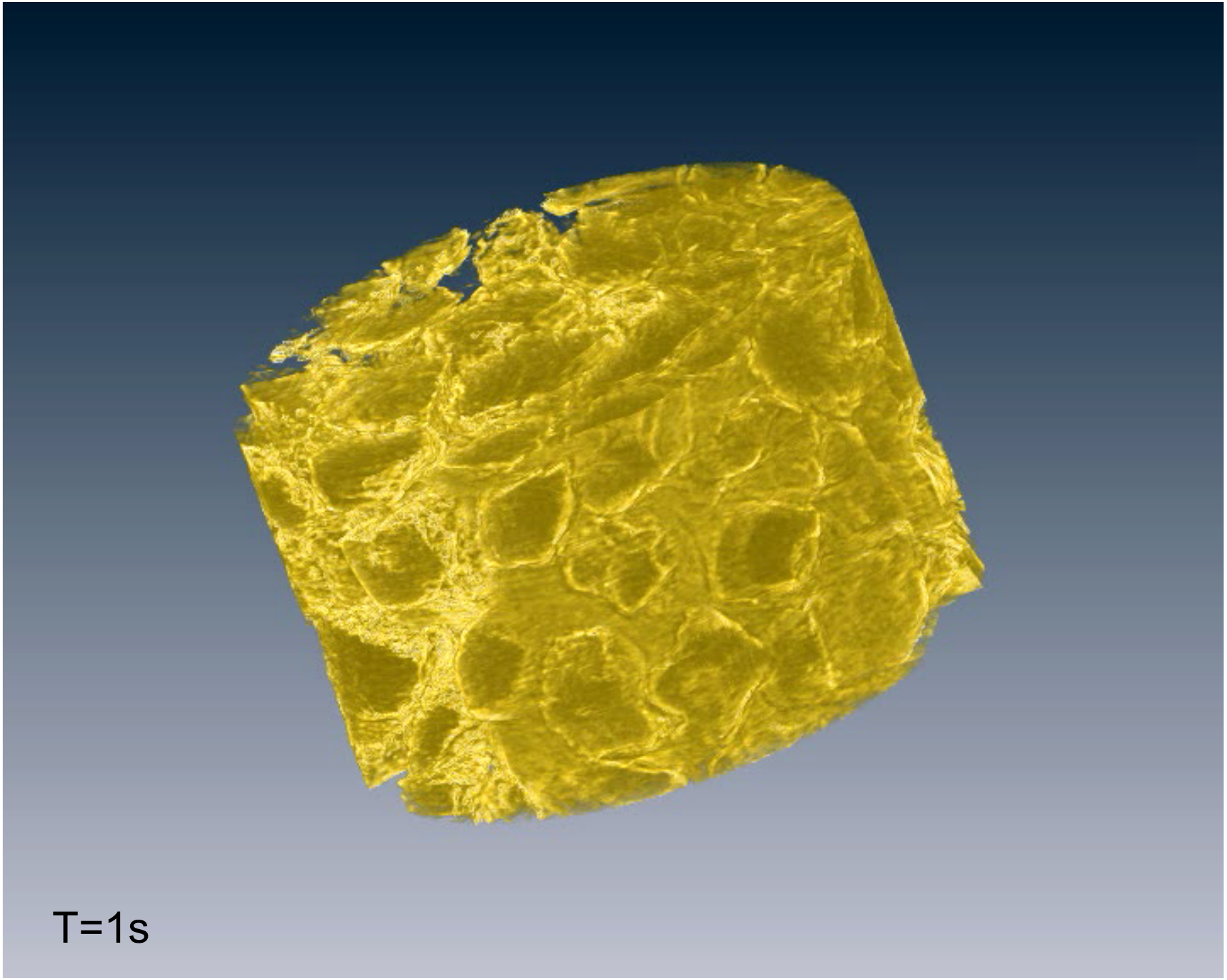
T=1s

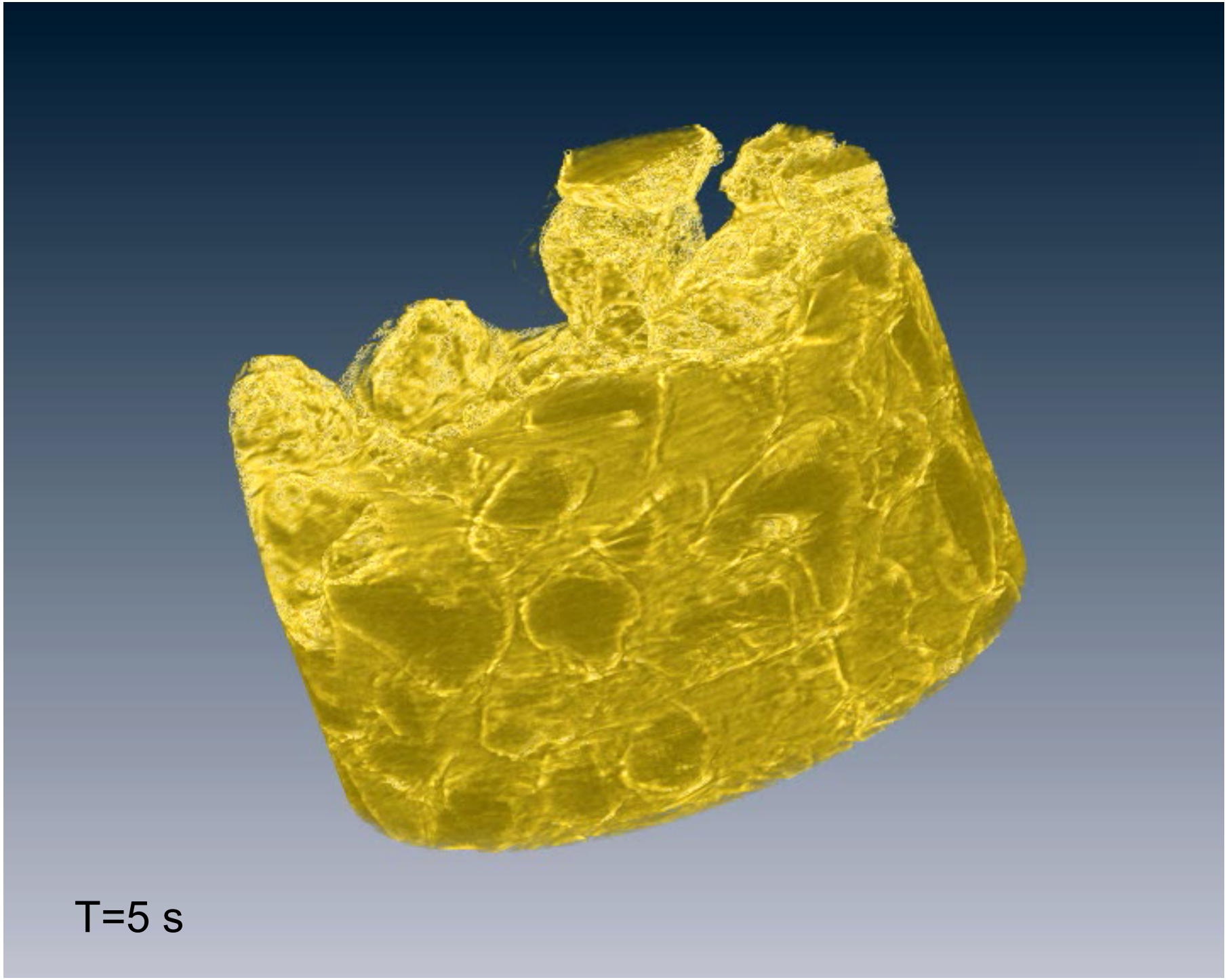
T=5 s

Utilizing Synchrotron Time structure

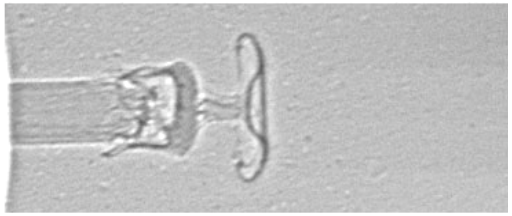

X-ray

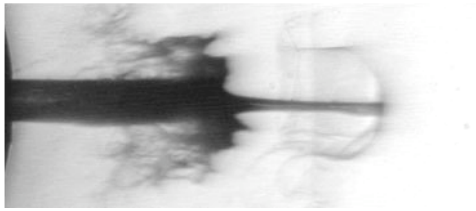

Visible light

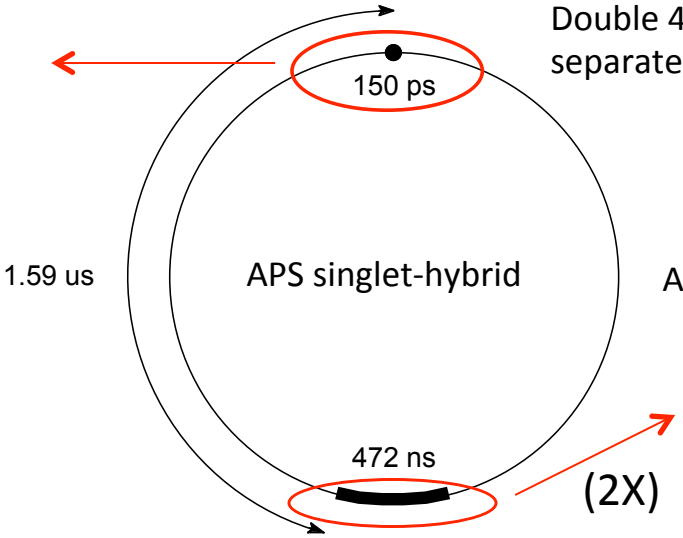

Double 472 ns exposure
separated by 3.68 us.

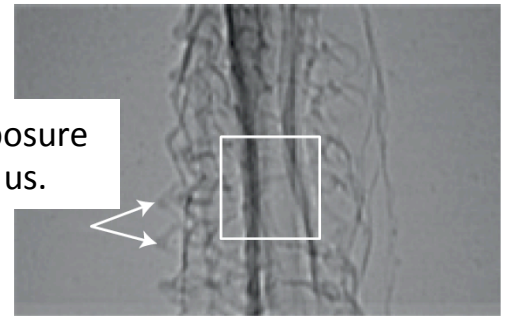

Autocorrelation

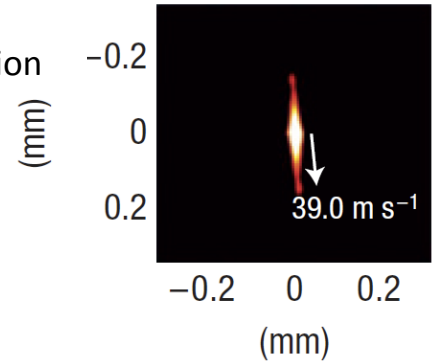

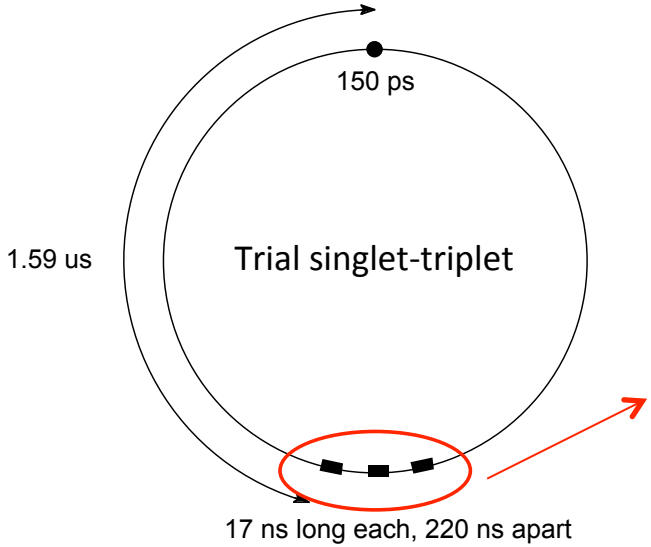

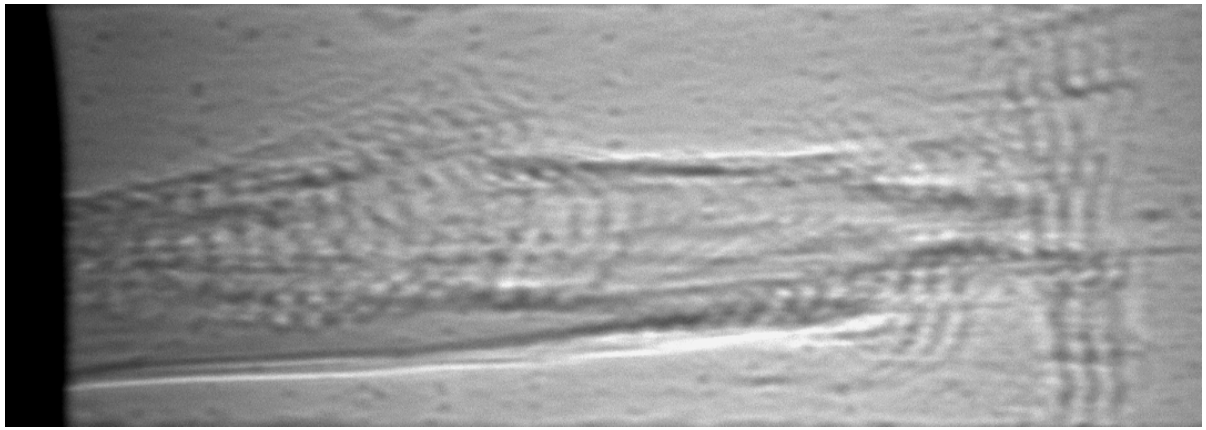

Triple 17 ns exposure separated by 220 ns
Liquid jet moving at ~ 200 m/s

What imaging technique to use?

Q: What do I want to see?

- is x-ray imaging the right too?
- what are the size features I want to see? (Spatial resolution)
- how fast do I need to image? (Time resolution)
- what contrast mechanism do I need? (Phase or absorption or ?)

General guide:

Below ~ 0.5 microns spatial resolution: Use TXM
Highest speed: Filtered white beam absorption/propagation technique
Slowly varying phase (eg tumor): Analyzer based techniques or long distance propagation
Quantitative phase: Holotomography (propagation at several distances) or interferometry
Qualitative phase: Propagation or analyzer based
Samples that scatter a lot: Analyzer based techniques

Some thoughts….

- Full-field x-ray imaging is a keystone technique.
- It complements other x-ray modalities: microfluorescence, scattering.
- Tackles realistic samples; ie, living animals and fuel injectors.
- Technique is extremely versatile and flexible; enabling all types of realistic environments to be incorporated
- In the foreseeable future, synchrotron-based x-ray imaging will remain unchallenged for the study of dynamics.

	10 keV	20 keV	30 keV	40 keV	50 keV
Water, β	4.9e-9	2.6e-10	4.6e-11	1.4e-11	5.3e-12
Water, δ	2.3e-6	5.8e-7	2.6e-7	1.4e-7	9.2e-8
Al, β	6.6e-8	4.0e-9	7.6e-10	2.3e-10	9.1e-11
Al, δ	5.5e-6	1.4e-6	6.0e-7	3.4e-7	2.2e-7
Fe, β	1.3e-6	9.6e-8	2.0e-8	6.4e-9	2.6e-9
Fe, δ	1.5e-5	3.8e-6	1.7e-6	9.5e-7	6.1e-7

This table will be used for homework and exam question.